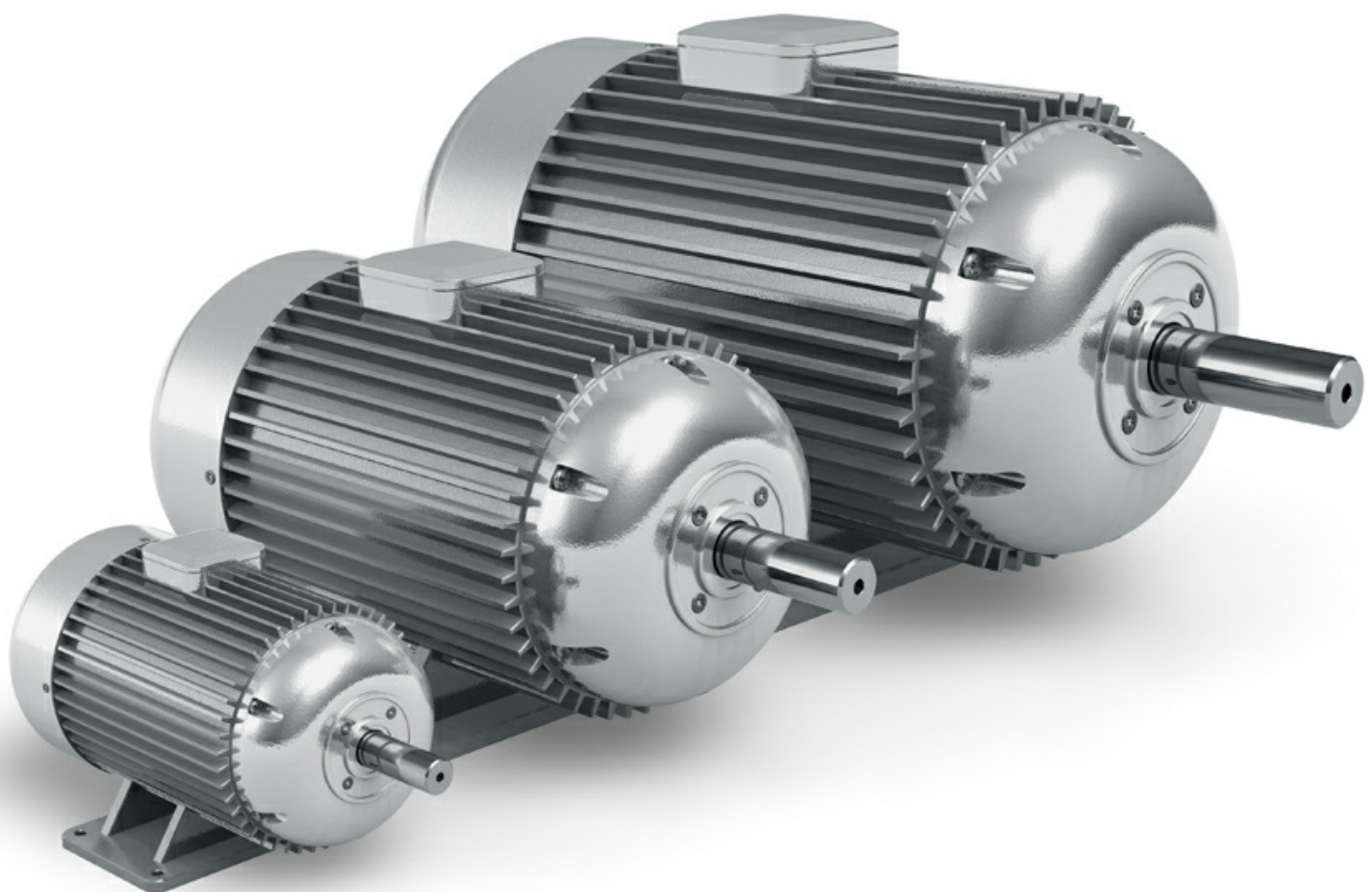


Electric Drive Dimensioning and Tuning

Valery Vodovozov



Download free books at

bookboon.com

Valery Vodovozov

Electric Drive Dimensioning And Tuning

Electric Drive Dimensioning And Tuning
© 2012 Valery Vodovozov & bookboon.com
ISBN 978-87-403-0247-9

Contents

Designations	6
Indexes	6
Abbreviations	7
Preface	8
1 Project Planning	9
1.1 Project requirements	9
1.2 Operating modes	15
1.3 Motor dimensioning	19
1.4 Design stages	25
2 Load Calculations	30
2.1 Moments of inertia	30
2.2 Load calculation formulae	32
2.3 Friction forces	35
3 Mechanical Transmissions	40
3.1 Travel functions	40

I joined MITAS because
I wanted **real responsibility**

The Graduate Programme
for Engineers and Geoscientists
www.discovermitas.com

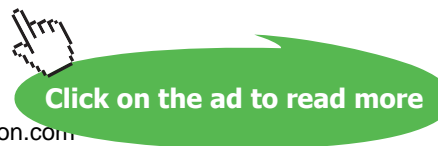


Real work
International opportunities
Three work placements



Month 16
I was a construction supervisor in the North Sea advising and helping foremen solve problems

 MAERSK



3.2	Reflecting of forces and torques	45
3.3	Elasticity forces	50
3.4	Load gaps and backlashes	56
4	Regulators and Filters	59
4.1	Transfer functions and block diagrams of drive components	59
4.2	Analogue regulators and filters	64
4.3	Digital filters and regulators	66
4.4	Static accuracy of electric drive	70
5	Control Principles of Electric Drives	74
5.1	Modal control and standard settings	74
5.2	Sequential correction of simple objects	77
5.3	Sequential correction of complex objects	80
5.4	Cascading	83
6	Tuning the Electric Drives	86
6.1	Speed control	86
6.2	Combined speed-current control	92
6.3	Path control	96
6.4	Electric drives with elastic load	100



www.job.oticon.dk

oticon
PEOPLE FIRST

Designations

BR	speed sensor	<i>F</i>	force, magneto-motive force, MMF
BQ	position sensor	<i>G</i>	Young's modulus, rigidity
C	capacitor	<i>GD</i> ²	flywheel torque
L	winding, load	<i>I</i>	current
M	motor	<i>J</i>	moment of inertia
R	resistor	<i>L</i>	inductance
		<i>L</i> ₁₂₃	phases
<i>a</i>	coefficient	<i>P</i>	power
<i>f</i>	frequency	<i>Q</i>	square
<i>g</i>	gravity acceleration	<i>R</i>	resistance
<i>h</i>	depth, height, step	<i>T</i>	torque
<i>i</i>	reduction rate	<i>U</i>	voltage
<i>k</i>	factor, gain	<i>V</i>	volume
<i>l</i>	length, path	<i>W</i>	energy
<i>m</i>	mass	<i>W(s)</i>	transfer function
<i>m</i> ₁₂	phase number		
mod	module	β	rigidity
<i>n</i>	rotation frequency	γ	overshoot, ratio
<i>p</i>	pole pair number	δ	error, loss
<i>q</i>	productivity	η	efficiency
<i>r</i>	radius	μ	coefficient of friction
<i>s</i>	differential operator	ξ	damping factor
<i>t</i>	time	ρ	density, resistivity
<i>v</i>	velocity	σ	leakage
<i>y</i>	control variable	τ	time constant
<i>z</i>	number of teeth, steps	τ°	temperature
		φ	angle
<i>A</i>	heat emission	χ	disturbance
<i>B</i>	induction	ψ	flux linkage
<i>C</i>	capacity	ω	angular speed, angular frequency
<i>E</i>	electromotive force, EMF		

Indexes

₀	input, synchronous, delay	₂	rotor
₁	stator	_a	armature
₁₂	rotor relative to stator, mutual	_c	self-oscillation, cutoff

<i>d</i>	dynamic, running	<i>c</i>	converter
<i>dif</i>	differential	<i>G</i>	gear
<i>e</i>	electromagnetic	<i>J</i>	inertia
<i>f</i>	filter	<i>L</i>	load
<i>int</i>	integral	<i>M</i>	motor
<i>l</i>	linear	<i>T</i>	mechanical
<i>max</i>	maximal	β	elastic, inner friction
<i>min</i>	minimal	μ	small, friction, stiffness
<i>n</i>	rated, normal	δ	error, variation
<i>o</i>	object	Σ	total
<i>opt</i>	optimal	τ^o	thermal
<i>q</i>	braking	σ	leakage
<i>rg</i>	regulator	*	set-point

Abbreviations

ac	alternating current	FOC	field-oriented control
cdf	cyclic duration factor	I	integral control
dc	direct current	IP	Ingress Protection standard
rad	radian	ISO	International Standard Organisation
rms	root mean square	HPF	high-pass filter
rpm	revolutions per minute	LPF	low-pass filter
AI	artificial intelligence	MMF	magneto-motive force
ANN	artificial neuron network	MO	modulus optimum
BDCM	brushless dc motor	P	proportional control
BPF	band-pass filter	PD	propotional-differential control
BSF	band-stop filter	PI	propotional-integral control
CCW	counter-clockwise	PID	propotional-integral-differential control
CFC	current-frequency control	PM	permanent magnet
CSI	current source inverter	PMSM	PM synchronous motor
CW	clockwise	PWM	pulse-width modulation
D	differential regulator	SO	symmetrical optimum
DTC	direct torque control	SRM	switched-reluctance machine
DSP	digital signal processor	SVM	space vector modulation
EMC	electromagnetic compatibility	THD	total harmonic distortion
EMF	electromotive force	UPS	uninterruptible power supply
EO	exponential optimum	VFC	voltage-frequency control
FESM	field-excited synchronous motor	VSI	voltage source inverter

Preface

Each point of our life is the point of choice

Yuly Daniel

There is always an increasing demand for most modular, flexible, and integrated solutions. This in turn is causing designers to find ways of enhancing their product offerings in response to such demand. Designs are fast becoming more commonplace, in part because technology advances are making them easier and also because an integrated solution functions more effectively as a whole rather than the sum of the individual elements that comprise it.

An electric drive is the electromechanical system that converts electrical energy to mechanical motion of the driven machine. As a rule, it has more capability than the separate motor, gear, or power converter in their composition. To meet the application requirements, every component must be evaluated according to its own capability before selecting it for use on a drive. This must be considered when selecting and tuning multiple motor-gear-converter combinations.

This book is intended primarily for the university-level learners of an electromechanical profile, including the bachelor and master students majored in electrical engineering and mechatronics. It will help also technicians and engineers of respective specialities. Those who have completed the basics of electric drive are welcome to this advanced course.

The proper choice of the driving equipment to meet the load requirements called dimensioning is discussed in the first three sections of this book. The amount of power and torque produced by a drive must always be at least equal those required by the load. If the drive cannot produce sufficient values, it will either fail to start the load, stall, or run in an overloaded condition. The book illustrates how the load can be determined. In order the machine to perform without excessive overshoot, settle within adequate time periods, and have minimum errors, the electric drive must be tuned. In the last three sections of the book, the control systems are discussed which are the basis of the adjustable converter-fed electric drives. They implement motor speed, position, flux, and torque management, realise coordinated motion of multiple mechanisms, and convert information of the automatic process. As the electric drives exhibit highly coupled, nonlinear, and multivariable structures, their control generally requires complex algorithms that can be performed by microprocessor controllers along with fast-switching power converters.

I wish you much success in designing and tuning electric drives.

Author

1 Project Planning

1.1 Project requirements

Request for proposal. To find an optimum system composition the complex *project planning* is conducted. As a rule, this process begins from the *request for proposal*, which clarifies the types of motors, gears, and power converters as well as the system organisation to obtain the highest reliability, best dynamic and static properties, minimum dimensions or loss, and acceptable cost. An equipment type has to satisfy the required technical and economic indices.

To start the project planning, the load data, such as mass, speed, forces, frequency, operating times, geometry of wheels and shafts as well as the performance conditions are collected. Using these data, the required amount of power in regard to efficiency is calculated, and the output speed is determined. Then, the gears, motors, and power converters are selected from the manufacturer catalogs and databases observing the individual operating conditions. For fast and effective determination of the drive components, the leading vendors suggest the project planning programs where extensive data of electronic catalogs are available as the datasheets. Thus, the user can choose between uncontrolled and controlled drive systems, required components, and their accessories.

Drive specifications. Failure to proper specifying of a motor drive can result in a conflict between the equipment supplier and the end user. To avoid such a problem, the design specifications should reflect the operating and environmental conditions listed:

- performance conditions and duty
- supply conditions and harmonics
- supply voltage, current, and frequency
- power and torque ratings
- speed range, minimum, and maximum values
- accuracy and time response
- efficiency and power factor
- service life expectancy
- standards, rules, and regulations

Both an equipment supplier and a customer should work as partners and cooperate from the beginning of the project until successful commissioning and handover. It is advisable that the customer procure the complete drive system, including system engineering, commissioning, and engineering support, from one competent supplier. It is one of the first priorities to identify applicable national and international standards on issues related to EMC, harmonics, safety, and noise, smoke emissions during faults, dust, and vibration. Overspecifying the requirements could often result in a more expensive solution than necessary. The customer must have an idea about the drive interfaces, voltages, mechanical power, and shaft speed because the torque and current are calculated from these. The frequency and the power factor depend on the choice of the motor and the gear. For a high-power drive, it is always recommended to carry out a “harmonic survey” which will reveal the existing level of harmonics and quantify approaching the new levels.

Other classifications, not listed above, include the following:

- working voltage: low (less than 690 V) or medium
- current type: ac or dc
- mechanical coupling: direct, via a gearbox, or indirect
- packaging: integrated motors as opposed to separate ones
- movement: rotary, vertical, or linear motion
- drive configuration: stand-alone, system, dc link bus, etc.
- braking mode: regenerative or non-regenerative
- cooling method: direct and indirect air, liquid, etc.

Classification by applications. Every application is targeted to the specific load. The way the drive performs is very much dependent on the load characteristics. With regard to applications, four main groups of motor drives are available, namely appliance drives, general-purpose drives, system drives, and servo drives. Table 1.1 describes typical applications and main features of these groups.

Feature	Appliances	General-purpose drives	System drives	Servo drives
Applications	Home appliances,	Fans, pumps, compressors, mixers	Test benches, cranes, elevators, hoists	Robots, lathes, machine tools
Performance	Middle	Low	High	Very high
Power rating	Low	Whole range		Low and middle
Motor	Mainly induction motors		Mainly servomotors	
Converter	Simple, low cost	Open-loop ac and dc	Expensive, high quality	
Typical feature	Home, mass production	Process, cost sensitive, low performance	High accuracy and high dynamic, high precision and linearity	

Table 1.1 Electric drive classification by applications

Electrical requirements. Electrical rules regulate the kind of electrical power and technical characteristics of the primary supply circuit and the load.

The drives are designed to operate in a wide range of supply voltages, from low voltage to higher voltage at supply frequencies of 47...63 Hz. Many supplies vary outside those levels. For example, supplies at the end of long power lines in remote areas can rise excessively when large loads are no longer present. Industries with locally controlled and generated supplies can have poor regulation and control. Power systems in certain parts of the world may not meet expected tolerances. The supply circuit sometimes has steady or transient asymmetry. Thus, operation outside the stated supply levels will probably cause damage and must be avoided.

In the case of ac supply, input voltages, currents, frequencies, and the number of phases are rated as well as the quality of electrical supply as a whole. In the group of quality factors, the steady state and dynamic stability, possible non-sinusoidal shape of waves, time, and periodicity of dynamic disturbances are included. In the case of low-power supply source, the harmonic content of the input current, the power factor, and the timing diagrams are limited. In the case of long cabling distances, the electrical resistance of the wiring is to be taken into account. When the high harmonic currents flow through the cables, the distributed inductances and distributed capacitances are also significant. Thus, the resonant phenomena and signal shape distortion should often be eliminated or limited.

In the past four years we have drilled
81,000 km

That's more than **twice** around the world.

Who are we?
We are the world's leading oilfield services company. Working globally—often in remote and challenging locations—we invent, design, engineer, manufacture, apply, and maintain technology to help customers find and produce oil and gas safely.

Who are we looking for?
We offer countless opportunities in the following domains:

- **Engineering, Research, and Operations**
- **Geoscience and Petrotechnical**
- **Commercial and Business**

If you are a self-motivated graduate looking for a dynamic career, apply to join our team.

What will you be?

Schlumberger

careers.slb.com

In the case of dc supply, input rated voltages and currents as well as the power supply quality are also indicated. Among the quality factors, the steady state and dynamic stability, possible time and periodicity of dynamic disturbances are listed. The ripple level and frequency are the important features of dc supply. Again, in the case of low-power source, the supply line dynamic value of electrical resistance is limited. This parameter helps to evaluate the influence of the input current on the output voltage, commutation spikes and drops under the load rising and lowering.

An electric drive is supplied with ground and phase fault protection, overheating and overcurrent protection. Table 1.2 illustrates the difference of protection equipment (2 – Full protection, 1 – Partial protection, 0 – No protection).

Malfunctions of electric drive	Current protection		Thermal protection	
	Fuse	Automatic breaker	Thermistor	Bimetallic breaker
Short circuit	1	2	2	2
Overcurrent more than 200%	0	2	2	2
Start-stop mode, more than 60 cycles/h	0	1	2	2
Phase break	0	1	2	2
Voltage fluctuation	0	2	2	2
Frequency fluctuation	0	2	2	2
Overheating	0	0	2	2

Table 1.2 Current and thermal protection equipment

A designer must take into account the full scope of protection grounding standards. The grounding methods and elements should have constant transient rated resistance during the full time of duty. Other standards and technical rules concern different technological and production modes. Particularly, they are: electrical connectors and leads, marking, signal sizes and levels, cabling circuits, metrological devices, ergonomics, etc.

The following standards regulate possible variants of the used equipment:

- IEC 60034 – Rotating electrical machines. Rating and performance. Converter-fed cage induction motors.
- IEC 60072 – Rotating electrical machines. Dimensions and output series.
- EN 50347 – General purpose three-phase induction motors.
- IEC 72 – Rotating electrical machines. Frame numbers.
- EN 60204 – Safety of machinery. Electrical equipment of machines. General requirements.
- EN 60146 – Semiconductor converters. General requirements and line commutated converters.

Converter type defines an *electromagnetic interference level (EMI)* and *electromagnetic compatibility level (EMC)* of electric drive. Both indexes are regulated by directives EEC 89/336, EN 61800-3, EN 50081, EN 50082, by international standards IEC 801 and national standards. Manufacturers support the required levels of *emission* by radiation and conductivity, electrostatic charge, pulse noise, and radio frequency *immunity*, as well as supply voltage and magnetic fields deviation protection.

Table 1.3 summarizes main techniques used to overcome problems associated with EMI at source as well as at load.

Effect	Frequency	Counter-measure	
		At source	At load
Mains	Up to 100 Hz	Avoid circulating currents	Balanced signal circuits. Avoid earth loops in signal paths
Mains harmonics	100 Hz...2,5 kHz	Line and/or dc link reactor on rectifiers. Higher pulse number rectifier. Avoid loops in signal paths. Low-impedance supply. Harmonic filters	Balanced signal circuits. Avoid loops in signal paths. Filtering
Intermediate	2,5 kHz...150 kHz	Filters	Filtering. Screening. Balanced signal circuits
Low frequency	155 kHz...30 MHz	Filters. Cable screening	Filtering
High frequency	Higher than 30 MHz	Screening. Internal filtering	Screening

Table 1.3 Motor drive EMI protection techniques

Equipment enclosure. The drive design depends on the maintenance conditions and functional place of equipment, such as autonomous, built-in, or a part of another device. An autonomous module is the most commonly employed type, thus the requirement of standard housing is typical. Mechanical resistance to shocks, vibrations, etc. is another characteristic. Methods of control, repair, and reconstruction processes are very important also. When the influence of humidity and water is high, plus an aggressive environment, hermetic sealing is the solution of the problem. The same concerns the storage conditions.

An *enclosure* holds the drive components together and also protects the internal components from moisture and containments. The degree of protection and cooling depends on the enclosure type. There are two categories of enclosures, open and totally enclosed. Open enclosures permit cooling air to flow through the motor. In some applications, the air surrounding the motor contains corrosive or harmful elements which can damage the internal enclosure parts of a motor. A totally enclosed non-ventilated enclosure limits the flow of air in this case.

To suit the demands of the prevailing ambient conditions, such as high humidity, aggressive media, splash-water and jet-water, dust accumulation, etc., equipments are available in the corresponding enclosure class according to EN 60529 with Ingress Protection coding (IPXY). Here X is a first classification figure and Y is the second one (Table 1.4).

IP	X – protection against accidental contact	Y – protection against penetration of water
0	No protection	No protection
1	Large surface and solid objects exceeded 50 mm in diameter	Dripping water (vertical falling drops)
2	Fingers and solid objects exceeded 12 mm in diameter	Water drops falling up to 15° from the vertical
3	Tools and solid objects exceeded 1 mm in diameter	Spray water up to 60° from the vertical (rain)
4		Deck water (splash water from all directions)
5	Any object and harmful dust deposits, which can interfere with operation	Jet water from all directions
6	Any contact and any kind of dust	Temporary flooding (deck of a ship)
7		Effects of brief immersion
8		Pressurized water

Table 1.4 IP coding of enclosure classes

**INDEPENDENT MINDED
LIKE YOU**

We believe in equality, sustainability and a modern approach to learning. How about you?
Apply for a Master's Programme in Gothenburg, Sweden.

PS. Scholarships available for Indian students!

www.gu.se/education

Normally, IP54, IP55, or IP56 are recommended. Increased corrosion protection for metal parts and additional impregnation of the winding (protection against ingress of moisture and acids) are possible, as well as delivery of explosion-protected type motors and brake motors in conformity with enclosure class EExe (increased safety), EExed (motor increased safety, brake explosion-proof), and EExd (explosion-proof).

1.2 Operating modes

Cooling methods. Every motor is ultimately rated dependently its thermal loading. At overheating caused by inadequate *cooling* or overloading, the machines *fall out*. Therefore, the motors are supplied with *thermal protection* against *overheating*, *overvoltage protection*, *overload protection*, and time-current protection called *It monitoring*.

From the viewpoint of cooling, all the machines are divided in accordance with the IC (International Cooling) scale MEC 34 as *enclosed motors*, *protected motors*, *natural air cooling motors*, *self-ventilation motors*, and *forced ventilation motors*.

Because of the great variety of the thermal conditions the motor *rated data* are referred to the ambient temperature 40 °C. When the motor is expected to work upon other temperatures, the load is recalculated in respect to the rated one. The conversion factors are usually given in the motor datasheets. For example, to exclude overheating at low speeds the motors of increased power (derated motors) are recommended to apply. For example, Omron requires the derating level of 40...45% for continuous operation at 5 Hz and 25...30% for operation at 10 Hz.

Some vendors design their equipment with the *service factor* indicated in the nameplate of the machine. Service factor is a number that is multiplied by the rated power to determine the power at which the motor can be operated. Therefore, a motor designed to operate at or below its nameplate power rating has a service factor of 1.0. The motors designed for a service factor higher than 1.0 can, at times, exceed their rated power. For example, a service factor of 1.15 permits operation at 15% above the rated power. Of course, any motor operating continuously above its rated power will have a reduced service life.

Heat balance. Let the motor is a homogeneous body. Then, the heat dissipated is defined by electrical losses $\delta_{\tau^o} = P_l - P$ as follows:

$$W_{\tau^o} \approx \delta_{\tau^o} dt$$

The part of this heat is emitted to the environment,

$$W_A = A\tau^o dt$$

where A is the heat emission factor and τ° is an excess of the motor temperature over the ambient temperature. The remaining part of energy heats the motor,

$$W_C = Cd\tau^\circ$$

where C is the heating capacity. The heat balance is as follows:

$$W_{\tau^\circ} = W_A + W_C.$$

Heat dissipation is described by the following first order differential equation:

$$\delta_{\tau^\circ} = A\tau^\circ + C \frac{d\tau^\circ}{dt},$$

represented by an exponential curve of the temperature rise with the thermal time constant $\tau_{\tau^\circ} = \frac{C}{A}$. As the motor heat capacity is proportional to its volume and the motor heat emission factor is proportional to its area, the enclosed low-speed motors of high power are heated and cooled down slowly whereas the small machines do it faster. Thus, the induction wound rotor motors and dc machines have $\tau_{\tau^\circ} = 1\dots270$ minutes and induction squirrel-cage self-ventilated motors have $\tau_{\tau^\circ} = 0.1\dots30$ minutes. For instance, for the motor series 1LA from Siemens at 0.06 kW $\tau_{\tau^\circ} = 11$ s and at 75 kW $\tau_{\tau^\circ} = 50$ s.

The *thermal classification* is provided in accordance with EN 60034. An ability of the motor insulation to handle heat is defined by motor insulation class. The four insulation classes are A, B, F, and H. The classes identify the possible temperature rise from an ambient temperature of 40° C of the surrounding air. Classes B and F are the most commonly used. Starting from an ambient temperature of 40°C, the winding temperature of the Class B motors may increase by a maximum of 120°C.

An ambient temperature, that is the temperature, is an important heat parameter also. It shows the temperature of the motor windings before starting the motor, assuming the motor has been stopped long enough. The temperature rises in the motor windings as soon as the motor is started. The combination of an ambient temperature and a permissible temperature rise equals the maximum rated winding temperature. If the motor is operated at a higher winding temperature, service life will be reduced. An increase of the operating temperature of 10°C above the permissible maximum can halve the motor insulation life expectancy. Every insulation class has a margin allowed to compensate for the motor hot spot, a point at the center of the motor's windings where the temperature is higher.

To find the temperature curve of the working drive, the thermal balance equation needs to be solved. Nevertheless, for the electric drives operated at the above given *alternating loads* with often start-ups and stops, the curve would be very complex. Such approach to the power counting is very laboriousness and its accuracy seems low. Therefore, other methods are used for the motor heating calculation upon the cycling and acyclic loads.

Duty modes. The rated power of a drive is always associated with a specific mode of operation. Operating modes are classified in accordance with EN 60034. They are normally specified for *continuous operation*, *short-term operation*, and *periodic operations*. To this aim, the *load diagrams*, primarily the *torque patterns* and the *power patterns* are used.

The size of the driven motors is generally chosen for continuous operation at a rated output, yet a considerable proportion of motor drives are used for duties other than continuous. As the output upon such deviating conditions may differ from the continuous rating, accurate specification of the duty is an important prerequisite for proper planning. The number of possible duty types is strongly limited. In high-performance applications, such as traction and robotics, the load and speed demands vary with time. While the traction equipment accelerates, the startup torque must be higher (typically twice the nominal torque). As the torque varies with time, so does the motor current (and motor flux linkage level). The electric, magnetic, and thermal loading of the motor and the electric and thermal loading of the power electronic converters have definite constraints in a drive specification. Table 1.5 categorizes *operating duties* into eight major types.

Type	Duty	Description
S1	Continuous running	Operation at constant load of sufficient duration for the thermal equilibrium to be reached.
S2	Short-term	Operation at constant load during a given time, less than required to reach thermal equilibrium, followed by de-energizing of sufficient duration to reestablish machine temperatures.
S3	Intermittent periodic	A sequence of identical duty cycles, each including a time of operation at constant load and a de-energizing time. In this duty type, the cycle is such that the starting current does not significantly affect the temperature rise.
S4	Intermittent periodic at a high startup torque	A sequence of identical duty cycles, each including a significant period of starting, a period of operation at constant load, and a de-energizing time.
S5	Intermittent periodic at a high startup torque and electric braking	A sequence of identical cycles, each consisting of a time of starting, a time of operation at constant load, a time of rapid electric braking, and a de-energizing time.
S6	Continuous periodic	A sequence of identical duty cycles, each consisting of a time of operation at constant load and a time of no-load operation without de-energizing.
S7	Continuous periodic at a high startup torque and electric braking	A sequence of identical duty cycles, each consisting of a time of starting, a time of operation at constant load, and a time of electric braking without de-energizing.
S8	Continuous periodic at related load-speed changes	A sequence of identical duty cycles, each consisting of a time of operation at constant load at a predetermined followed by one or more periods of operation at other constant loads at different speeds without de-energizing.

Table 1.5 Motor drive duty modes

The drive is normally specified for the *continuous S1 operation mode* (Fig. 1.1 (a)), that is, operation at a permanent load power P_L , the duration of which is sufficient to reach the thermal steady state condition, that is $t_L > (3...4)\tau_{\tau^0}$. Here, the *thermal time constant* $\tau_{\tau^0} = \frac{C}{A}$ is the ratio of the motor heat capacity C to its heat emission A at the temperature τ^0 . This is the conventional mode for fans, pumps, compressors, conveyers, spinning machines, textile equipment, and papermaking machines.

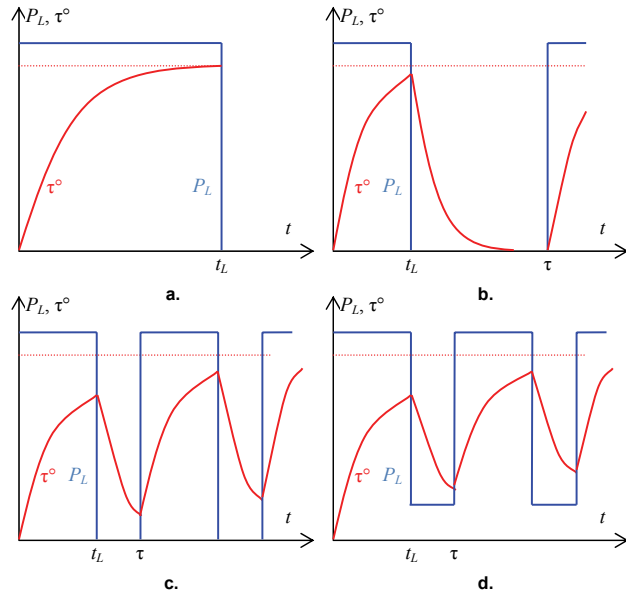


Fig. 1.1 Operating modes of electric drive



Linköping University –
innovative, highly ranked,
European

Interested in Engineering and its various branches? Kick-start your career with an English-taught master's degree.

→ [Click here!](#)



The S2 mode is a *short-term operation*, i.e. operation with a constant load state for a specific limited time t_L followed by a pause until the motor reaches the ambient temperature once again (Fig. 1.1 (b)). Here, the *service time* or *load cycle* $t_L \leq (3\dots4)\tau_{\tau^{\circ}}$ and the pause $t_0 > (3\dots4)\tau_{\tau^{\circ}}$ accomplish the full *cycle duration* τ . In this mode some crane mechanisms and the *rapid traverse drives* of the machine-tools operate.

The S3 mode is a *periodic operation* without impact of the start-up procedure on the motor warning-up. This mode is presented by a sequence of similar cycles (Fig. 1.1 (c)), each comprising a cycle duration τ with a constant load t_L and a pause t_0 in which the motor is at standstill. The motor temperature during the service time $t_L < (3\dots4)\tau_{\tau^{\circ}}$ does not reach the steady-state level whereas in a pause $t_0 < (3\dots4)\tau_{\tau^{\circ}}$ the machine has no time to cool down. This mode is characterized by a *cyclic duration factor*

$$cdf = \frac{t_L}{t_L + t_0} = \frac{t_L}{\tau}$$

Thus, the *cdf* represents the ratio of the service time duration t_L to the full cycle duration. Maximum cyclic duration of periodical motor drives is 10 minutes.

Often the cyclic duration factor is expressed by percent and is applied as 15%, 25%, 40% or 60%. For example, the cyclic duration 60% per minute corresponds to the motor operation 60 seconds with the following 40-second standstill. This mode is used in hoists, robots, drill machines, woodworking and grinding machines, some saws, fans, and conveyers.

An *intermittent duty* S6 (Fig. 1.1 (d)) is typical for many machine-tool drives. This periodic operation where the start-up procedure influences the warning-up is characterized by a cyclic duration factor and, in the case of induction motor, the *number of stops and starts* per hour. Every cycle consists of the loading work and the idle. The period continuation here is enough short thus the machine temperature does not reach the steady-state value.

The drive duty cycle also affects the *reliability* and the *service life* expectancy of power devices. Repetitive load cyclic duty results in additional thermal stresses on power devices. Frequent drive acceleration and deceleration result in repetitive junction temperature rise and falls at the cyclic duty. The life expectancy of devices is often determined by the maximum allowed number of cycles for a given power device junction temperature rise.

1.3 Motor dimensioning

Safety factor. *Specification* of the driving motor should meet the requirements of the driven machine in all the working modes, primarily in torque and power. Motor overloading causes fast isolation wear and mechanical damage. At the same time, unwarranted derating results in the *frame size* and cost increasing as well as the power loss deterioration. Therefore, it is required to bring the motor usage to the load characteristics as close as possible, with justified reserve.

In machine-tool constructions and robotics, the *safety factor* is accepted as 1.2...1.4 whereas in metallurgy, for instance, it reaches 1.8...2.2. In hoist mechanisms the motor dimension derates in units. Mass relation, backlashes, gaps, and transient requirements play an important role. The *service factors* (ratios of derated and rated powers, torques, currents, etc) are not normalized therefore the motor manufacturers set them basing on different criteria.

Long-term duty. Dimensioning procedure for the long-term duty upon the *steady load* includes the choice of the nearest machine, which specification meets the *full load* $P_M \geq kP_L$ and $T_M \geq kT_L$ where P_M and T_M are the rated motor power and torque.

The problem of the motor selection in the case of alternating loads is more sophisticated. Many machines have the cyclic operation mode in which the working cycle often fits either the single operation or the separate operation or technological step. The loading diagram of each cycle usually has the sections of constant power or torque of the definite duration. The curved diagram is often subjected to approximation by the stepped line. After that, both the *rated capacity* and the required motor torque are counted using one of the four following methods: the average loss method, the equivalent (rms) current method, the equivalent (rms) torque method, or the equivalent (rms) power method.

Average losses. As the permissible temperature of the motor is restricted

$$\tau^\circ = \frac{\delta_M}{A}$$

at $\delta_M \approx P_M \left(\frac{1}{\eta_M} - 1 \right)$ where η_M is the motor rated efficiency and A is the heat emission, the method of average losses seems to be rational. The following conditions must be satisfied at this method:

$$\tau^\circ < \tau^\circ_M, \quad \delta_{\tau^\circ} < \delta_M.$$

The method of average losses is based on the timing diagram of motor losses. The motor winding temperature is assumed to be less than the permissible one while the cycle average losses do not overcome the rated drive losses, that is

$$\delta_{\tau^\circ} = \frac{\sum_k \delta_k t_k}{\tau} = \frac{\delta_1 t_1 + \delta_2 t_2 + \dots + \delta_n t_n}{\tau},$$

where $k = 1, 2, \dots, n$ – cycle section number, δ_k – motor losses in the k -th section, t_k – k -th section duration, $\tau = \sum_k t_k$ – cycle duration. At the end of each section, the temperature $\tau^\circ = \frac{\delta_{\tau^\circ}}{A}$ is reached.

Nevertheless, an application of this method seems problematic due to the need in calculation of losses at the particular loading using the detailed motor datasheets. Therefore in practice the method of average losses is used only to validate the preliminary chosen machines being counted, for example, using the average static load with some empirical safety factor,

$$P_M > \sqrt{\frac{1}{\tau} \int P_L^2(t) dt}, T_M > \sqrt{\frac{1}{\tau} \int T_L^2(t) dt}$$

or, shortly,

$$P_M > \frac{\sum_k P_{Lk} t_k}{\tau}, T_M > \frac{\sum_k T_{Lk} t_k}{\tau}.$$

Such approach is suitable as the computer “fitting” of different motors to the given load.

Equivalent current. In practice, the method of equivalent (rms) current is more accessible. Here, the losses are considered as approximately proportional to the current square:

$$\delta_{\tau^0} \approx I^2 R,$$

$$I = \sqrt{\frac{\sum_k I_k^2 t_k}{\tau}} = \sqrt{\frac{I_1^2 t_1 + I_2^2 t_2 + \dots + I_n^2 t_n}{\tau}}$$

**STUDY FOR YOUR MASTER'S DEGREE
IN THE CRADLE OF SWEDISH ENGINEERING**

Chalmers University of Technology conducts research and education in engineering and natural sciences, architecture, technology-related mathematical sciences and nautical sciences. Behind all that Chalmers accomplishes, the aim persists for contributing to a sustainable future – both nationally and globally.

Visit us on **Chalmers.se** or **Next Stop Chalmers** on facebook.

CHALMERS
UNIVERSITY OF TECHNOLOGY

where I and R are the motor current and resistance. It should be mentioned that, due to the pauses in the working cycle, average losses calculated for the equivalent long-term mode should overcome the actual steady-state losses. In other words, the error of this method is proportional to the pause duration. To count the running (t_d), braking (t_q), and pausing (t_0) sections, the cooling deterioration factor k_c may be used as follows:

$$\tau = k_c(t_d + t_q + t_0) + t_s,$$

where t_s – duration of the steady-speed operation. Usually, it is assumed $k_c = 0.75$ for the dc motors and $k_c = 0.5$ for the induction machines.

Additional motor heating is caused by the semiconductor power converters which are the sources of the pulsing current. Such heating is counted by the pulsing factor

$$k_p = \frac{I_{\max} - I_{\min}}{I_{\max} + I_{\min}},$$

where I_{\max}, I_{\min} – pulsing current extremes. At $k_p = 0.15$ the motor heat increases by 2...3%, at $k_p = 0.25$ – by 5...7%, and at $k_p = 0.35$ – by 15...22%. Therefore, manufacturers recommend the F class isolated motors for the semiconductor-fed drives.

To use the method of equivalent current, the rated current limit is to be set as $I_M \geq I$. This limit is suitable to validate the power and torque of the preliminary selected motor.

Transients and resulted dynamic loading normally increase the required motor power. The intermittent duties cause additional problems in motor dimensioning. Particularly, to work upon the alternating load in press industry the *flywheels* are applied. The principle of the flywheel drive is based on the idea that the *peak (shock) load* affects only the useful work whereas in the loose running it is insignificant. Thanks to the flywheel, an excess energy of inertia mass is accumulated in idling, which then is consumed in the working part of the cycle. In this way, accumulated energy of the moment of inertia J applied at the speed change from ω_{\max} to ω_{\min} ,

$$W = \frac{J(\omega_{\max}^2 - \omega_{\min}^2)}{2}$$

saves the required motor power within the work cycle τ . Assume energy supplied the load from the mechanism and energy returned from the mechanism to the load within the work cycle is $W = P_L \tau$. Assume also an average cycle speed is $\omega = \frac{\omega_{\max} - \omega_{\min}}{2}$ and an irregularity factor is $\delta_{\omega} = \frac{\omega_{\max} - \omega_{\min}}{\omega}$. Now, the required moment of inertia of an electric drive is defined as $J = \frac{W}{\omega^2 \delta_{\omega}}$, and moment of inertia of the flywheel is $J_{\max} = J_{\Sigma} - J_M - J_L$. Acceleration is limited by the flywheels, though, in some cases, the flywheels increase energy acquisition in running and braking modes.

Equivalent torque. The method of equivalent torque may be used instead of the method of equivalent current if assume the proportionality of the torque and current. Then,

$$T = \sqrt{\frac{\sum_k T_k^2 t_k}{\tau}} = \sqrt{\frac{T_1^2 t_1 + T_2^2 t_2 + \dots + T_n^2 t_n}{\tau}}.$$

This approach has more error than the method of equivalent current has because the assumed proportionality cannot be satisfied in many aspects.

Equivalent power. The method of equivalent power has even more error as it is based on the proportionality of the torque and the power ($P \approx T\omega$). Equivalent power is as follows:

$$P = \sqrt{\frac{\sum_k P_k^2 t_k}{\tau}} = \sqrt{\frac{P_1^2 t_1 + P_2^2 t_2 + \dots + P_n^2 t_n}{\tau}}.$$

At the same time, the main advantage of this method concerns the suitability of the loading diagram applying. Nevertheless, while the motor speed alternates within the broad range, this approach cannot be used.

Applying of both the methods of equivalent torque and equivalent power is suitable for the motor choice basing on the rated value restrictions, such as

$$T_M \geq T, P_M \geq P.$$

Periodic duty. The specialised periodic duty motors are featured by the rated cyclic duration factors cdf_M for the 10-minute cycle τ . While the load cyclic duration cdf is equal to one of the standard cdf_n values, the motor is selected from the datasheet as $P_M \geq P_L, cdf_M = cdf$.

At the most, the given condition is not fulfilled. In this case, the equivalent work time is derived $t_s = \sum_k t_{sk}$ as well as the equivalent pause time $t_0 = \sum_k t_{0k}$, actual cyclic duration factor $cdf = \frac{t_s}{t_s + t_0} = \frac{t_s}{\tau}$, equivalent torque T , and equivalent power P . Then, the motor is selected which meets the conditions

$$T_M \geq T \sqrt{\frac{cdf}{cdf_M}}, P_M \geq P \sqrt{\frac{cdf}{cdf_M}}.$$

If the required periodic duty motors are absent, the S1 motor is to be selected which rated power is to be increased by the derating factor k . For instance, Sew Eurodrive proposes the following derating factors for S3: $cdf = 15\%$ corresponds $k = 1.1$; $cdf = 40\%$ corresponds $k = 1.15$; $cdf = 25\%$ corresponds $k = 1.3$; and $cdf = 15\%$ corresponds $k = 1.4$. When the speed varies in the range 5...10, this company recommends the long-term motor application. For the larger ranges, the motor of the nearest small dimension with forcing cooling is selected.

Short-term duty. For the short-term mode, the standard cycle durations τ are 30, 60 and 90 minutes. The specific short-term motors are very rare manufactured therefore the S1 motor is selected the rated power of which must be increased by the derating factor. For instance, Sew Eurodrive proposes the following factors for S2: $\tau = 60$ minutes – 1.1; $\tau = 30$ minutes – 1.2; and $\tau = 10$ minutes – 1.4.

Also, for the short-term mode the S1 motor power may be defined using the ratio of short-term losses δ_{S2} to long-term losses δ_{S1} called an *overheating factor*:

$$\lambda_{\tau^\circ} = \frac{\delta_{S2}}{\delta_{S1}}.$$

To be fully used in the short-term mode, the motor should be loaded in the way that the isolation temperature does not exceed the permissible limit to the end of the work cycle.

If the use of the common-mode long-term motors in this situation seems unsuitable, the periodic duty motors come to practice, counting $cdf_M = 15\%$ for $\tau \leq 30$ minutes, $cdf_M = 25\%$ for $\tau \leq 60$ minutes, and $cdf_M = 40\%$ for $\tau \leq 90$ minutes.

Starting frequency. Very common ac drive systems are found which have a high starting frequency and a small counter-torque, for example a travel drive. In this case the power demand is in no way decisive for the motor selection, but rather the number of starts. The high starting current flows each time the motor is switched on and heats up the motor over-proportionally. If the heat absorbed is greater than the heat dissipated by the motor ventilation system, the windings will heat up to an inadmissible level. The thermal load capacity of the motor can be increased by a suitable choice of the thermal classification or by forced cooling.

By some manufacturers, the permissible starting frequency of an ac motor is given as so-called *no-load starting frequency* at $cdf_M = 50\%$ (cdf_{50}). This value expresses how often the motor can accelerate the moment of inertia of its rotor without a counter-torque at cdf_{50} per hour to the maximum motor speed. If an additional moment of inertia has to be accelerated or if the loading occurs, the run-up time of the motor increases. Since current flows during this run-up time, the motor is more severely thermally loaded and the permissible starting frequency drops.

Often, the mechanism work cycle does not reach 10 minutes though the required starting frequency is high. In this case, an impact of the start-up and braking losses becomes the determinative factor of the motor choice for operation in S4 and S5 periodic duties. Hence, for an induction motor selection the hour *permissible starting frequency* is additionally calculated to heat the motor without over-temperature

$$f_{\tau^\circ} = 3600\delta_n \frac{k(1 - cdf) + cdf \left(1 - \frac{\delta_{\tau^\circ}}{\delta_M}\right)}{W_d + W_q - (t_d + t_q) \left(\frac{1+k}{2} \delta_M + \delta_s - \delta_M\right)} \approx 3600\delta_M \frac{k(1 - cdf)}{W_d + W_q}$$

Here $cdf = \frac{t_d + t_s + t_q}{t_d + t_s + t_q + t_0}$, $k = 0.25...0.35$ for protected motors and $0.45...0.55$ for close induction machines, W_d – dissipated energy of loading motor at running, W_q – dissipated energy of counter-current braking.

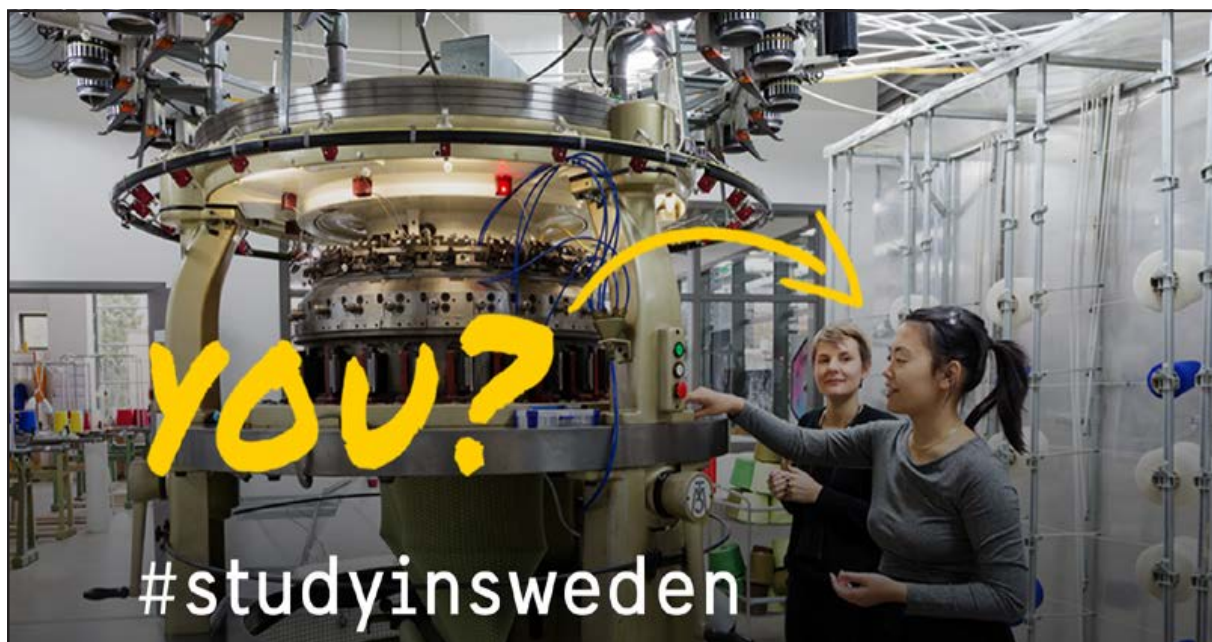
The idling small machines permit 500...1500 switching per hour. As the power increases 50 kW, this value drops to 15...150. Here, the bigger values refer to the slow motors of less power. Moreover, the protected motors have higher permissible starting frequency than the enclosed machines. Often this value is inscribed into the standard line 30, 60, 120 or 240.

Sometimes a manufacturer defines the permissible starting frequency for the no-load mode upon cdf_{50} . To calculate the permissible starting frequency, he indicates the correction factors in the datasheets, which depend on inertia (k_1), load (k_2), and actual $cdf(k_3)$:

$$cdf = k_1 k_2 k_3 cdf_{50}.$$

1.4 Design stages

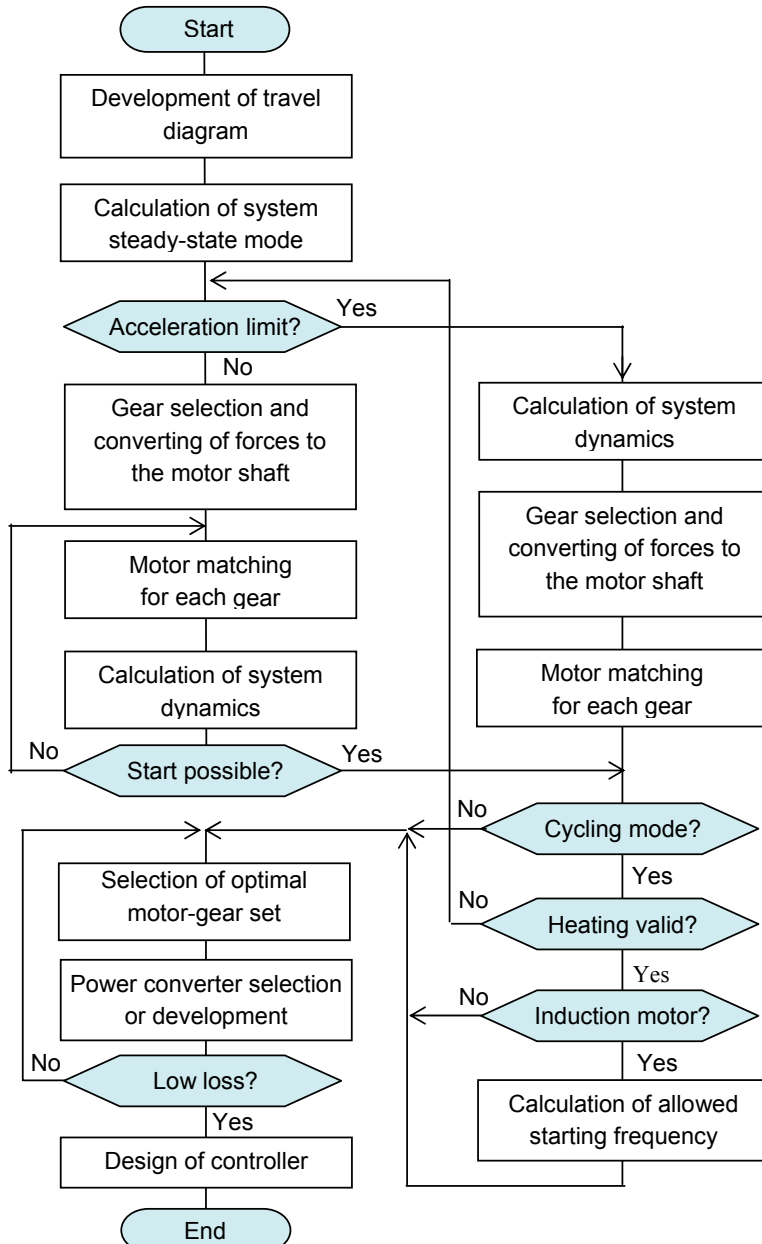
Design algorithm. The design algorithm is presented in Fig. 1.2. The overall design process includes some stages. First, initial selection of motors and gears is carried out. Then, the planned equipment is tested and more specific information is obtained if necessary. After that, the final selection is executed from multiple variants. Next steps are devoted to the choice of power converter, design the control system, and its tuning



Striking a match, reconnecting with your family through Skype or over a phone network from Ericsson, refurbishing your apartment at IKEA or driving safely in your Volvo - none of this would be possible if not for Sweden. Swedish universities offer over 900 international master's programmes taught entirely in English.

Don't just pick a place - pick a future.
[>studyinsweden.se](http://studyinsweden.se)



**Fig. 1.2** Flowchart of an electric drive design algorithm

Some particular cases of the described technology deal with the problem of equipment modernization when the gearboxes or the motors are specified beforehand. Often, mechanical units are designed together with electric drives thus the dimensioning starts as the first stage of design.

In any case, three groups of databases are available, namely A_M , A_G , and A_C . The first group includes motors, which differ in powers P_M and speeds ω_M . Each motor has the rated and maximum shaft torques, moment of inertia, mass, efficiency, and electrical parameters. The group A_G includes mechanical transmissions that differ in their power P_G and gear ratio i . Each gear has rated and maximum torques, input and output speeds, moment of inertia, dimension, and efficiency. The group A_C involves power converters.

Gear selection. On the first stage of dimensioning, the set A_G is restricted by the required load power, torque, moment of inertia, and speed, $A_{G1} \subset A_G$. These requirements are defined by the travel diagrams and necessary safety factors as well as by operational features, weight, and other indexes. To calculate the forces, the mechanism load diagrams are used.

When the load is constant and works continuously, to calculate the power the kinematical diagrams and equipment technical data are used. When the load changes, *effective* (rms) values of parameters are calculated taking into account the alternating modes. When the machine works shortly or periodically, the appropriate calculation methods are applied.

To keep up the constant torque, the gear rated power and rated torque should meet the maximum load power. At that, a gear requires the necessary overload capacity to operate normally on the maximum speed. Some mechanisms maintain two speed ranges: low constant torque range and high constant power range. In this case, the gear is selected in accordance with these ranges.

Anyway, the gear has to be selected with a safety factor, which depends on the load type. The machines of the first type have a safety factor of 1. Among these are fans, compressors, pumps, conveyers, and carriers which velocities change slightly during operation as well as the units with inertia ratio $\gamma_J = \frac{J_M + J_L}{J_M}$ less than 1.2. The second group has the safety factor of 1.25 and includes such mechanisms as elevators, balanced machines and hoists with some speed range requirements as well as the units with inertia ratio below 3. The third group has the safety factor of 1.5, and covers mixers, crushers, roll-tables, lathers, and robots, operated in the broad speed ranges.

**TAKE THE
RIGHT TRACK**

**Click here
to learn more**

**Give your career a head start
by studying with us. Experience the advantages
of our collaboration with major companies like
ABB, Volvo and Ericsson!**

**Apply by
15 January**

**World class
research**

www.mdh.se

**MÄLARDALEN UNIVERSITY
SWEDEN**

The mechanisms differ not only in their load character but in the calculation methods. Thus, the hoist drives usually have no typical service cycle. Their mode of operation depends on a number of factors and the load changes in the broad restraints. Elevator mechanisms have very strong requirements on the smooth adjustment and weak damping. The tunnel boring machines and the excavators have long kinematical transmissions, which may oscillate and jam. Different lathes require high accuracy and quick action. The specific peculiarity of plotters, mills, mixers, centrifuges, and ship rigging deals with the high starting torque and broad temperature range as well as operation in high humidity and current-conducting dust. The counter-torque of pumps and fans depends on the speed. Conveyors and mills have the transitional distributed loads whereas the robots operate under the alternating moment of inertia. For the machines that operate with heavy starting and braking modes, the gear manufacturers state high utility factors, up to 1.8 or 2. All these features have to be taken into account in the dimensioning, placing, assembling, and connection processes.

Motor selection. Following the permissible gear limiting, the motor capacity restrictions are imposed. The rated motor torque, power, and speed should exceed the respective load values. Motor moment of inertia commonly comes to 1...100% of the load inertia. For all that, the low-dynamic units accept the smaller values and the high-dynamic machines – the greatest quantities. Every gear associates with all possible motors that power and torque meet the load requirements as well as the speed meets the transmission requirements.

First, the presence of the geared motors is examined. The low inertia motors are preferable for apparatus, printers, small robots and other fast-speed units. Remaining groups of machines require the common-mode motors. Accurate mechanisms use servomotors whereas the induction machines are used in low-precision open loop systems. To build powerful industrial machinery, the large-scale induction and synchronous motors employ. In the particular cases, special motors are introduced.

Next, the quality of transients and steady-state processes of each motor-gear pair is examined. To that end, the system analytical optimization or the computer dynamic simulation may be used to derive full information concerning the quality of the designed system. The library of the drive models serves as the major part of the optimization methods.

Then, obtained estimation is used to sort the selected motor-gear pairs on descending of the quick-action, power, cost, etc. Thereafter, each selected motor is tested on the equivalent thermal load and starting possibilities using the drive *duty diagrams* including their torque and power patterns. The duty diagram differs from the load diagram by the start-up and braking areas that correspond to the possible system accelerations and decelerations. Particularly, the drive dynamic torque is calculated by these diagrams as:

$$T_d = \frac{J\ddot{\omega}}{t_d}$$

where t_d is the time needed to accelerate (or decelerate) the inertia J to the speed ω .

The thermal mode is satisfactory if the motor rated torque and rated power exceed the effective quantities, which have been calculated on the base of duty diagrams. To check the start-up conditions, the full load and maximum sticking friction is to be taken into account. If some conditions are failed, it is the reason to exclude the motor from the list of candidates.

Selection of power converter. Further, selection of a power converter begins. Most manufacturers have their own methods for the converter choice dependently on the required adjustment mode (speed, torque, path, etc.), speed range, and accuracy.

During the final optimal motor-gear-converter set selection process, a designer takes into account the start-up time, braking, steady-state motion and additional estimations, properties, and features of the desired system. As well, he pays need to reliability, brand name, *service life* as well as maintainability, guaranty, and so on.

As a rule, this procedure is automated to a great extend by the existing computer aided design systems. Computers serve both for calculations and for the component selection and section agreement, sorting, and search the optimal variants. The last problem belongs to the non-linear programming area and its solution depends in many ways on the used algorithms and software.

Further, the general design stages are discussed in conformity with the above presented algorithm.

2 Load Calculations

2.1 Moments of inertia

Elementary moments of inertia. According to the main equation of the electric drive motion,

$$T = T_L + J \frac{d\omega}{dt} = T_L + Js\omega$$

where $s = \frac{d}{dt}$, the dynamic torque $T_d = Js\omega$ (also the dynamic force $F_d = ms\omega$) defines the rate of the change in kinetic energy, that is the system speed of response. Moment of inertia of the load on the motor shaft is associated with the load mass: $J_L = mr_L^2$, where r_L is the radius of inertia.

Particularly, moment of inertia of a *solid cylinder* of the radius r , the length l , and the density ρ (Fig. 2.1 (a)) is equal to

$$J_L = \frac{mr^2}{2} = \frac{\rho\pi r^4 l}{2}$$



ADVANCE YOUR CAREER IN UMEA!

- modern campus • world class research • 32 000 students
- top class teachers • ranked nr 1 in Sweden by international students

Master's programmes:

- Architecture • Industrial Design • Science • Engineering



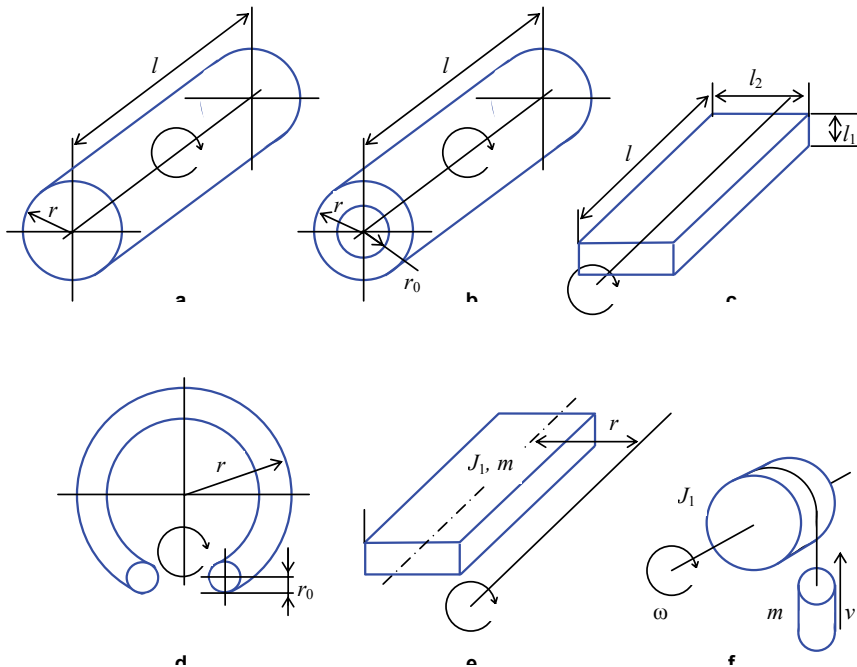
UMEÅ
UNIVERSITY

FACULTY OF SCIENCE & TECHNOLOGY

Download brochure here!



Click on the ad to read more

**Fig. 2.1** Simple geometrical figures

Density values ρ of steel, aluminum, and copper are 7.8, 2.5 and 9.0 10^3 kg/m^3 respectively. Here, an inertia radius is $\sqrt{2}$ times less than a cylinder radius. This equation is used particularly to calculate the moments of inertia of the shafts and the actuating screws.

Moment of inertia of a *hollow cylinder* of an inner radius r_0 (Fig. 2.1 (b)) is equal to

$$J_L = \frac{m(r^2 + r_0^2)}{2} = \frac{\pi\rho l}{2}(r^4 - r_0^4).$$

In the case of $r_0 \rightarrow r$, moment of inertia is $J_L \rightarrow mr^2$. This equation is used particularly to calculate the moments of inertia of the gear-wheels, pulleys, and drums.

Moment of inertia of a *parallelepiped* (Fig. 2.1 (c)) is equal to

$$J_L = \frac{m(l_1^2 + l_2^2)}{12} = \rho l l_1 l_2 \frac{l_1^2 + l_2^2}{12}.$$

Moment of inertia of a *ring* of a radius r and a thickness $2r_0$ (Fig. 2.1 (d)) is equal to

$$J_L = \frac{m(4r^2 + 3r_0^2)}{4} = \rho\pi^2 r r_0^2 \frac{4r^2 + 3rr_0^2}{2}.$$

Moment inertia of a body in respect to the shifted axis (Shtaner's law) (Fig. 2.1 (e)) is equal to

$$J_L = J_1 + mr^2$$

where J_1 is moment of inertia of the body of the mass m in respect to the axis, which passes through the centre of gravity and r is the distance between the axes. The same formula is typically used to calculate moment of inertia of a translational movement mass m (Fig. 2.1 (f)), but here J_1 is moment of inertia of the rotational body. Taking into account the ratio between the linear and angular speeds,

$$v = \omega r$$

the equation may be rewritten as follows:

$$J_L = J_1 + \frac{mv^2}{\omega^2}.$$

The overall moment of inertia of the motor rotor with the loading shaft is calculated as the sum

$$J = J_M + J_L.$$

Experimental determination of moments of inertia. To find the moment of inertia of a machine, an experimental method may be used based on the equation of the free run $-T_L = J\omega$. For this purpose, a mechanism runs with some speed ω_L which power P_L is measured and the torque is calculated as follows:

$$T_L = \frac{P_L}{\omega_L}.$$

Then, the motor is unplugged and the trace of the freewheel stop $-\omega(t)$ is acquired. The tangent of this speed trace at $t = 0$ determines the derivative $s\omega = \frac{\Delta\omega_L}{\Delta t}$. The same process is repeated at 2 to 5 other speeds ω_L . Finally, moment of inertia is calculated as an average value of the defined moments of inertia,

$$J = \frac{T_L}{s\omega}.$$

In such a way, the dynamic component of the driven load is determined by the geometric characteristics of the decelerated or accelerated machine, its density, and required acceleration. The more is this component, the more powerful should be an electric drive. Usually, the high precision machine-tools, robots, servo- and positioning systems have the highest dynamic requirements in distinct from the pumps, fans, and auxiliary drives.

2.2 Load calculation formulae

To calculate the *driven load*, the specific mechanism features should be taken into account. In most kinds of machines, the static components of the driving force develop the work counter-forces F_{LW} , counter-torques T_{LW} , and powers P_{LW} on the one hand and overcome the transmission and motor friction, F_μ , T_μ , P_μ , on the other hand,

$$\begin{aligned} F_L &= F_{LW} + F_\mu, \\ T_L &= T_{LW} + T_\mu, \\ P_L &= P_{LW} + P_\mu. \end{aligned}$$

Metal-cutting equipment. The cutting strength of the metal-cutting equipment depends on the cutting depth h , the cutting tool edge width l , and the tool geometrical properties. By applying the safety factor k_s to take into consideration the material features, the next formulae may be used to describe the cutting strength and torque:

$$F_{LW} = k_s h l$$

$$T_{LW} = F_{LW} r_L$$

The radius of applied force r_L is the property of the grinding wheel, the milling cutter, or the leading gear size. If some non-right angle φ_L occurs between the cutting strength and the rotation axis, the torque formula will change as follows:

$$T_{LW} = F_{LW} r_L \sin \varphi_L$$

The feed velocity v defines the cutting power as follows:

$$P_{LW} = F_{LW} v$$

Hoists and robots. Concerning the hoists, the main problem is to exceed the gravity force. The similar goal is typical for some drives of the drilling, milling, and grinding machines. Rising and lowering strengths of the mass m are calculated through the gravity acceleration g ,

$$F_{LW} = mg$$



We ask you
**WHERE DO YOU
 WANT TO BE?**

TOMTOM 

TomTom is a place for people who see solutions when faced with problems, who have the energy to drive our technology, innovation, growth along with goal achievement. We make it easy for people to make smarter decisions to keep moving towards their goals. If you share our passion - this could be the place for you.

Founded in 1991 and headquartered in Amsterdam, we have 3,600 employees worldwide and sell our products in over 35 countries.

For further information, please visit tomtom.jobs



Click on the ad to read more

The radius of the applied force and the transport velocity define the static torque and power of the drive. When the counter-mass m_L appears,

$$F_{LW} = (m - m_L)g$$

To design an electric drive of the rotational mechanisms, the torque caused by the unbalanced gravity forces of the moved weights and constructional elements is to be taken into consideration:

$$T_{LW} = mgr_L$$

where r_L is the distance between the rotational axis and the centre of gravity. In robots, the static torque often depends on the rotational angle φ_L of the mechanism. It varies while the robot moves the load and this relation may be differently non-linear. Therefore, graphics and sheets are used to produce calculation in these cases.

Conveyers. Conveyer systems have the distributed load of the carried materials and the conveyer tape, thus their strength,

$$F_{LW} = mg\mu,$$

depends on the specific resistance μ of the supporting. The overall torque is defined by the forces of the tape and the static resistance of other elements. It is determined through the tension difference of the oncoming (F_{LWon}) and outgoing (F_{LWout}) brunches of the tape:

$$T_L = (F_{LWon} - F_{LWout})r_L$$

Here, r_L is the radius of the leading drum. To calculate the conveyer power, the angular speed of the drum ω_L is used:

$$P_{LW} = T_{LW}\omega_L$$

Often, the conveyer power is connected with the volume capacitance q as follows:

$$P_{LW} = qgp(\mu l \pm h)$$

where $\mu = 3$ to 30 , l is the length of the horizontal projection of the path, h is the height of the material lifting or lowering, and ρ is the material density.

In the cases discussed above, the work torque is practically independent on the speed thus it is considered as a constant value.

Compressors, fans and pumps. The compressor power is a function of the productivity q and may be calculated as follows:

$$P_{LW} = \frac{q(W_i + W_a)}{2V}$$

Here, W_i and W_a are the works of an isothermal and adiabatic compressions and V is the working body volume. The working torque of the compressors, the loading generators, and the same mechanisms alternates.

The fan power is calculated through the gas pressure F_{LW} on the area Q as follows:

$$P_{LW} = q \frac{dF_{LW}}{dQ} .$$

The pump power depends on the productivity as well,

$$P_{LW} = k_s h \rho q g$$

where $k_s = 1.1$ to 1.3 , h is the pressure height, and ρ is the liquid density. The power diagrams of the fans, centrifugal pumps, and conveyors have the cubical dependence on the velocity, and their static torque has a squared relation.

2.3 Friction forces

Definition. Friction is the resistance for the relational motion of the contacted bodies in their contact points. Dependently on the motion mode, the slipping friction and the rolling friction are distinguished. *Slipping friction* of the pressed surfaces is caused by the micro unevenness because of which the contact area occupies a very small part of the full square (from 0.001 to 1%). Thus, even at the very low loading there is a great specific pressure in the contiguities. Slipping friction depends on the contact area conditions and on the lubricants. In vacuum, *frictionless* is possible without any pellicles and chemical combinations. *Coulomb's friction* occurs in air without lubricants and pollutions causing jerking and *cogging* at the low-speed motion. *Border friction* takes place in the case of the thin pellicles, often of oil. *Oil friction* occurs when the solid layer of a lubricant divides hard surfaces. *Semi-oil friction* is a composition of oil and border friction.

Friction force. The vector of the slipping friction strength has an opposite direction to the vector of the relational motion velocity in the tangent plane of the rubbed surfaces. The maximum *retarding force* of the relational motion of the rubbed bodies, which arises at the motion starting instant is known as *sticking friction* or *friction of rest*, $F_{\mu s}$. It always exceeds motion friction F_μ .

According to the *Amonton-Coulomb's law*, the simple model of the Coulomb's friction (Fig. 2.2 (a)) is described by the following equations

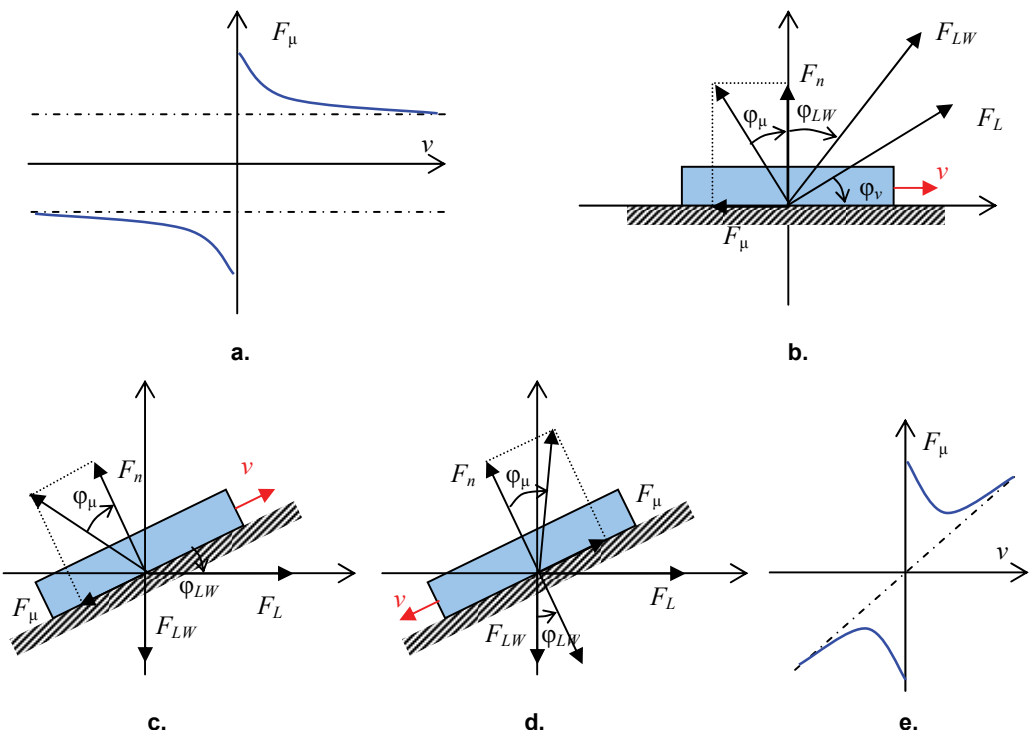
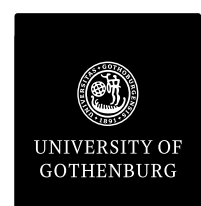


Fig. 2.2 Friction forces

INNOVATIVE LIKE YOU.

If you're hoping for a truly modern education, one where you're encouraged to speak your mind and to think long-term, both when it comes to your own future and the future of the planet. Then the University of Gothenburg is the place for you.

Study a Master's programme in Gothenburg, Sweden | www.gu.se/education



$$F_{\mu} = \begin{cases} F_{LW}\mu \operatorname{sgn} v & (v \neq 0) \\ F_n\mu_s \operatorname{sgn} F & (v = 0) \end{cases}$$

Here, F_{LW} and F_n are the motoring and the normal pressure forces, v is the motion velocity, and μ , μ_s are the motion and sticking friction factors. In accordance with this model, the Coulomb's friction does not depend on the velocity value.

The slipping friction factor depends on the friction angle φ_{μ} between the F_n and F_{μ} vectors,

$$\tan \varphi_{\mu} = \frac{F_{\mu}}{F_n} = \mu, \quad \varphi_{\mu} = \arctan \mu.$$

Particularly, when some bodies move along the horizontal flatness (Fig. 2.2 (b)), an electric drive has to overcome the force

$$F_L = F_{LW} \frac{\sin(\varphi_{LW} - \varphi_{\mu})}{\cos(\varphi_v - \varphi_{\mu})}$$

Here, F_{LW} is the work force; φ_{LW} is the angle between F_{LW} and F_n , whereas φ_v is the angle between the vectors of the velocity and the motoring force. On the inclined plane, the horizontally directed motoring force of the upward moving mass (Fig. 2.2 (c)) is equal to:

$$F_L = F_{LW} \tan(\varphi_{LW} + \varphi_{\mu}).$$

When the motoring force is directed in parallel with the slipping plane,

$$F_L = F_{LW} \frac{\sin(\varphi_{LW} + \varphi_{\mu})}{\cos \varphi_{\mu}}.$$

When the mass pulls down (Fig. 2.2 (d)),

$$F_L = mg(\cos \varphi_L \cdot \tan \varphi_{\mu} - \sin \varphi_L)$$

If the relational motion of the bodies upon the friction and gravity is impossible, a kinematical pair brakes itself.

In Table 2.1, the friction factors of some mechanisms and materials are presented. Here, μ_r is a *rolling friction factor* or a rolling shoulder, which has the dimension of length.

Slipping guides	μ	Rolling guides	μ	μ_r mm
Bronze vs bronze	0.06	Gearboxes	0.005	0.1
Steel vs steel	0.09	Crane running wheels	0.008	0.2
Steel vs bronze	0.08	Rolling machines	0.010	0.3
Cast iron vs bronze	0.15	Tires	0.750	5.0
Fluoroc plastics vs steel	0.04			

Table 2.1 Slipping and rolling friction factors

The oil friction curves plotted in Fig. 2.2 (e) are described by the following model:

$$F_{\mu} = \frac{Qv\beta_L \operatorname{sgn} v}{h}.$$

Here, Q is the slipping area, h is the thickness of the liquid layer, β_L is the inner friction factor. As the oil friction factor depends on the velocity, it significantly differs from the Coulomb's friction.

Friction torque. The slipping friction torque depends on the radius r of the applied friction force as follows:

$$T_{\mu} = F_{\mu}r ..$$

In the rotational pairs two kinds of torques are developed. The torque caused the radial slipping force, which stresses the support *bearings*, is equal to:

$$T_{\mu} = \frac{4}{3}F_{\mu}\mu r$$

The torque from the axle loading force is equal to:

$$T_i = \frac{2}{3}F_i i r.$$

Particularly, the screw pairs have the friction torque

$$T_{\mu} = F_{LW}r \tan(\varphi_L + \varphi_{\mu}).$$

Here, F_L is the axis retarding force, r is the average thread radius, φ_L is the angle of the thread slope, $\varphi_{\mu} = \arctan \frac{\mu}{\cos 2\varphi_v}$ is the friction angle, φ_v is the thread profile angle.

The static torque of the axle journal rotation in the *sleeve bearing* is as follows:

$$T_{\mu} = F_{LW}r_L\mu,$$

where F_{LW} is the strength of journal pressing and r_L is the journal radius.

Rolling friction. When a body rotates, the motoring force overcomes both the slipping friction and the *rolling friction* simultaneously. The latter causes the deformation of the contacted surfaces and the oscillation due to the crumpling of the rotational surfaces,

$$F_{\mu} = \frac{\mu_r F_n}{r}.$$

Here F_n is the strength of the normal pressure and μ_r is a rolling friction factor. The torque of the rolling friction force is calculated as follows:

$$T_i = F_i r = \mu_r F_n$$

The friction torque of the *roller bearings*, particularly *ball bearings*, may be evaluated approximately on the base of the fitting radius r using the formula

$$T_\mu = 10^{-10} r^2 \text{ Nm.}$$

The static torque of the wheel having the radius r and the journal radius r_L is

$$T_L = \mu_\Sigma F_n$$

where $\mu_\Sigma = \frac{\mu_r + \mu r_L}{r}$.

Antifriction measures. To decrease the friction impact on the load operation, different means have been proposed. Thus, in the positioning mode of multi-operational machine-tools, the rolling guides provide fast and precision output. In the contouring mode of bidirectional milling machines, the slipping guides with very low friction are in use. When the strengths are high and velocities reach 0.1 m/s, the combine slipping/rolling guides are suitable. The hydrostatic systems are popular in the heavy milling machines.

3 Mechanical Transmissions

3.1 Travel functions

Transmission requirements. The motor serves as the source of mechanical power to drive the mechanical system and carry out the useful work. The power is proportional to the motor size and speed, that is:

$$P = T\omega = BlIr\omega = k_m\omega .$$

Here, B is induction, l is an active length of winding, I is a current, r is an average rotor radius, k_m is a provisional motor mass factor. In other words, the machine size and speed determine its power. The motors of high mass and low speed ($m \rightarrow \max, \omega \rightarrow \min$) are usually taken out of the operational area and have low mechanical transmission ratio. In this way, high motor mass and size do not disturb the mechanism design. The motors of low mass and high speed ($m \rightarrow \min, \omega \rightarrow \max$) are often encapsulated into the mechanism. In this way, the light and high-speed motors are connected to the load by gearboxes or other transmissions. The first tendency is suitable mainly for machine building and equipment for metallurgy and transport. The second principle is typical in robotics and instrument industry, though these borders are enough conventional. Along with the low-speed, linear, and synchronous machine improvement, the *direct (gearless) drives* are introduced.



Scholarships



Lnu.se

Open your mind to new opportunities

With 31,000 students, Linnaeus University is one of the larger universities in Sweden. We are a modern university, known for our strong international profile. Every year more than 1,600 international students from all over the world choose to enjoy the friendly atmosphere and active student life at Linnaeus University. Welcome to join us!

Linnaeus University
Sweden

Bachelor programmes in
Business & Economics | Computer Science/IT | Design | Mathematics

Master programmes in
Business & Economics | Behavioural Sciences | Computer Science/IT | Cultural Studies & Social Sciences | Design | Mathematics | Natural Sciences | Technology & Engineering

Summer Academy courses

Kinematical circuits of technological equipment require small gaps and backlashes, low elastic deformations, and simple design. The following three main properties qualify the kinematic designs – transmission ratio, efficiency, and rigidity.

First, an ideally *solid mechanical system* is examined here.

Transmission ratio. The motion ratio of the driving and driven units is described by a *travel function*. When this function ties *momentary speeds* or paths, it is called a *transmission ratio*:

$$i = \frac{\omega}{\omega_L} = \frac{s\varphi}{s\varphi_L} = \frac{\varphi}{\varphi_L}.$$

Here, ω and φ are the angular speed and rotation angle of the driving shaft as well as ω_L and φ_L are the angular speed and angle of the driven shaft.

Linear ratio. A travel function, which describes linear velocities or *straight-line displacements*, is called a *linear ratio*,

$$i = \frac{v}{v_L} = \frac{sl}{sl_L} = \frac{l}{l_L}.$$

Here, v and l are the linear velocity and displacement of the driving shaft as well as v_L and l_L are the linear velocity and displacement of the driven shaft. Simplify this equation, taking into account that the linear velocity v is proportional to the rotational point distance r_L from the axis of rotation:

$$v = \frac{2\pi r_L}{\tau_L} = \omega_L r_L$$

where τ_L is the period of rotation. Introduce a *referred radius* as a travel function, which ties the instant linear velocities with the angular speeds as follows:

$$r_i = \frac{v}{\omega} = \frac{\omega_L r_L}{\omega} = \frac{r_L}{i}.$$

Particularly, when $i = 1$ all radii are equal, $r_i = r_L = r$. In the general case, the referred radius makes up the i -th part of the driven wheel radius.

Transmission of multi-section mechanisms. The travel function of a multi-section mechanism may be calculated as a product of the travel functions of the consecutively connected elementary sections:

$$i = \prod_m i_m \prod_n \frac{1}{r_{in}}$$

In the *parallel geared mechanical transmissions* and *coaxial geared mechanical transmissions* with the equal velocities v of the contact point the gear ratio is as follows:

$$i = \frac{v}{r} \cdot \frac{r_L}{v} = \frac{r_L}{r}$$

where r and r_L are the average radii of the driving and driven gears or *pulleys*.

Toothed gears. Quite often this ratio relates to the *toothed gears* (Fig. 3.1 (a)) with the following parameters:

$$\frac{r_L}{r} = \frac{z_L}{z}, \text{ mod} = \frac{h}{\pi}, h = \frac{2\pi r}{z}$$

where z and z_L are the number of teeth of the driving and driven gears, mod is the tooth engagement module, and h is the engagement step.

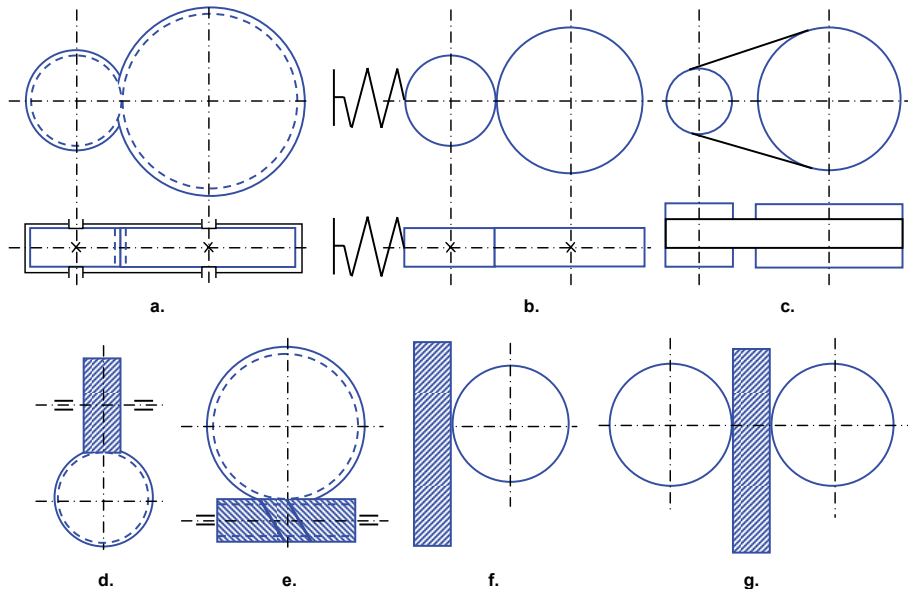


Fig. 3.1 Mechanical transmissions

The toothed gearboxes are widely applicable in industry. They are produced as both the separate assembly units and the coupled motor-gear sets. The geared wheels are manufactured from the tempered metals and then subject to grinding or polishing. The broad range of ratios in the single-, double-, and three-step models provides the universality of the gearbox applications. The gears with cylindrical toothed wheels and ratios from 0.2 to 10 develop the highest speeds. The *spur bevel gears* with external engagement have higher wear resistance and better smoothing, noiseless and heightened speeds. Thanks to the decrease of the teeth number of the small wheel, their size is less than other gears. The gears with cylindrical wheels and inner engagement are of high compact, high overload, low slip, but they are of less technological from the production point of view.

Efficiency of a pair of the toothed wheels depends on the number of teeth, gearing properties, circular force, and friction factor μ . The steel teeth usually have $\mu = 0.08$ to 0.12 . The steel worms, toothed wheels, and bronze teeth of the driven wheels have $\mu = 0.15$ to 0.25 on the velocities up to 2 m/s.

Efficiency of a cylindrical pair is approximately

$$\eta_L = 1 - \mu\pi \left(\frac{1}{z_1} + \frac{1}{z_2} \right) = 0.95 \text{ to } 0.99 .$$

Efficiency of the *bevel gear* is of the same order.

Other transmissions. *The friction transmissions* with parallel axes (Fig. 3.1 (b)) are popular in instrument-making industry where they alter the speeds by 2 to 5 times.

Rim, rope, cord and chain flexible transmissions (Fig. 3.1 (c)) transmit the long-distance motions of 2 to 10-times speed variations with the broad nomenclature of the pulley diameters.

To raise the torque on the shaft of a rotational mechanism i times relatively the torque of the prime mover of the same power, the parallel and cross-axis transmissions are used. The following relation describe the mechanisms with crossing axes:

$$i = \frac{\omega}{\omega_L} = \frac{z_L}{z} = \frac{r_L}{r} .$$

This ratio concerns of the *helical* (Fig. 3.1 (d)) and *worm* (Fig. 3.1 (e)) gears. To convert rotation into the forward motion, the *rack-toothed gears* (Fig. 3.1 (f)), *friction couplings* (Fig. 3.1 (g)), *camshafts*, and hinge-lever mechanisms are in use.

In the rack gears, rotation is converted into the forward motion thanks to the gear rotation in respect to the straight toothed rack. A gear revolution corresponds to the linear motion of $2\pi r$, whereas the reflected radius is equal to:

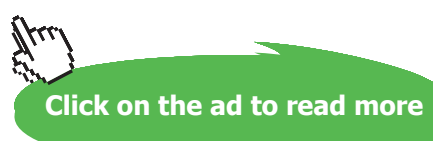
$$r_i = \frac{v}{\omega} = \frac{2\pi r r_L}{2\pi r} = r_L .$$

Cynthia | AXA Graduate

AXA Global Graduate Program

Find out more and apply

redefining / standards **AXA**



The same method is used to calculate the travel functions of the *wheel gears*, *pulley-rope*, and *drum-rope* transmissions.

To build the high-precision or noiseless joints as well as to pass the high forces, the *screw-nut* and *ball-screw gears* are recommended, which accompany the screw motion by the travel of the lathe component connected to the screw-nut. To exclude the *dead point* in these transmissions, a pair of springing nuts joints upon which a nut revolution corresponds to the linear motion equal to the screw step:

$$r_i = \frac{v}{\omega} = \frac{h}{2\pi}.$$

Efficiency of the screw-nut transmission is $\eta_L = 0.5$ to 0.8. The rack-toothed and planetary gear efficiencies are usually 0.92 to 0.98. The next formula defines the transmission ratio of the worm gear:

$$i = \frac{\omega}{\omega_L} = \frac{r_L}{r \tan \varphi_L} = \frac{z_L}{z}.$$

Here, ω is the worm rotational speed, ω_L is the worm wheel speed, φ_L is the spiral slope angle, $r = \frac{z \text{ mod}}{2 \tan \varphi_i}$, and $r_L = \frac{z_L \text{ mod}}{2}$ are the worm and worm wheel radiiuses, z is the number of worm threading, z_L is the number of wheel teeth, $\text{mod} = \frac{h}{\pi}$ is the worm gearing module, h is the worm step. The linear velocity of the worm motion is

$$v = \frac{r\omega}{\cos \varphi_L}.$$

The worm coupling with $z = 1$ to 4 and $z_L > 26$ ensures the ratio range $i = 7$ to 360. In contrast to other cross-axes transmissions (screw, friction, camshaft) having the equal motoring and motor torques, the worm gear increases the torque $\frac{r_L}{r_i}$ times. In the worm gear, the worm spiral slope angle is $\varphi_L = 0.01$ to 0.1, the friction angle is $\varphi_\mu = \arctan \mu$. The self-braking condition of the screw and worm pairs is $\varphi_L < \varphi_\mu$. Efficiency of the screw and worm gears is calculated as follows:

$$\eta_L = \frac{\tan \varphi_L}{\tan(\varphi_L + \varphi_\mu)}.$$

Usually $\eta_L = 0.65$ to 0.85.

In addition to the described gears, some other transmission types are applied in instrument-making, machine-building and robotics, particularly adjustable *planetary transmissions* of ratios 3 to 1500. Examples are the built-in planetary gears of Siemens of the backlash less than 6 angular minutes and very low moment of inertia.

The *wave gears* have significant ratios. When properly mounted, they slow down the rotation by 10 to 270 times and ensure the high overload capability and low backlashes. Thanks to the wave generator with the elastic mechanical link, this gear has a plenty of simultaneously geared teeth (up to 20 %) that contribute to raising the transmitted power and accuracy. It is convenient to pass the motion in the hermetic machines. Wave gear efficiency is usually 0.7 to 0.9.

Clutches are the integral parts of machine-building. The electromagnetic toothed clutches ensure the reliable shaft connection and pass the rotation without *freewheeling*. Specially shaped teeth allow to synchronize rotation and to convert speeds by the clutches. The same problems are resolved by electromagnetic disc clutches with air and oil cooling and by magnetic and non-magnetic discs having ratios of 1 to 5. Efficiency of the leading clutches is in the range of 0.95 to 0.98 whereas the disc clutches have efficiency 0.75 to 0.92.

3.2 Reflecting of forces and torques

Referred mass. To calculate an electric drive, all external masses, forces, and moments of inertia that influence the mechanism are to be reflected to the reduction unit, usually to the motor shaft with mass m_M and moment of inertia J_M as shown in Fig. 3.2 (a, b).

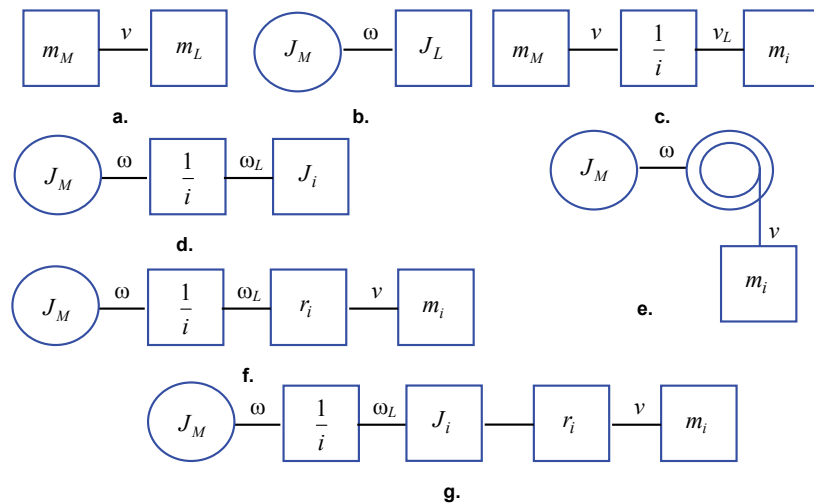


Fig. 3.2 Reflecting circuits for moments of inertia

A *referred mass* is a suspended mass m_L , which reference point moves at a velocity v and has kinetic energy W equal to the mechanism kinetic energy (Fig. 3.2 (c)). The kinetic energy equivalence

$$W = \frac{m_L v^2}{2} = \frac{m_i v_L^2}{2}$$

yields

$$m_L = \frac{m_i v_L^2}{v^2} = \frac{m_i}{i^2}.$$

Referred moment of inertia. A *referred moment of inertia* is a suspended moment of inertia J_L of a revolving component having an angular speed ω and kinetic energy W equal to the mechanism kinetic energy (Fig. 3.2 (d)). The kinetic energy equivalence

$$W = \frac{J_L \omega^2}{2} = \frac{J_i \omega_L^2}{2}$$

yields

$$J_L = \frac{J_i \omega_L^2}{\omega^2} = \frac{J_i}{i^2}.$$

For the translation mechanism (Fig. 3.2 (e))

$$W = \frac{J_L \dot{u}^2}{2} = \frac{m_i v^2}{2}$$

that is

$$J_L = \frac{m_i v^2}{\omega^2} = m_i r_i^2$$

where $r_i = \frac{v}{\omega}$ is a referred radius. In the *double-stage gears* (Fig. 3.2 (f))

$$J_L = \frac{m_i v^2}{\omega_L^2 i^2} = \frac{m_i r_i^2}{i^2}$$

..... Alcatel-Lucent 

www.alcatel-lucent.com/careers

What if you could build your future and create the future?

One generation's transformation is the next's status quo. In the near future, people may soon think it's strange that devices ever had to be "plugged in." To obtain that status, there needs to be "The Shift".



Click on the ad to read more

where $r_i = \frac{v}{\omega_L}$. When an intermediate link of the moment of inertia J_i occurs as shown in Fig. 3.2 (g),

$$J_L = \frac{m_i r_i^2}{i^2} + \frac{J_i}{i^2}$$

In a general case

$$J_L = \sum_k m_k \left(\frac{v_k}{\omega} \right)^2 + \sum_n J_n \left(\frac{\omega_n}{\omega} \right)^2 = \sum_k m_k r_{ik}^2 + \sum_n \frac{J_n}{r_n^2}$$

Overall moment of inertia. An overall moment of inertia of an electric drive is equal to $J = J_M + J_L$. In the low-speed mechanisms, particularly hoists with the inertia ratio $\gamma_J = \frac{J_M + J_L}{J_M} < 2$, the moment of inertia J_M may be taken into account using a safety factor of 30%:

$$J = k_s J_M \approx 1.3 J_M$$

On the contrary, in the mechanisms with the high-speed motors, the motor's own moment of inertia may be omitted:

$$J \approx J_L$$

Referred torque. A *referred force* is a suspended force F_L , which power in the referred point is equal to the power of forces applied to the mechanism (Fig. 3.3 (a)). The torque T_L of the referred force is called a *referred torque*. Particularly, in the lathes and milling machines where an electric drive rotates the instrument as shown in Fig. 3.3 (b), an equation of the static balance is as follows:

$$P = T_L \omega = \frac{T_i \omega_L}{\eta_L}$$

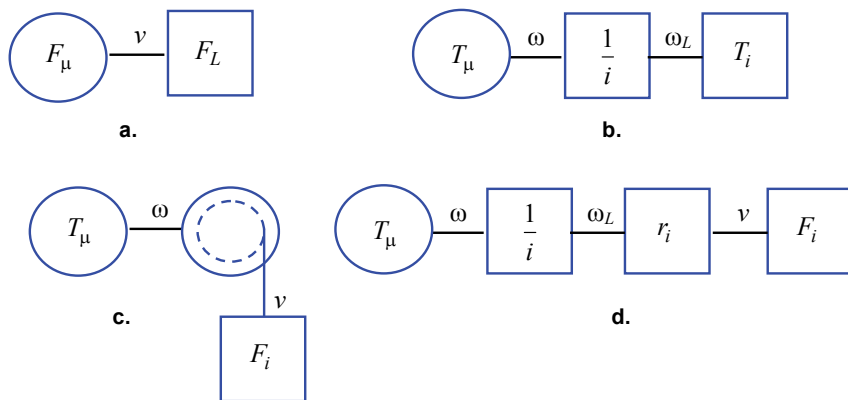


Fig. 3.3 Reflecting circuits for forces and torques

Thus, the following torque expression takes place:

$$T_L = \frac{T_i \omega_L}{\omega \eta_L} = \frac{T_i}{i \eta_L}$$

For the translation mechanisms, for example hoists (Fig. 3.3 (c)), an equation of the static balance is as follows:

$$T_L \omega = \frac{F_i v}{\eta_L}$$

Consequently,

$$T_L = \frac{F_i v}{\omega \eta_L} = \frac{F_i r_i}{\eta_L}$$

In the two-stage gears of the feed drives (Fig. 3.3 (d)), the rotor rotation is converting firstly to the lead screw revolving and then to the mechanism forward motion thus the balance equation is as follows:

$$T_L = \frac{F_i v}{\omega \eta_L} = \frac{F_i r_i}{i \eta_1 \eta_2}$$

where $r_i = \frac{v}{\omega_L}$ and $i = \frac{\omega}{\omega_L}$. The counter-torque of the screw pair:

$$T_s = (F_L + \mu(mg + F_T)) \frac{v}{\omega \eta}$$

Here, F_L and F_T are the work force and the screw tension, m is the motoring mass, g is the gravity acceleration, μ is the friction factor, whereas v , ω , and η are the speeds and efficiency.

The working torque of an elevator drive in the lifting mode for the cabin of the mass m_1 , the pulley, and the counter-mass m_2 is calculated as follows:

$$T_L = \frac{(m_1 - m_2)gv}{\omega \eta}$$

In the lowering mode:

$$T_L = \frac{(m_2 - m_1)gv\eta}{\omega}$$

In the multistage gears, $i = i_1 i_2 \dots i_n$, $r_i = r_1 r_2 \dots r_n$. In the general case,

$$T_L \omega = \sum_k \frac{F_k v_k}{\eta_{Lk}} + \sum_n \frac{T_n \omega_n}{\eta_{Ln}},$$

Here, F_k is a force applied to the k -th section, v_k is a velocity of F_k force application point, T_n is a torque of the forces applied to the n -th section, ω_n is an angular speed of the n -th section. Consequently,

$$T_L = \sum_k \frac{F_k v_k}{\eta_{Lk} \omega} + \sum_n \frac{T_n \omega_n}{\eta_{Ln} \omega}$$

Thus, F_L and T_L depend on the driven forces, torques, and speed ratio.

Example. Calculate the counter-torque of the motor shaft and find the inertia formula for the mechanism shown in Fig. 3.4. The shaft rotation of the motor M is delivered to the load shaft 1 through the power geared transmission, then to the shaft 2 through the instrument gear. The shaft 2 is connected to the shaft 3 of the position sensor BQ by the disk clutch. Gear ratios are shown in the diagram. The load torque $T_L = 0.2 \text{ Nm}$, static torque on the sensor shaft $T_3 = 0.012 \text{ Nm}$, power gear efficiency $\eta_1 = 0.98$, instrument gear efficiency $\eta_2 = 0.66$, clutch efficiency $\eta_3 = 0.81$, gear friction torques $T_{\mu 1} = 0.0018 \text{ Nm}$ and $T_{\mu 2} = 0.0009 \text{ Nm}$.

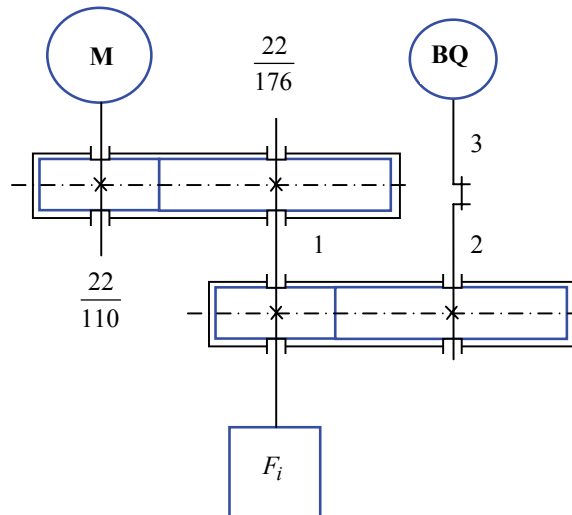


Fig. 3.4 Example of reflecting

Nido

Luxurious accommodation

Central zone 1 & 2 locations

Meet hundreds of international students

BOOK NOW and get a £100 voucher from voucherexpress

Nido Student Living - London

Visit www.NidoStudentLiving.com/Bookboon for more info.

+44 (0)20 3102 1060

The static torque on the shaft 2 is equal to $T_2 = \frac{T_3}{\eta_3} + T_{\mu 2} = 0.0157$ HM and on the motor shaft $T_L = \frac{T_1}{i_1 \eta_1} = 0.042$ Nm. The moment of inertia of the mechanism:

$$J_{L\Sigma} = J_{22} + (J_{110} + J_{22} + J_L) \cdot \left(\frac{22}{110} \right)^2 + (J_{176} + J_{BQ}) \cdot \left(\frac{22}{110} \cdot \frac{22}{176} \right)^2$$

3.3 Elasticity forces

Definition. When the long shafts, chains, or ropes are used to transmit the motion, the droops, *lags*, and movement distortion occur because of elastic deformation. Elastic sections provoke various oscillations in the mechanism:

- free oscillations upon the reference change and load torque variation;
- forced oscillations caused by external periodical forces irrespective of the system motion;

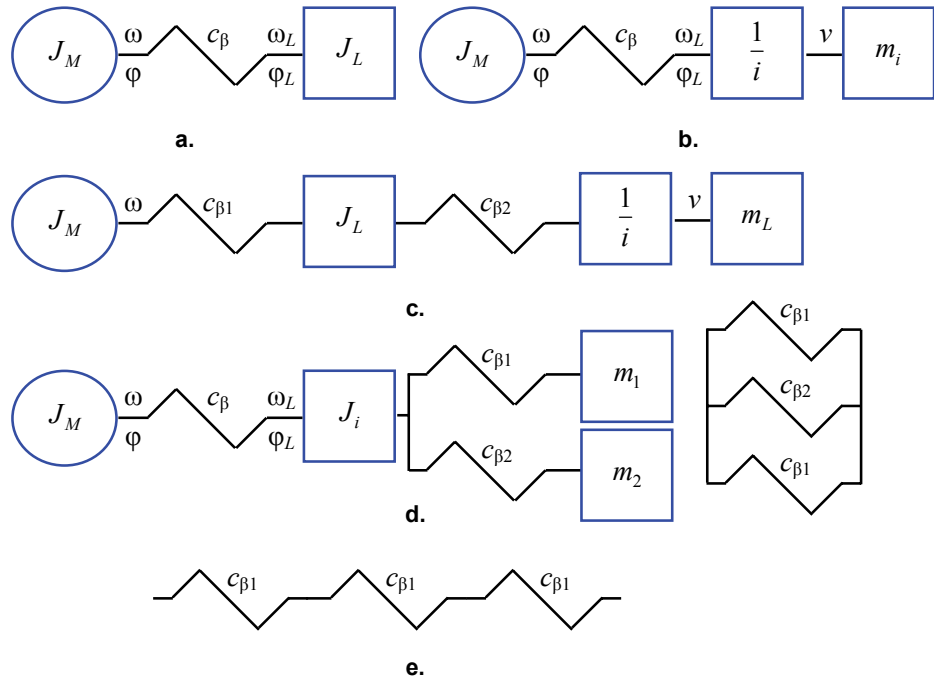
hunting induced by an interaction of the motoring object and external energy sources;

audio oscillations (*noise*).

If the external periodic force coincides with the frequency of one of these oscillations, a *resonance* will appear. This results in the mechanism ware and breakage as well as in the production of quality deterioration. To eliminate elastic oscillations and to accelerate their damping, the transmission rigidity and the viscous friction are to be increased.

Double-mass system. An electric drive with elastic sections is considered as a *multi-mass system* in distinct to earlier discussed *single-mass systems*. In the most cases, an elastic mechanism may be simulated as a *double mass system* where the pair of masses replaces all moving parts as shown in Fig. 3.5 (a). The first mass is concentrated on the motor shaft. It has moment of inertia J_M , rotated with the speed ω and traveling along the angular path φ . The second mass is separated from the motor by an elastic section. This mass has a moment of inertia J_L revolving with the speed ω_L and passing an angular path φ_L . An *elastic torque* causes deformation by sagging, lengthening δ_l , or twisting δ_φ ,

$$\delta_\varphi = \varphi - \varphi_L .$$

**Fig. 3.5** Reflecting circuits for elastic systems

Referencing to the gearbox of a ratio i shown in Fig. 3.5 (b), change δ_φ as following:

$$\delta_\varphi = \varphi - \varphi_L i.$$

The system rigidity affects both the path and the speed.

Solid and elasticity factors. A *solid factor* c_β displays the possibility of a mechanical system to withstand a deformation δ_l or δ_φ . It is described by the following ratio of an *elastic force* F_β or torque T_β to the induced deformation:

$$c_\beta = \frac{F_\beta}{\delta_l} \text{ or } c_\beta = \frac{T_\beta}{\delta_\varphi}. \quad (3.1)$$

Particularly in the case of the translation of a rod of the profile area Q , length l , and *Young's modulus* G , the formula is as follows:

$$c_\beta = \frac{GQ}{l}.$$

In the case of a revolving shaft of the radius r , the length l , and the shift module G , this expression is as follows:

$$c_\beta = \frac{Gr}{l}.$$

The solid factor formulae of the typical kinematical sections of the driven mechanisms are presented in Table 3.1.

Kinematical section	c_β , Nm/rad	Designations
Cylindrical or tongue-and-groove shaft	$\frac{\pi Gr^4}{2l}$	l – length, r – radius
Shaft with a pivotal hole	$\frac{\pi Gr^4}{2lk_c}$	$k_c = \frac{1}{1 - \left(\frac{r_{Lc}}{r}\right)^4}$, r_{Lc} – hole radius
Conical shaft with a pivotal hole	$\frac{\pi Gr^4}{2lkk_c}$	$k = \frac{r_{Lc}}{3r} \left(1 + \frac{r_{Lc}}{r} + \frac{r_{Lc}^2}{r^2}\right)$, r, r_{Lc} – big and small radiiuses
Shaft with a dowel groove	$\frac{\pi Gr_{Lc}^4}{2l}$	$r_{Lc} = r - 0.3h$, h - groove height

Table 3.1 Formulae of the solid factor for typical kinematical sections

The inverse quantity of c_β , which defines the mechanism compliance, is called an *elasticity factor*.

To account for an elasticity of a hoist, the replacement circuit may be figured as a three-mass system shown in Fig. 3.5 (c)). Here, the mass on the motor shaft, the mass of the drum with a rope, and the weight mass are emphasized. In the circuit, next designations are assumed: J_L – moment of inertia of a drum with the rope, m_L – weighting mass, $c_{\beta 1}$ - gearbox solid factor and $c_{\beta 2}$ – rope solid factor. In the special cases, this circuit may be simplified. Thus, if the backlashes occur, $m = 0$ may be considered because $c_{\beta 1} \gg c_{\beta 2}$. In the hoisting up mode with the grab, $c_{\beta 1} \rightarrow \infty$ and the two first masses link together. When the *stalling* or freezing weight starting is discussed, $m_L \rightarrow \infty$ is considered.

Multi-mass system. Sometimes, the branchy multi-mass circuit is used (Fig. 3.5 (d)) where the drum rotation courses the mass m_1 hoisting up and the mass m_2 hauling down. In this circuit, one have to consider the motor shaft moment of inertia J_n , the drum with a rope moment of inertia J_L tied with J_n by $c_{\beta 1}$, and masses m_1 and m_2 linked to the drum by elastic sections $c_{\beta 2}$ and $c_{\beta 3}$. In the case of parallel elastic connection shown in Fig. 3.5 (e), $c_\beta = \sum_k c_{\beta k}$, and in the case of a series connection (Fig. 3.5 (f)), $c_\beta = \frac{1}{\sum_k \frac{1}{c_{\beta k}}}$.

As a rule, the solid factor of a toothed belt does not exceed $0.2 \text{ N}/\mu$, and $1 \text{ N}/\mu$ in the case of the chain transmission. This index for the lathe rack-pinion transmissions reaches 100 to 300 N/μ whereas for the ball-screw pairs it exceeds 1200 N/μ .

Reflecting of elastic sections. The method of the speed damping in the *elastic system* depends on the inner friction factor,

$$\beta_L = \frac{F_\beta}{\delta_v} \text{ or } \beta_L = \frac{T_\beta}{\delta_\omega}. \quad (3.2)$$

The forces of inner viscous friction are proportionate to the deformation speed and act towards this speed. The following formulae reflect the solid factors c_{β_i} and the inner friction factors β_{Li} to the motor shaft:

$$c_{\beta} = \frac{c_{\beta_i}}{i^2}, \quad \beta_L = \frac{\beta_{Li}}{i^2}.$$

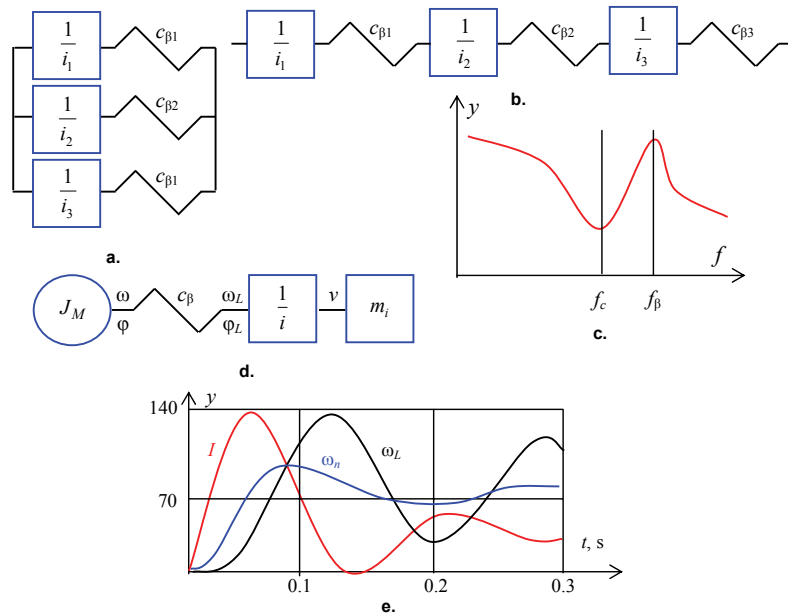


Fig. 3.6 Examples of elastic systems

SIMPLY CLEVER

ŠKODA



**WE WILL TURN YOUR CV
INTO AN OPPORTUNITY
OF A LIFETIME**



Do you like cars? Would you like to be a part of a successful brand?
As a constructor at ŠKODA AUTO you will put great things in motion. Things that will
ease everyday lives of people all around. Send us your CV. We will give it an entirely
new new dimension.

Send us your CV on
www.employerforlife.com



For the elastic section shown in Fig. 3.6 (a)

$$c_\beta = \frac{c_{\beta 1}}{i_1^2} + \frac{c_{\beta 2}}{i_2^2} + \frac{c_{\beta 3}}{i_3^2}.$$

For the elastic section shown in Fig. 3.6 (b) the same formula is as follows:

$$c_\beta = \frac{1}{\frac{i_1^2}{c_{\beta 1}} + \frac{i_1^2 i_2^2}{c_{\beta 2}} + \frac{i_1^2 i_2^2 i_3^2}{c_{\beta 3}}}.$$

Elastic oscillations. The elastic torque T_β causes oscillations in the elastic sections of the mechanical transmission. In the general case, the amplitude of the elastic oscillations depends on the motor and load torques, T and T_L is as follows:

$$T_{\beta \max} = \frac{J_M T_L + J_L T}{J_M + J_L}. \quad (3.3)$$

The period of the free oscillations in the elastic system τ_β is defined by the inertia ratio γ_J ,

$$\tau_\beta = \sqrt{\frac{J_M J_L}{(J_M + J_L) c_\beta}} = T_c \sqrt{\frac{1}{\gamma_J}} = T_M \sqrt{1 - \frac{1}{\gamma_J}}. \quad (3.4)$$

The period of the mechanism free oscillation at the immovable motor and the period of the motor shaft oscillation at the immovable mechanism are as follows:

$$\tau_c = \sqrt{\frac{J_L}{c_\beta}} = \tau_\beta \sqrt{\gamma_J} \quad (3.5)$$

$$\tau_M = \sqrt{\frac{J_M}{c_\beta}} = \frac{\tau_\beta \sqrt{\gamma_J}}{\sqrt{\gamma_J - 1}} \quad (3.6)$$

Figure 3.6 (c) shows a *frequency response* of the elastic section with the marked frequencies of the system and mechanism elastic oscillations

$$f_\beta = \frac{1}{2\pi\tau_\beta}, \quad f_c = \frac{1}{2\pi\tau_c}.$$

Usually, these frequencies are restricted by 0.1 Hz in the mine hoists, drags, and sluices as well as by 300 to 700 Hz in the high precision lathes. Referred rigidity of the feed drive for the control numerical control lathe occupies the range from 100 to 1300 N/μ, thus the amplitude of the linear oscillation is in the range 1 to 5 μkm and the amplitude of the angular oscillation does not exceed 0.01 radians.

The damping factors of elastic oscillations are calculated as follows:

$$\xi_\beta = \frac{\beta_L}{2c_\beta\tau_\beta} = \frac{\ln \frac{\nu_{\max 1}}{\nu_{\max 2}}}{2\pi}. \quad (3.7)$$

$$\xi_c = \frac{\beta_L}{2c_\beta\tau_c}$$

It is customary to retain the dumping factor within the range of 0.05. Equivalent damping of robots, excavators, and mining hoists falls in the range 0.1 to 0.3. It reaches 0.4 in rolling mills and hoisters.

Overall system description. As a case in point, describe the motion of the double mass elastic system shown in Fig. 3.6 (d) assuming deformation in accordance with the *Hook's law* (constant rigidity):

$$\begin{aligned} T &= T_\beta + J_M s\omega \\ T_\beta &= T_s + J_L s\omega_L i \\ T_\beta &= c_\beta \delta_\phi + \beta_L \delta_\omega \end{aligned}$$

Here $\delta_\omega = \omega - \omega_L i$, $\omega_L = s\phi_L$, $\omega = s\phi$. Double differentiation of the third equation and substitution data from other equations yields

$$s^2 T_\beta + \left(\frac{\beta_L}{J_M} + \frac{\beta_L}{J_L} \right) s T_\beta + \left(\frac{c_\beta}{J_M} + \frac{c_\beta}{J_L} \right) T_\beta = \frac{c_\beta}{J_L} T_c + \frac{c_\beta}{J_M} T + \frac{\beta_L}{J_M} s T$$

where $s^2 = \frac{d^2}{dt^2}$. Timing it by τ_β^2 yields

$$\frac{J_M J_L}{(J_M + J_L) c_\beta} s^2 T_\beta + \frac{\beta_L}{c_\beta} s T_\beta + T_\beta = \frac{J_M T_c + J_L T}{J_M + J_L} + \frac{\beta_L}{c_\beta} \frac{J_L}{J_M + J_L} s T$$

In the more compact form, represent the equation of the mechanical system motion as follows:

$$\tau_\beta^2 s^2 T_\beta + 2\xi_\beta \tau_\beta s T_\beta + T_\beta = \frac{J_M T_c + J_L T}{J_M \gamma_J} + 2\xi_\beta T_\beta \frac{J_L}{J_M \gamma_J} s T.$$

When the dumping factor ξ_β slightly affects the transients, a conservative section with an elastic torque

$$T_\beta \approx T_{\beta \max} \left(1 - \cos \frac{t}{\tau_\beta} \right). \quad (3.8)$$

will serve as a first approximation of the elastic system. At the step torque disturbance, the period of the second mass oscillation is equal to τ_β whereas at the immovable motor the mechanism free oscillation period is as follows:

$$\tau_c = \tau_\beta \sqrt{\gamma_J}$$

Example. Figure 3.6 (e) shows the transients of the slightly damped double-mass system having the following parameters: $U_M = 220$ V, $I_M = 5.4$ A, $\omega_M = 105$ rad/s, $R_M = 0.68$ Ω, $L_M = 0.02$ H, $J_M = 0.09$ kgm², $T_L = 1$ Nm, $c_\beta = 11$ Nm/rad, $\beta_L = 0.05$ Nms/rad.

While $c_\beta \rightarrow \infty$, the system may be considered as an absolutely rigid drive disregarding its elastic properties. All remaining cases should be subdivided into the weakly, essentially, and strongly connected systems. In the case of the weak connection ($\gamma_r < 1.5$) as well as in the case of the strong connection ($\gamma_r > 10$) an electric drive poor dumps the load oscillations. At the same time, since the inertia ratio approaches a unit, the load affection the motor becomes weaker. Otherwise, an elastic connection may provoke significant system flapping, which depends on the inertia ratio γ_r .

3.4 Load gaps and backlashes

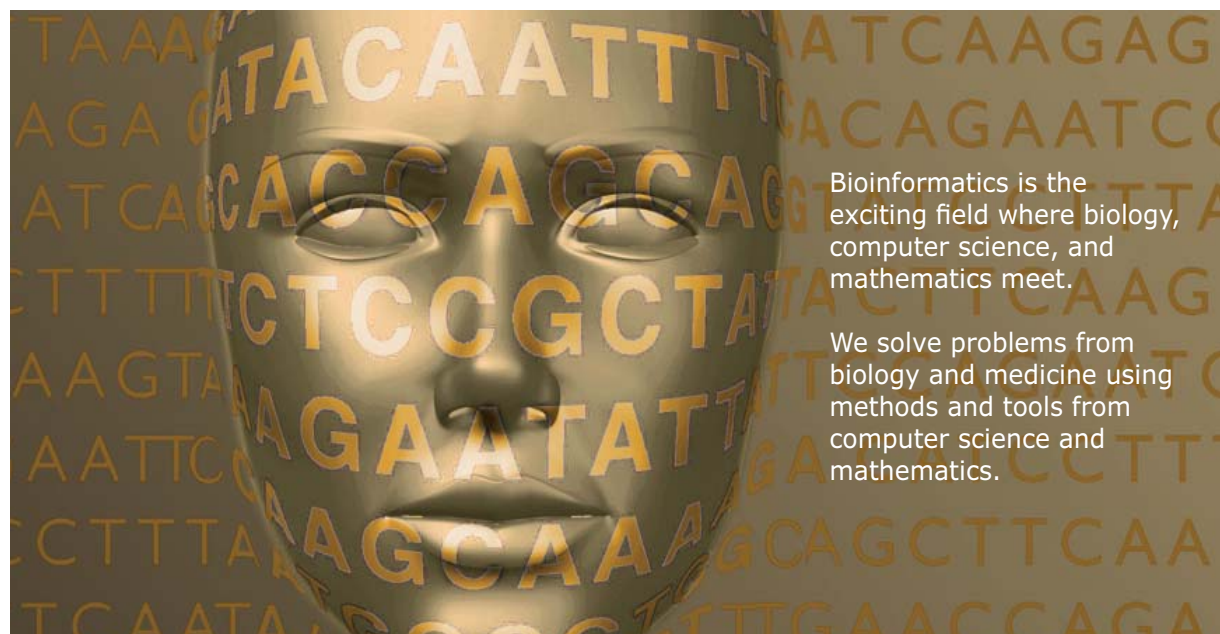
Gap. A *gap* is the mechanism area δ_l or δ_φ causing the path difference within which an elastic force is equal to zero. As far as the path difference exceeds this area, the gap locks and the mechanism sections continue their interaction. An example of the elastic circuit with a gap is given in Fig. 3.7 (a). The gap model (Fig. 3.7 (b)) is the following:

$$T_\beta = \begin{cases} c_\beta \left(\delta_\varphi - \frac{\varphi_\beta}{2} \operatorname{sgn} \delta_\varphi \right) & \text{within } |\delta_\varphi| > \frac{\varphi_\beta}{2} \\ 0 & \text{within } |\delta_\varphi| \leq \frac{\varphi_\beta}{2} \end{cases}$$



UPPSALA
UNIVERSITET

Develop the tools we need for Life Science
Masters Degree in Bioinformatics



Bioinformatics is the exciting field where biology, computer science, and mathematics meet.

We solve problems from biology and medicine using methods and tools from computer science and mathematics.

Read more about this and our other international masters degree programmes at www.uu.se/master



Click on the ad to read more

where φ_β is the gap width. Often, the gap is simulated by a relay characteristic like a dead space or a lag (Fig. 3.7 (c)):

$$T_\beta = \begin{cases} T_L \operatorname{sgn} \delta & \text{within } |\delta_\varphi| > \frac{\varphi_\beta}{2} \\ 0 & \text{within } |\delta_\varphi| \leq \frac{\varphi_\beta}{2} \end{cases}$$

where T_L is a torque transmitted through the gap.

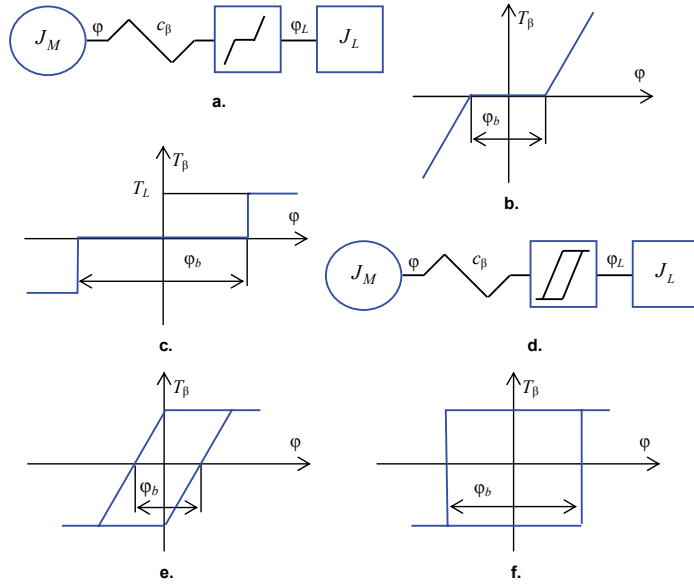


Fig. 3.7 Models of gaps and backlashes

Backlash. Other parameter of the elastic mechanical systems is called a *backlash*, or a *plug* (Fig. 3.7 (d)). The backlash causes non-identical drive response upon the identical set-points, which differ only in their sign. It blights significantly to the follow-up system sensitivity. The backlash action determines by the motion direction that is by the speed sign $\omega_L = \frac{d\varphi_L}{dt}$. The backlash model is as follows (Fig. 3.7 (e)):

$$T_\beta = \begin{cases} c_\beta(\delta_\varphi - \frac{\varphi_b}{2} \operatorname{sgn} \delta_\varphi) & \text{within } \omega_L > 0 \\ c_\beta(\delta_\varphi + \frac{\varphi_b}{2} \operatorname{sgn} \delta_\varphi) & \text{within } \omega_L \leq 0 \end{cases}$$

Frequently, the backlash is simulated by a relay characteristic like a rectangle hysteresis shown in Fig. 3.7 (f)):

$$T_\beta = \begin{cases} T_L & \text{within } \delta_\varphi \geq \frac{\varphi_b}{2} \\ T_L & \text{within } \frac{\varphi_b}{2} \geq \delta_\varphi > -\frac{\varphi_b}{2}, \omega_L \geq 0 \\ -T_L & \text{within } -\frac{\varphi_b}{2} \leq \delta_\varphi < \frac{\varphi_b}{2}, \omega_L < 0 \\ -T_L & \text{within } \delta_\varphi < -\frac{\varphi_b}{2} \end{cases}$$

Protection measures. To exclude the gaps and backlashes from the precision lathes, the screw kinematic pairs strain preliminary or automatic gap excretion applies. Thereto, the split adjusted toothed wheels are used often. As well, additional toothed transmissions and specific adjusted clutches are introduced. Totally, gaps and backlashes of the precision units do not exceed 0.1 to 10 μm .

Fig. 3.8 displays the drive responses of different set-points (a) with a gap (b) and backlash (c) into the transmission.

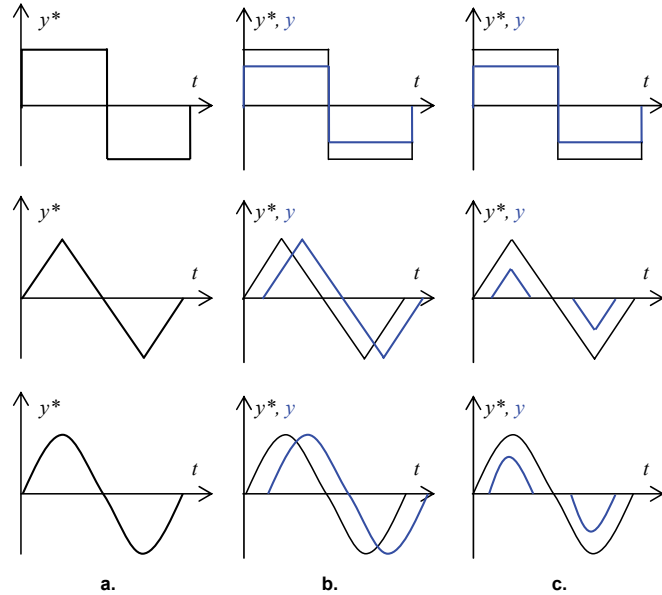


Fig. 3.8 Responses on typical input signals

4 Regulators and Filters

4.1 Transfer functions and block diagrams of drive components

To tune electric drives, the linear models are best suited thanks to the classical theory of the linear system control. The drive components, which can be described by the linear models, are expressed mathematically by the operator Laplace transformation using transfer functions and block diagrams.

A *transfer function* is the mathematical model of a linear chain. It describes the operator image of one of the output variables with respect to one of the input variables at zero starting conditions. To proceed from the differential equations to the Laplace images, the differential operator called a *Laplace operator* is used being considered as an algebraic value. In symbols,

$$s = \frac{d}{dt}, s^2 = \left(\frac{d}{dt} \right)^2, s^3 = \left(\frac{d}{dt} \right)^3, \text{etc.}$$

Therefore, by introducing the single quantity s , we get a lot in return – many differential equations can now be solved algebraically. This is quite a general method because the linear equations are often more easily solved than the differential ones.

UNIVERSITY OF COPENHAGEN





Copenhagen
Master of Excellence

Copenhagen Master of Excellence are two-year master degrees taught in English at one of Europe's leading universities

Come to Copenhagen - *and aspire!*

Apply now at
www.come.ku.dk

cultural studies

religious studies

science

Thanks to the technical linearization and control arrangement, all the motor types operated in the close loop drive systems may be represented by the linear models. At the no-load condition ($T_L = 0$) they are described by the second-order differential equations

$$\tau_T \tau_e s^2 \omega + \tau_T s \omega + \omega = \omega_0, \quad (4.1)$$

$$\tau_T \tau_e s^2 I + \tau_T s I + I = \frac{\tau_T}{R} s U. \quad (4.2)$$

The equations (4.1) and (4.2) can be compared with quadratic equations in a sense which solutions are an interesting combination of some particular cases.

In (4.1) and (4.2), the mechanical time constant is used,

$$\tau_T = \frac{J\omega_0}{T_d} = JRk_{ME}k_{MT},$$

and the electromagnetic time constant of the winding circuit τ_e also. To build the motor operator model using these equations, introduce the following *transfer factors* or *gains*:

$$k_{ME} = \frac{\omega_M}{E_M} - \text{the motor EMF gain,}$$

$$k_{MT} = \frac{I_M}{T_M} - \text{the motor torque gain.}$$

Here, $E_M = U_M - I_M R$ is the motor EMF, ω_M , I_M , T_M , U_M are the motor rated values, J is moment of inertia reflected to the motor shaft, ω_0 is the synchronous motor speed, and T_d is the run-up torque.

In the case of the dc motor, an armature inductance is $L = L_2 = L_a$ and resistance is $R = R_2 = R_a$. Thanks to the proper motor design,

$$k_{ME} = k_{MT} = \frac{1}{\psi_1}.$$

where $\psi_1 = \Phi$ is the stator permanent flux linkage.

In the case of induction electric drive, in which $\psi_1 = \text{const}$ is arranged,

$$k_{ME} = \frac{1}{p^2 \psi_1}, \quad k_{MT} = \frac{2}{m_1 p \psi_1} = \frac{2p}{m_1} k_{ME}, \quad L = \sigma L_1, \quad R = R_1 + R_2 \frac{k_1}{k_2},$$

Here, p is the pole pair number and m_1 is the stator phase number, R_1 and R_2 are the stator resistances, L_1 , L_2 and L_{12} – stator, rotor and mutual inductances, $k_1 = \frac{L_{12}}{L_1}$, $k_2 = \frac{L_{12}}{L_2}$, $\sigma = 1 - \frac{L_{12}^2}{L_1 L_2} = 1 - k_1 k_2$.

In the case of induction electric drive, in which $\psi_{12} = \text{const}$ is arranged,

$$k_{ME} = \frac{1}{p \psi_{12}}, \quad k_{MT} = \frac{2}{m_1 p \psi_{12}} = \frac{2}{m_1} k_{ME}, \quad L = L_1 + L_2 k_2, \quad R = R_1 + R_2 k_2.$$

In the case of induction electric drive, in which permanent rotor flux $\psi_2 = \text{const}$ is arranged,

$$k_{ME} = \frac{1}{k_2 p \psi_2}, \quad k_{MT} = \frac{2}{m_1 p \psi_2} = \frac{2k_2}{m_1} k_{ME}, \quad L = \sigma L_1, \quad R = R_1 + R_2 k_2^2.$$

In the case of the synchronous servo motor with $\psi_2 = \text{const}$,

$$k_{ME} = \frac{1}{p \psi_2}, \quad k_{MT} = \frac{2}{m_1 p \psi_2} = \frac{2}{m_1} k_{ME}, \quad L = L_1, \quad R = R_1.$$

Now, replace (4.1) and (4.2) by the Laplace operator expressions that describe the motor angular frequency and current responses, excited by the step reference E at the constant torque,

$$\begin{aligned}\omega &= E \frac{k_{ME}}{\tau_T \tau_e s^2 + \tau_T s + 1} \\ I &= E \frac{\tau_T s}{R(\tau_T \tau_e s^2 + \tau_T s + 1)}\end{aligned}$$

The following pair of the Laplace equations describes the transients caused by the step load disturbance T_L at the constant reference signal:

$$\begin{aligned}\omega &= -T_L \frac{\tau_T (\tau_e s + 1)}{J(\tau_T \tau_e s^2 + \tau_T s + 1)} \\ I &= T_L \frac{k_{MT}}{\tau_T \tau_e s^2 + \tau_T s + 1}\end{aligned}$$

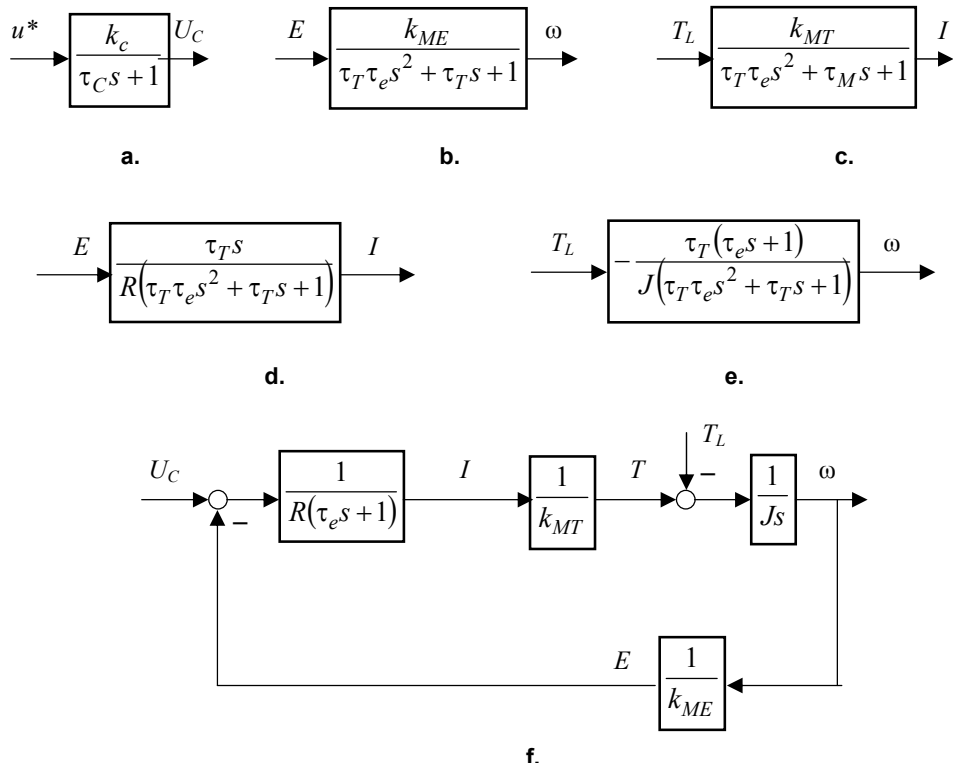
Based on these Laplace expressions, the transfer functions in regard to the reference EMF (without disturbance) are as follows:

$$\begin{aligned}W_M(s) &= \frac{\omega}{E} = \frac{k_{ME}}{\tau_T \tau_e s^2 + \tau_T s + 1} \\ W_{MI}(s) &= \frac{I}{E} = \frac{\tau_T s}{R(\tau_T \tau_e s^2 + \tau_T s + 1)}\end{aligned}\tag{4.3}$$

Accordingly, the motor transfer functions in regard to the disturbance (without the reference) are as follows:

$$\begin{aligned}W_{ML} &= \frac{\omega}{T_L} = -\frac{\tau_T (\tau_e s + 1)}{J(\tau_T \tau_e s^2 + \tau_T s + 1)} \\ W_{MIL} &= \frac{I}{T_L} = \frac{k_{MT}}{\tau_T \tau_e s^2 + \tau_T s + 1}\end{aligned}\tag{4.4}$$

Given equations are used to represent the converter and motor models by the *block diagrams* shown in Fig. 4.1. Each block diagram in Fig. 4.1 (a...e) corresponds to a particular transfer function. The detailed block diagram shown in Fig. 4.1 (f) describes the motor as the close loop system of elementary components, which have the current, torque, and EMF at the particular outputs.

**Fig. 4.1** Block diagrams of the drive components

Brain power

By 2020, wind could provide one-tenth of our planet's electricity needs. Already today, SKF's innovative know-how is crucial to running a large proportion of the world's wind turbines.

Up to 25 % of the generating costs relate to maintenance. These can be reduced dramatically thanks to our systems for on-line condition monitoring and automatic lubrication. We help make it more economical to create cleaner, cheaper energy out of thin air.

By sharing our experience, expertise, and creativity, industries can boost performance beyond expectations.

Therefore we need the best employees who can meet this challenge!

The Power of Knowledge Engineering

Plug into The Power of Knowledge Engineering.
Visit us at www.skf.com/knowledge

SKF

Because of the second-order transfer functions (4.3) and (4.4), the step responses of the motor speed and current may be presented by the periodic or non-periodic traces the shape of which depends on the time constant ratio. At $\tau_T > 4\tau_e$ they are exponential or non-periodic, but while $\tau_T < 4\tau_e$ they oscillate as is plotted in Fig. 4.2 by the dotted, dashed, and solid lines.

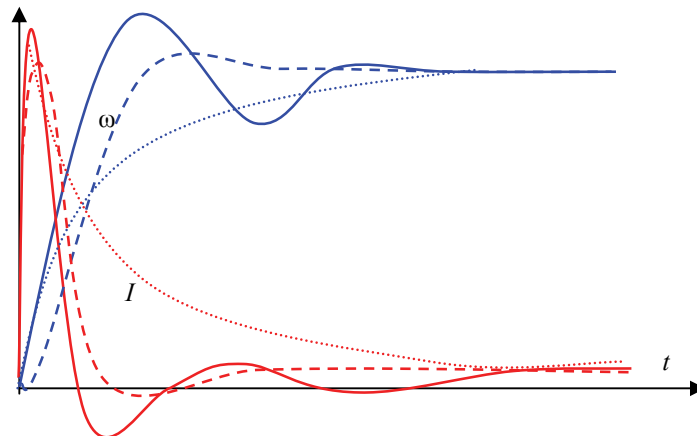


Fig. 4.2 Typical drive step responses

As a rule, the major transient impact results from the mass of the running inertia evaluated by the mechanical time constant τ_T . At the non-oscillating process, the electromagnetic time constant τ_e has low impact on the dynamic characteristic. On the contrary, the oscillating processes are significantly defined by the electromagnetic time constant.

Power converters of motor drives are often modeled as simple linear circuits described by the differential equation of the first order (Fig. 4.1 (a)) with a transfer function

$$W_c(s) = \frac{k_C}{\tau_C s + 1}.$$

Here, k_C is the converter gain, which depends of the converter function. It may be the ratio of the output voltage to the reference signal of the controlled rectifier, or the ratio of the output frequency to the input current of the inverter, etc. The time constant τ_C defines the average converter delay. In the case of thyristor devices,

$$\tau_C = \tau_{Cf} + \frac{1}{2mf_1},$$

where $\tau_{Cf} = 1\dots10$ ms is the time constant of the input filter, m is the number of ripples, and f_1 is the supply frequency. The transistor power converters are normally considered as non-inertia units except for the elastic and non-linear chains.

4.2 Analogue regulators and filters

To implement the discussed above drive topologies, continuous and discrete automatic elements or the program tools are used. *Analogue, or continuous, converters* are realised on the basis of the linear amplifiers.

Figure 4.3 presents the circuit diagrams and time responses $y(t)$ of the different analogue regulators – *proportional (P) controller*, *PI controller*, *PID controller* and their combinations built on operational amplifiers. In Table 4.1 the formulae for their calculation are collected.

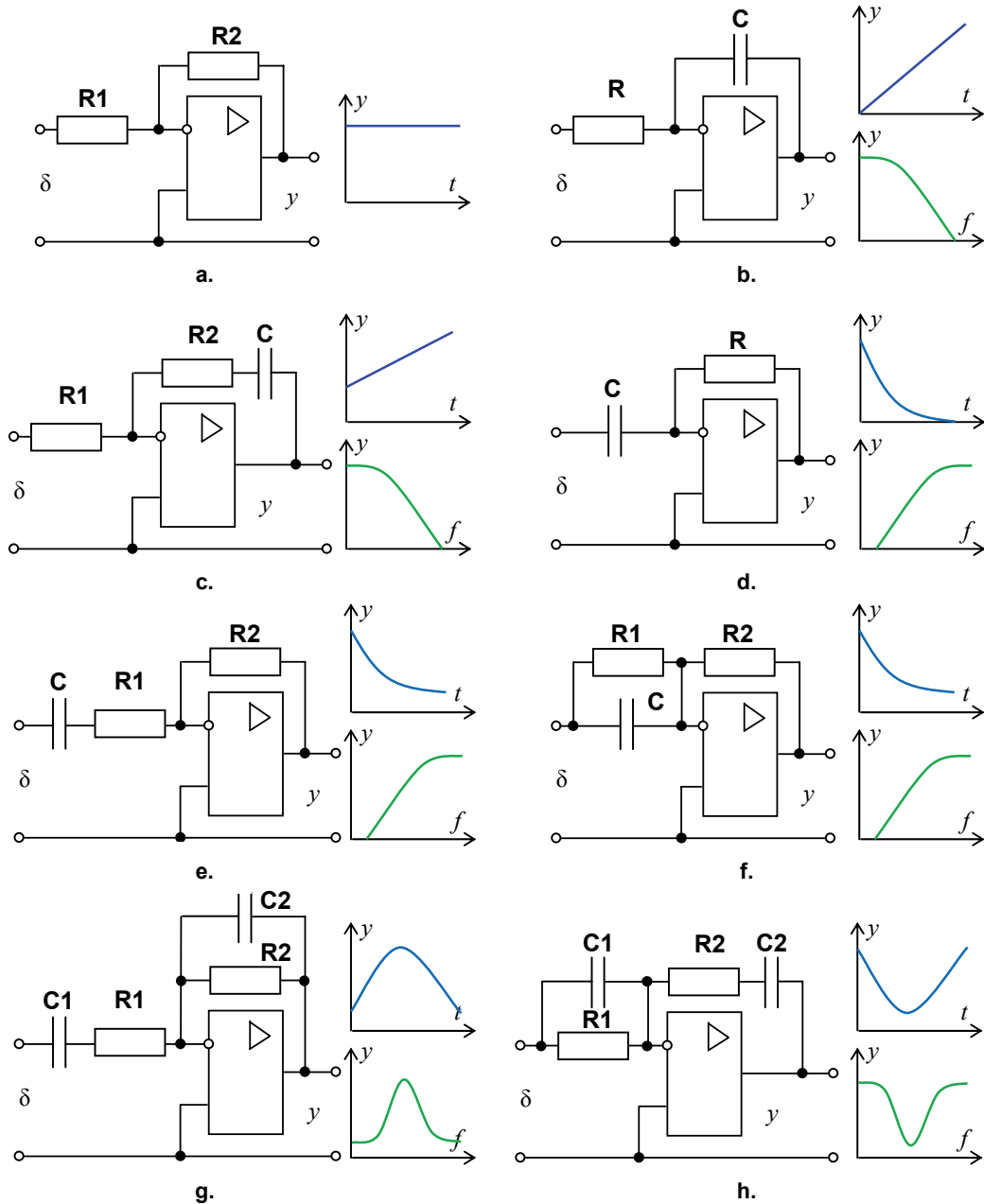


Fig. 4.3 Analogue regulators and active filters

Fig.	Regulator	Transfer function	Parameters
a	P	$-k_r$	$k_r = \frac{R_2}{R_1}$
b	I	$-\frac{1}{\tau_{int}s}$	$\tau_{int} = R\tilde{N}$
c	PI	$-k_r \frac{\tau_{int}s + 1}{\tau_{int}s}$	$k_r = \frac{R_2}{R_1}, \tau_{int} = R_2\tilde{N}$
d	D	$-\tau_{dif}s$	$\tau_{dif} = R\tilde{N}$
e	PD1	$-k_r \frac{\tau_{dif}s}{(\tau_{int}s + 1)}$	$k_r = \frac{R_2}{R_1}, \tau_{dif} = R_2C, \tau_{int} = R_1C$
f	PD2	$-k_r(\tau_{dif}s + 1)$	$k_r = \frac{R_2}{R_1}, \tau_{dif} = R_1C, R_1 < R_2$
g,h	PID	$-k_r \left(1 + \frac{1}{\tau_{int}p} + \tau_{dif}p \right)$	$k_r = \frac{R_2}{R_1}, \tau_{int} = R_2\tilde{N}_2, \tau_{dif} = R_1\tilde{N}_1, R_1 < R_2$

Table 4.1 Formulae for regulator calculations

Trust and responsibility

NNE and Pharmaplan have joined forces to create NNE Pharmaplan, the world's leading engineering and consultancy company focused entirely on the pharma and biotech industries.

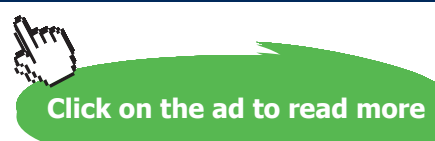
Inés Aréizaga Esteva (Spain), 25 years old
Education: Chemical Engineer

– You have to be proactive and open-minded as a newcomer and make it clear to your colleagues what you are able to cope. The pharmaceutical field is new to me. But busy as they are, most of my colleagues find the time to teach me, and they also trust me. Even though it was a bit hard at first, I can feel over time that I am beginning to be taken seriously and that my contribution is appreciated.



NNE Pharmaplan is the world's leading engineering and consultancy company focused entirely on the pharma and biotech industries. We employ more than 1500 people worldwide and offer global reach and local knowledge along with our all-encompassing list of services. nnepharmacplan.com

nne pharmaplan®



To calculate regulators, the apparatus of the transfer function operation calculus is applied.

Circuits used to remove unnecessary variations of dc and ac signals are known as *filters*. Depending on the passive and active components, filters are classified as *passive filters* and *active filters*. The first are built on resistors, capacitors, and inductors, whereas the active filters use only resistors and capacitors together with op amps and are considerably easier in design than passive filters. The circuit diagrams of the filters are similar to those of the regulators. The frequency responses $y(f)$ of the active filters are also given in Fig. 4.3 above. Table 4.3 collects the formulae for their calculation.

Fig.	Filter	Transfer function	Parameters
b	LPF	$-k_f \frac{1}{\tau_{\text{int}} s + 1}$	$k_f = \frac{R_2}{R_1}, T_{\text{int}} = R \tilde{N}$
e	HPF1	$-k_f s \frac{1}{\tau_{\text{dif}} s + 1}$	$k_f = \frac{R_2}{R_1}, \tau_{\text{dif}} = R_1 C$
f	HPF2	$-k_f (\tau_{\text{dif}} s + 1)$	
g	BPF	$-k_f s \frac{1}{(\tau_{\text{dif}} s + 1)(\tau_{\text{int}} s + 1)}$	$k_f = R_2 C_1, \tau_{\text{dif}} = R_1 C_1, \tau_{\text{int}} = R_2 \tilde{N}_2$
h	BSF	$-k_f - \frac{1}{\tau_{\text{int}} s} - \tau_{\text{dif}} s$	$k_f = \frac{R_2}{R_1} + \frac{C_1}{C_2}, \tau_{\text{dif}} = R_2 C_1, \tau_{\text{int}} = R_1 \tilde{N}_2$

Table 4.2 Formulae for filter calculations

The following filters are presented here: *low-pass filters (LPF)*, *high-pass filters (HPF)*, a *band-pass filter (BPF)* and a *band-stop filter (BSF)*. To calculate filters the apparatus of the transfer function operation calculus is also used.

4.3 Digital filters and regulators

Digital filters and *digital regulators* built using the microprocessor technique and computer software have some specific features. As a rule, a digital unit replaces a group of analogue devices. Moreover, it usually processes additional functions, such as the testing modes, automatic auxiliary calculations, self-tuning, signal override control, information exchange, diagnostic, and alarm generation. An arbitrary filter function is represented by the digital device as an algorithm and the corresponding program. The software may be corrected before running and during maintenance, and the tuning range is typically broad enough. At the same time, digital devices have some drawbacks, such as lower accuracy as compared to their analog prototypes because of the limited calculation step τ_0 .

Using the direct approach to the digital controller implementation, present the model of the PID controller as follows:

$$y(t) = k_r \left[\delta(t) + \frac{1}{\tau_{int}} \int_0^t \delta(\tau_c) d\tau_c + \tau_{dif} \frac{d\delta(t)}{dt} \right],$$

where k_r – regulator gain, τ_{int} – integral time constant, τ_{dif} – differential time constant, τ_c – discrete interval. For the k -th small quantizing intervals $\tau_0 = \tau_c$ and this equation may be transformed using the finite difference method. Replace the derivative by the first-order difference and the integral by the sum as follows:

$$y_k = k_r \left[\delta_k + \frac{\tau_0}{\tau_{int}} \sum_{i=1}^k \delta_{i-1} + \frac{\tau_{dif}}{\tau_0} (\delta_k - \delta_{k-1}) \right]. \quad (4.5)$$

At $\tau_{dif} = 0$ this equation describes the PI controller, at $\tau_{int} \rightarrow \infty$ PD controller, as well as at $\tau_{dif} = 0$ and $\tau_{int} \rightarrow \infty$ P controller. The smaller is τ_0 , the nearer the digital system approaches its analogue prototype. The practical recommendation is as follows:

$$\frac{\tau_0}{t_d} \leq \left(\frac{1}{4} \dots \frac{1}{15} \right),$$

where t_d is the response time of the loop containing the digital device. Accordingly the Shannon theorem,

$$\tau_0 \leq \frac{\pi}{\omega_c}$$

where ω_c is the self-oscillation frequency of the processed signals.

To build a recurrent algorithm, derive the current signal y_k through its value from the previous calculation step y_{k-1} with some correction. For this, find the difference between (4.5) and an equation

$$y'_{k-1} = k_r \left[\delta_{k-1} + \frac{\tau_0}{\tau_{int}} \sum_{i=1}^{k-1} \delta_{i-1} + \frac{\tau_{dif}}{\tau_0} (\delta_{k-1} - \delta_{k-2}) \right].$$

which results in

$$y_k - y_{k-1} = q_0 \delta_k + q_1 \delta_{k-1} + q_2 \delta_{k-2},$$

where

$$q_0 = k_r \left(1 + \frac{\tau_{dif}}{\tau_0} \right), \quad q_1 = -k_r \left(1 + 2 \frac{\tau_{dif}}{\tau_0} - \frac{\tau_0}{\tau_{int}} \right), \quad q_2 = k_r \frac{\tau_{dif}}{\tau_0}.$$

This is the fast practical algorithm because it calculates only current control values without keeping the previous values in memory.

Now, build the recurrent algorithms of the digital implementation for the main blocks of electric drive. As shown above, most of the automatic system units including regulators and filters can be described by the second-order transfer function

$$W(s) = \frac{y(s)}{\delta(s)} = \frac{\tau_1 s^2 + \tau_2 s + k_1}{\tau_3 s^2 + \tau_4 s + k_2}$$

or by the differential equation

$$\tau_3 s^2 y + \tau_4 s y + k_2 y = \tau_1 s^2 \delta + \tau_2 s \delta + k_1 \delta .$$

Using the finite differences, represent this equation as follows:

$$\begin{aligned} \frac{\tau_3}{\tau_0^2} [y_k - 2y_{k-1} + y_{k-2}] + \frac{\tau_4}{\tau_0} [y_k - y_{k-1}] + k_2 y_{k-1} = \\ \frac{\tau_1}{\tau_0^2} [\delta_k - 2\delta_{k-1} + \delta_{k-2}] + \frac{\tau_2}{\tau_1} [\delta_k - \delta_{k-1}] + k_1 \delta_{k-1}, \end{aligned}$$

where δ_k, y_k – input and output variables in the k -th calculation step. The solution of this equation yields:

$$y_k = -A_1 y_{k-1} - A_2 y_{k-2} + B_0 \delta_k + B_1 \delta_{k-1} + B_2 \delta_{k-2},$$

where $A_1 = \frac{k_2 \tau_0^2 - \tau_0 \tau_4 - 2\tau_3}{D}$, $A_2 = \frac{\tau_3}{D}$, $B_0 = \frac{\tau_0 \tau_2 + \tau_1}{D}$, $B_1 = \frac{k_1 \tau_0^2 - \tau_0 \tau_2 - 2\tau_1}{D}$, $B_2 = \frac{\tau_1}{D}$, $D = \tau_0 \tau_4 + \tau_3$.

This e-book
is made with
SetaPDF



PDF components for PHP developers

www.setasign.com



Click on the ad to read more

In Table 4.4 the examples of the program implementation for the typical electric drive components are shown at $\tau_{\text{int}} \geq \tau_0$.

Component	Model
LPF	$y_k = \left(1 - \frac{\tau_0}{\tau_{\text{int}}}\right) y_{k-1} + k_f \frac{\tau_0}{\tau_{\text{int}}} \delta_{k-1}$
PID regulator	$y_k = y_{k-1} + k_r \left[\left(1 + \frac{\tau_{\text{dif}}}{\tau_0}\right) \delta_k + \left(\frac{\tau_0}{\tau_{\text{int}}} - 2 \frac{\tau_{\text{dif}}}{\tau_0} - 1\right) \delta_{k-1} + \frac{\tau_{\text{dif}}}{\tau_0} \delta_{k-2} \right]$
PI regulator	$y_k = y_{k-1} + k_r \left[\delta_k + \left(\frac{\tau_0}{\tau_{\text{int}}} - 1\right) \delta_{k-1} \right]$
PD regulator	$y_k = y_{k-1} + k_r \left[\left(1 + \frac{\tau_{\text{dif}}}{\tau_0}\right) \delta_k - 2 \frac{\tau_{\text{dif}}}{\tau_0} \delta_{k-1} + \frac{\tau_{\text{dif}}}{\tau_0} \delta_{k-2} \right]$
I regulator	$y_k = y_{k-1} + k_r \left[\delta_k + \frac{\tau_0}{\tau_{\text{int}}} \delta_{k-1} \right]$
P regulator	$y_k = k_r \delta_k$

Table 4.3 Digital filter and regulators

The digital regulator delays an operation of the automatic system by amount of the quantising interval τ_0 . This delay can be described by the transfer function of the zero-order extrapolator as follows:

$$W_r(s) = \frac{1 - e^{-s\tau_0}}{\tau_0},$$

which tends to a unit at $\tau_0 < \frac{\pi}{\omega_c}$.

4.4 Static accuracy of electric drive

Recall the control topologies of electric drives. All variable-speed electric drives relate to the close loop systems. The system inputs y^* specify the required angular frequency ω^* , velocity v^* , or position φ^* as well as the demanded torque T^* , current I^* , or voltage U^* . The feedback signals are acquired from sensors coupled with the control objects, such as power converters, motors, and driving machines. These signals are processed by the controllers managed the control system. Thanks to the feedback, the referred signal is compared with the sensor signal using the subtracter in the case of the negative feedback or the summer in the positive feedback. Sometimes the regulators are mounted into the feedback loop but usually they are placed directly ahead the control object. In the former case shown in the block diagram of Fig. 4.4 (a) the feedback with the regulator of the transfer function $W_r(s)$ envelops the object $W_o(s)$. The reference (set-point signal) y^* is compared with the feedback signal ζ and their difference δ comes to the object as a reference impact. In the latter topology shown in Fig. 4.4 (b) the regulator directly affects the object whereas the feedback includes only sensors and filters described by the transfer function $W_y(s)$. This method is commonly used in the electric drive.

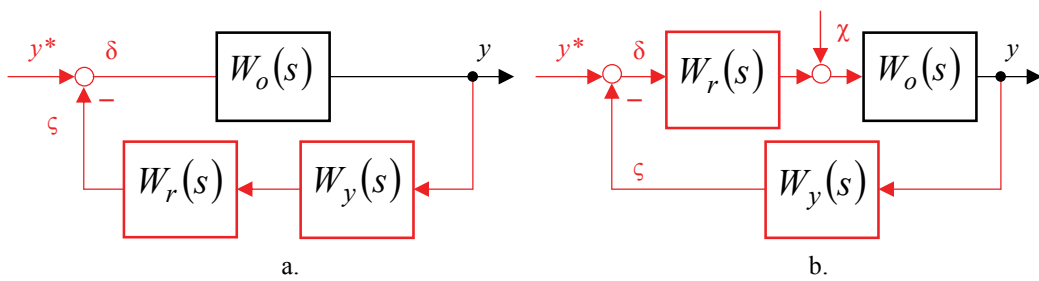


Fig. 4.4 Positioning of the regulator in the close loop system

The goal of a feedback is to increase the control accuracy by raising the static rigidity through the *speed holding*, which in turn increases the servo performance. Oppositely, in the systems those free oscillation period is harmonized with the run-up time the rigidity should be decreased to reduce the machine loading.

One of the main modes of the electric drive performance is the steady-state operation at the constant or smoothly changed inputs and disturbances. The major parameter of such performance is the steady-state error composed of both the error resulted from the set-point reproduction and the error resulted from the disturbance,

$$\delta = \delta^* + \delta_\chi .$$

Other errors caused by non-sensitivity and non-linearity of the regulators and sensors are usually eliminated by the system hardware and software.

In the system shown in Fig. 4.4 (b) the transfer function in respect to the input and the disturbance errors are as follows:

$$W_*(s) = \frac{1}{1 + W_y(s)W_r(s)W_o(s)},$$

$$W_\chi(s) = \frac{W_o(s)W_y(s)}{1 + W_y(s)W_r(s)W_o(s)}.$$

The errors depend on the transfer functions $W_r(s)$, $W_o(s)$, $W_y(s)$ and, particularly, on the gain of the open-ended system $k = k_r k_o k_y$ and its components k_r , k_o and k_y . If there are no integrated units in the forward loop, this equations describe a static system those errors are reversely proportional to k ,

$$\delta_* = \frac{y^*}{1+k}, \quad \delta_\chi = \frac{k_o k_y \chi}{1+k}.$$

If only $W_o(s)$ includes the integrated unit, like in the motor, the systems will become astatic in regard to the input. In this situation the set-point is processed without an error ($\delta_* = 0$) though the error from the disturbance is presented yet. If only $W_r(s)$ includes the integrated unit (for instance, I- or PI-controllers), the system will become astatic in regard to both the set-point and the disturbance, i.e. it has no steady-state errors at the fixed set-point and disturbance. When the system has two integrated units, the astatic system of the second order removes the steady-state errors of the permanently changing signals.



Sharp Minds - Bright Ideas!

Employees at FOSS Analytical A/S are living proof of the company value - First - using new inventions to make dedicated solutions for our customers. With sharp minds and cross functional teamwork, we constantly strive to develop new unique products - Would you like to join our team?

FOSS works diligently with innovation and development as basis for its growth. It is reflected in the fact that more than 200 of the 1200 employees in FOSS work with Research & Development in Scandinavia and USA. Engineers at FOSS work in production, development and marketing, within a wide range of different fields, i.e. Chemistry, Electronics, Mechanics, Software, Optics, Microbiology, Chemometrics.

We offer
A challenging job in an international and innovative company that is leading in its field. You will get the opportunity to work with the most advanced technology together with highly skilled colleagues.

Read more about FOSS at www.foss.dk - or go directly to our student site www.foss.dk/sharpminds where you can learn more about your possibilities of working together with us on projects, your thesis etc.

Dedicated Analytical Solutions

FOSS
 Slangerupgade 69
 3400 Hillerød
 Tel. +45 70103370
www.foss.dk




In the case of an arbitrary smooth set-point, the steady-state error can be defined by the following error factors:

$$\delta_* = C_0 y^* + C_1 s y^* + \frac{C_2}{2!} s^2 y^* + \frac{C_3}{3!} s^3 y^* + \dots$$

The error factors are derived using the transfer function of the set-point error and its derivatives at $s = 0$ as follows:

$$C_0 = W_*(s)|_{s=0}, \quad C_1 = \frac{dW_*(s)}{ds}|_{s=0} \dots$$

In the static systems, $C_0 = \frac{1}{1+k_{\delta\varphi}}$ meaning $k_{\delta\varphi}$ is the torque distortion quality. In the astatic systems, $C_0 = 0, C_1 = \frac{1}{k_{\delta\omega}}$ meaning $k_{\delta\omega}$ is the speed quality. In the second-order astatic systems, $C_0 = C_1 = 0, C_2 = \frac{1}{k_{\delta\omega}}$ meaning $k_{\delta\omega}$ is the acceleration quality. Therefore, when the demanded accuracy and input signals are known, the required quality can be calculated as well as the regulator gain.

In turn, the open-ended system gain relates to the frequency band of the inputs, which the electric drive processes at the given accuracy. This band is defined by the system bandwidth, $\omega_c = 2\pi f_c$. The more accurate is the system, the broader must be its bandwidth. The following Table 4.5 illustrates the relation of the bandwidth and the transfer function of the electric drive.

Open-ended transfer function	Bandwidth	Open-ended transfer function	Bandwidth
$\frac{k}{Ts}$	k	$\frac{k}{s(\tau_1 s + 1)(\tau_2 s + 1)}$	k
$\frac{k}{\tau s + 1}$	$\frac{k}{\tau}$	$\frac{k(\tau_1 s + 1)}{(\tau_2 s + 1)(\tau_3 s + 1)}$	$\frac{k\tau_1}{\tau_2^2}$
$\frac{k}{(\tau_1 s + 1)(\tau_2 s + 1)}$	$\frac{k}{\tau_1}$	$\frac{k(\tau_1 s + 1)}{s(\tau_2 s + 1)(\tau_3 s + 1)}$	$\frac{k\tau_1}{\tau_2}$

Table 4.4 Relation between bandwidths and transfer functions

Ignoring the EMF feedback and electromagnetic processes, the motor may be approximated by the integrated unit suitable for the draft calculations,

$$W_M(s) = \frac{1}{Jk_{MT}Rs},$$

In this case, the bandwidth of the system with the speed feedback (Fig. 4.4 (b)) is described as

$$\omega_c = \frac{k_{r\omega} k_C k_\omega}{JRk_{MT}}$$

therefore,

$$k_{r\omega} = \omega_c \frac{JRk_{MT}}{k_C k_\omega}.$$

Let $C_\omega = \frac{J_M R k_{MT}}{k_C k_\omega}$ is a speed loop factor. Then, $k_{r\omega}$ is as follows:

$$k_{r\omega} = \omega_c C_\omega \gamma_J.$$

When ignoring electromagnetic processes, the motor is described as the aperiodic unit with the mechanical time constant $\tau_T = JRk_{MT}k_{ME}$:

$$W_M(s) = \frac{k_{MT}}{\tau_T s + 1}.$$

In this case, $k_{r\omega} = \omega_c C_\omega \gamma_J$ again.

Therefore, the gain of the speed regulator may be preliminary counted for the demanded bandwidth of the speed loop, inertia ratio between the motor and the load, and the permanent parameters of the speed loop.



Click on the ad to read more

5 Control Principles of Electric Drives

5.1 Modal control and standard settings

Following the selection of the control topology, the regulators are to be designed. To provide the optimum settings, the control system has to follow some *principles*.

In distinct from the above discussed static properties, the system dynamic properties are defined by the transfer function, primarily by the roots of the characteristic polynomial. The *modal control principle* requires looping the controllable object with multiple feedbacks to reach the output transients having the typical (standard) distribution of the roots of the system characteristic polynomial. To generate the best dynamics, the *modal controllers* are required that process the all the possible object states. As not all the object variables are usually accessible by the sensors, these controllers should include the observers to reproduce inaccessible data mathematically, basing of the information acquired from sensors. In the simpler cases, the local regulators are designed to process the only accessible values, such as currents, voltages, speeds, paths, etc. measured by the feedback sensors.

Describe the close loop system shown in Fig. 4.4 (b) by the transfer function

$$W(s) = \frac{y}{y^*} = \frac{W_r(s)W_o(s)}{1 + W_r(s)W_o(s)W_y(s)}$$

accomplished by the images of the object $W_o(s)$, the regulator $W_r(s)$ and the feedback channel $W_y(s)$. To provide the demanded transient y^* , the transfer function of the regulator must be as follows:

$$W_r(p) = \frac{1}{W_o(s)} \cdot \frac{W(s)}{1 - W(s)W_y(s)}.$$

This regulator image includes the transfer function of the object and an additional part. The latter one depends on both the feedback $W_y(s)$ and the desired system model $W(s)$.

The engineering systems have the restricted *rate of response*. Call the minimum time of the system response as a *small equivalent time constant* τ_μ which serves as the measure of an electric drive response rate. Because of this unbalanced delay, any drive is described by a differential equation of, as minimum, the first order.

The system transfer functions $W(s)$ differ depending on their characteristic polynomials. Let the desired transfer function be described by the simplest first-order model having the characteristic polynomial

$$W_1(s) = a_1\tau_\mu s + 1$$

In this case, the motor drive will have very stable exponential step responses plotted above in Fig. 4.2 by the dotted curves.

If the desired transfer function of the drive is defined by the characteristic polynomial of the second order,

$$W_1(s) = a_1 \tau_\mu^2 s^2 + a_1 \tau_\mu s + 1$$

the system will be stable at $a_1 > 0$ in accordance with the Hurwitz's theorem. If $a_1 < 2$, the system will oscillate (solid lines in Fig. 4.2) whereas if $2 \leq a_1 < 4$, it will have the non-periodic transients (dashed traces in Fig. 4.2), and if $a_1 \geq 4$, the step responses will be again exponential.

The system having the desired transfer function with the characteristic polynomial of the third order,

$$W_1(s) = a_1 a_2 \tau_\mu^3 s^3 + a_1 a_2 \tau_\mu^2 s^2 + a_2 \tau_\mu s + 1$$

is stable at $a_1 > 0$ and $a_2 > 1$ as the Hurwitz's theorem states. The bounds between the non-periodic and oscillating processes are described by the Vyshnegradsky's equations:

$$\begin{aligned} 2a_1 a_2 - 9a_2 + 27 &= 0 \quad (a_1 a_2 < 27) \\ a_2^2 - 4 \left(a_1 a_2 + \frac{a_2^2}{a_1} \right) + 18a_2 &= 27 \quad (a_1 a_2 \geq 27) \end{aligned}$$

The plots of the given relations are displayed in Fig. 5.1 (a). Here area 1 envelops the oscillating processes, area 2 – non-periodic processes, and area 3 – unstable processes.

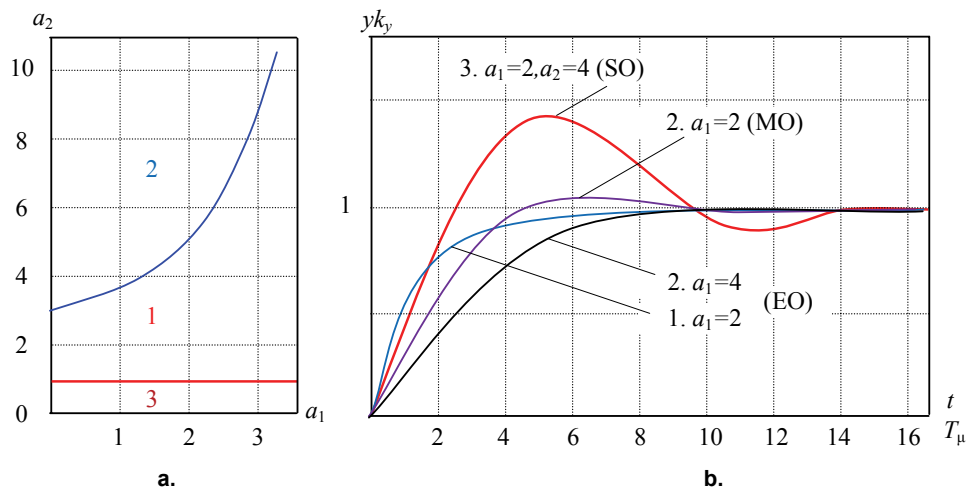


Fig. 5.1 Standard settings

Thus, the close loop drive transient shape, oscillation, and stability depend on the relation of the time constants rather than on their absolute values.

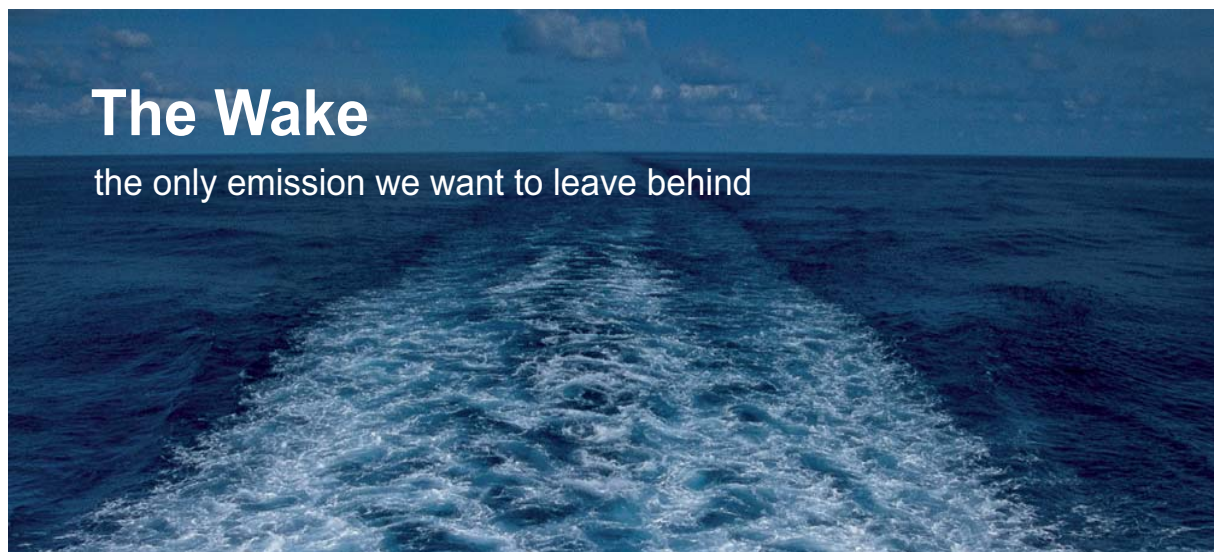
To select the factors a_1 and a_2 which provide the time optimal transients ($t_{d1}, t_d \rightarrow \min$ in Fig. 3.1 above), the so-called *standard tuning (setting)* is applied (Fig. 5.1 (b)).

The time-optimal non-periodic *exponential transient* (EO) in the second-order system takes place at $a_1 = 4$. Its running time is $9.5\tau_\mu$ without overshoot. In the third order system, a similar characteristic has the curve having $a_1 = 3$ and $a_2 = 9$. In the first-order system, a similar view is obtained by selection $a_1 = 2$.

The time-optimal monotonous (non-oscillating) step response in the second-order system takes place at $a_1 = 2$. Its running time area settles between $4.7\tau_\mu$ and $10.5\tau_\mu$ with the overshoot $\gamma = 4.3\%$ above the steady state value. This standard setting is called a *modulus optimum* (MO). In the third-order system a similar characteristic has the curve having $a_1 = 2.25$, $a_2 = 6$. In the first-order system a similar view is obtained by selection $a_1 = 2$.

The time-optimal oscillating transient in the third order system takes place at $a_1 = 2$ and $a_2 = 4$. Its running time is $3.1\tau_\mu$ with the overshoot $\gamma = 43\%$ above the steady state value. This standard setting is called a *symmetrical optimum* (SO). To obtain the similar characteristic in the second-order system, an inaccessible value of $a_1 = 0.25$ would be required. In the first-order system there are no oscillations.

Thus, the close loop drive running time and overshoot depend only on the loop model and the small equivalent time constant τ_μ . All the other parameters have no significance in the properly designed system with high linear characteristics.



Click on the ad to read more

5.2 Sequential correction of simple objects

The principle of the *sequential correction* requires the system to be divided into the loops each including the series-connected controller $W_r(s)$ and object $W_o(s)$ as Fig. 4.4 (b) shows. Normally, one of the object time constants (rarely two or three of them) is considered as the *large time constant* τ_o whereas other are the small time constants $\tau_{\mu i}$. The controller aims to balance the large time constant, thus converting the control loop into the simple system, preferably of the first order. Theoretically, it is desired to develop a fully inertia-free loop although in practice some non-sensing parameters are presented in the system, thus a small equivalent time constant τ_{μ} is kept in any case. The rules of such balancing are discussed further.

Let an object is described by the simple first-order model shown in Fig. 5.2 (a),

$$W_o(s) = \frac{k_o k_y}{\tau_o s + 1}$$

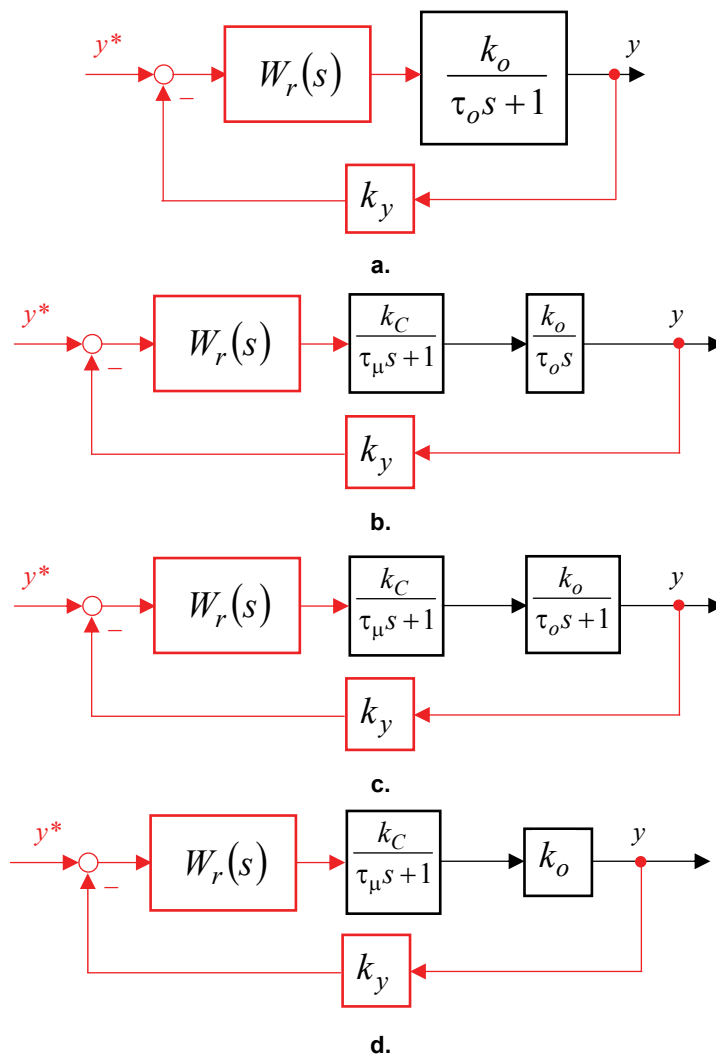


Fig. 5.2 Sequential correction of simple objects

To countervail the large time constant τ_o , the PI-controller is required which is described by the transfer function

$$W_r(s) = k_r \left(1 + \frac{1}{\tau_r s} \right) = k_r \frac{\tau_r s + 1}{\tau_r s}$$

$$k_r = \frac{1}{k_o k_y} \cdot \frac{\tau_0}{\tau_\mu}, \quad \tau_r = \tau_o$$

In this case, the resulting transfer function of the close loop becomes quite simple,

$$W(s) = \frac{W_r(s) W_o(s)}{1 + W_r(s) W_o(s)} = \frac{1}{k_y (\tau_\mu s + 1)}.$$

As the formula implies, now the loop properties depend merely on the feedback gain and the small time constant being independent of the object.

Observe further a more intricate loop shown in Fig. 5.2 (b). Here, the object includes the couple of time constants, τ_o and τ_μ , with the transfer function

$$W_o(s) = \frac{k_C k_o k_y}{\tau_o s (\tau_\mu s + 1)}.$$

To countervail the large time constant, use the P-controller

$$W_r(s) = k_r = \frac{1}{a_1 k_C k_o k_y} \cdot \frac{\tau_o}{\tau_\mu}.$$

As a result, the following second-order transfer function of the close loop is obtained:

$$W(s) = \frac{1}{k_y (\tau_\mu^2 s^2 + \tau_\mu s + 1)}.$$

For the objects described by the chain of the non-periodical members (Fig. 5.2 (c)) which have the sole large time constant τ_o , the PI-controller is applied with $k_r = \frac{\tau_o}{a_1 \tau_\mu k_C k_y k_i}$ and $\tau_r = a_2 \tau_\mu$.

Herewith,

$$W(p) = \frac{\frac{1}{k_y} \tau_o (a_2 \tau_\mu s + 1)}{a_1 a_2 \tau_\mu^2 s (\tau_\mu s + 1) (\tau_o s + 1) + \tau_o (a_2 \tau_\mu s + 1)}.$$

Particularly, when $\tau_r = a_2 \tau_\mu = \tau_o$ an application of the same PI-controller results in the above proposed transfer function of the second order. In the other cases, depicting $\tau_o = a_3 \tau_\mu$, the following system transfer function will be obtained:

$$W(s) = \frac{\frac{1}{k_y} a_3 \tau_\mu (a_2 \tau_\mu s + 1)}{a_1 a_2 \tau_\mu^3 s^3 + \frac{a_1 a_2 (a_3 + 1)}{a_3} \tau_\mu^2 s^2 + \left(\frac{a_1 a_2}{a_3} + a_2 \right) \tau_\mu s + 1}.$$

For reaching the above discussed transfer function of the third order, assume $\tau_o \gg \tau_\mu$, that is $a_3 \gg 1$,

$$\frac{a_3 + 1}{a_3} \approx 1, \text{ and } \frac{a_1 a_2}{a_3} \approx 0.$$

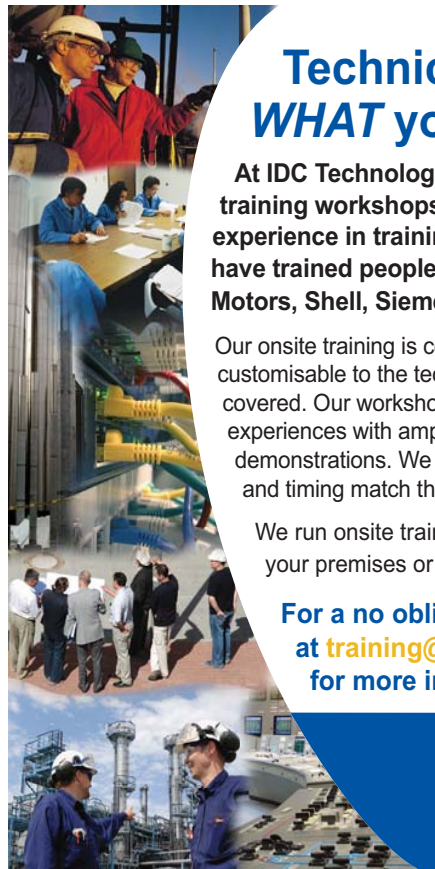
Sometimes, there is no large time constant in the object, as Fig. 5.2 (d) shows,

$$W_o(s) = \frac{k_C k_o k_y}{\tau_\mu s + 1}.$$

In this case, the following I-controller will be useful:

$$W_r(s) = \frac{k_r}{s} = \frac{1}{a_1 k_C k_o k_y} \cdot \frac{1}{\tau_\mu s}.$$

When many small time constants are involved in the direct and feedback channels of the loop, their sum is replaced by the common small time constant, i.e. $\sum \tau_{\mu i} = \tau_\mu$.



Technical training on ***WHAT*** you need, ***WHEN*** you need it

At IDC Technologies we can tailor our technical and engineering training workshops to suit your needs. We have extensive experience in training technical and engineering staff and have trained people in organisations such as General Motors, Shell, Siemens, BHP and Honeywell to name a few.

Our onsite training is cost effective, convenient and completely customisable to the technical and engineering areas you want covered. Our workshops are all comprehensive hands-on learning experiences with ample time given to practical sessions and demonstrations. We communicate well to ensure that workshop content and timing match the knowledge, skills, and abilities of the participants.

We run onsite training all year round and hold the workshops on your premises or a venue of your choice for your convenience.

**For a no obligation proposal, contact us today
at training@idc-online.com or visit our website
for more information: www.idc-online.com/onsite**

Phone: +61 8 9321 1702
Email: training@idc-online.com
Website: www.idc-online.com

**OIL & GAS
ENGINEERING**

ELECTRONICS

**AUTOMATION &
PROCESS CONTROL**

**MECHANICAL
ENGINEERING**

**INDUSTRIAL
DATA COMMS**

**ELECTRICAL
POWER**



Click on the ad to read more

5.3 Sequential correction of complex objects

In the above conversation the invariable part of the system contained the sole large time constant τ_o . In the common case, the control object may be more complex and include a number of inertial, boosting, integrated, and other members (Fig. 5.3 (a)). To countervail them, the more intricate regulators are needed. Thus, if the object is described by the transfer function

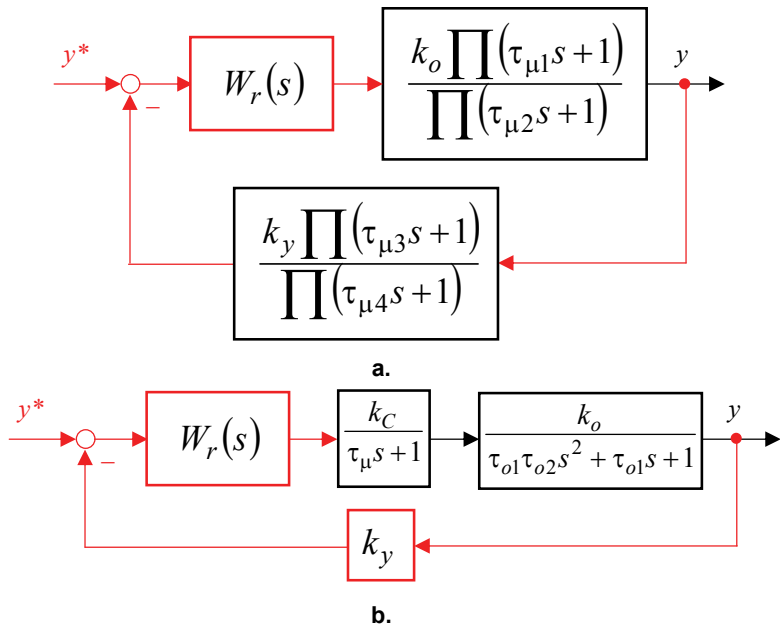


Fig. 5.3 Sequential correction of complex objects

$$W_o(s) = \frac{k_C k_o k_y}{(\tau_\mu s + 1)(\tau_{o1} \tau_{o2} s^2 + \tau_{o1} s + 1)},$$

(Fig. 5.3 (b)), the following PID-controller will compensate its inertia:

$$W_r(s) = k_r \left(1 + \frac{1}{\tau_{r1} s} + \tau_{r2} s \right),$$

which parameters are as follows: $k_r = \frac{\tau_{o1}}{a_1 \tau_\mu k_C k_\delta k_i}$, $\tau_{r1} = \tau_{o1}$, $\tau_{r2} = \tau_{o2}$. Such balancing results in the second-order transfer function of the close loop system. Besides, in the described case the *compensatory controller* may be used, for example like this one:

$$W_r(s) = k_r \left(1 + \frac{1}{\tau_{r1} s} + \tau_{r2} s \right) \left(1 + \frac{1}{\tau_{r3} s} \right)$$

where $k_r = \frac{\tau_{o1}}{a_1 \tau_\mu k_C k_\delta k_i}$, $\tau_{r1} = \tau_{o1}$, $\tau_{r2} = \tau_{o2}$, $\tau_{r3} = a_2 \tau_\mu$. In this situation the transfer function of the close loop system is of the third order.

The object with $\tau_{o1} > 4\tau_{o2}$ is converted as follows:

$$W_o(s) = \frac{k_C k_{o1} k_{o2} k_y}{(\tau_\mu s + 1)(\tau'_{o1}s + 1)(\tau'_{o2}s + 1)},$$

where $\tau'_{o1o2} = \frac{\tau_{o1}}{2} \pm \sqrt{\left(\frac{\tau_{o1}}{2}\right)^2 - \tau_{o1}\tau_{o2}}$. The PID-controller proper for the compensation of two large time constants τ'_{o1} , τ'_{o2} has the following transfer function:

$$W_r(s) = k_r \left(\frac{\tau_{r1} + \tau_{r2}}{\tau_{r1}} + \frac{1}{\tau_{r1}s} + \tau_{r2}s \right) = k_r \frac{(\tau_{r1}s + 1)(\tau_{r2}s + 1)}{\tau_{r1}s}$$

which parameters depend on the time constants τ'_{o1} , τ'_{o2} , τ_μ ratio. At $\tau'_{o1} > a_2\tau_\mu$ and $\tau'_{o2} < a_2\tau_\mu$, the gain $k_r = \frac{\tau'_{o1}}{a_1\tau_\mu k_C k_y k_{o1} k_{o2}}$ and the time constants $\tau_{r1} = a_2\tau_\mu$, $\tau_{r2} = \tau'_{o2}$ provide the third-order transfer function for the close loop system. Assuming $\tau'_{o1} = a_2\tau_\mu$, the second-order transfer function will take place. At $\tau'_{o2} > a_2\tau_\mu$, the gain $k_r = \frac{\tau'_{o1}\tau'_{o2}}{a_1a_2\tau_\mu^2 k_C k_y k_{o1} k_{o2}}$ and the time constants $\tau_{r1} = \tau'_{o2}$, $\tau_{r2} = a_2\tau_\mu$ result in the third-order transfer function. At $\tau'_{o2} = a_2\tau_\mu$ the close loop system is described by the second-order model.

The sequential correction of the objects

$$W_o(s) = \frac{k_C k_o k_y}{s(\tau_\mu s + 1)(\tau_{o1}\tau_{o2}s^2 + \tau_{o1}s + 1)}$$

is provided by the PID-controller with the parameters $k_r = \frac{1}{a_1\tau_\mu k_C k_y k_o}$, $\tau_{r1} = \tau_{o1}$, $\tau_{r2} = \tau_{o2}$. Herewith the close loop system is described by the second-order transfer function.

Finally, for the sequential correction of the objects with the transfer function

$$W_o(s) = \frac{k_C k_o k_y \tau_{o1}s}{(\tau_\mu s + 1)(\tau_{o1}\tau_{o2}s^2 + \tau_{o1}s + 1)}$$

the following compensatory controller is recommended:

$$W_r(s) = \frac{k_r}{s} \left(1 + \frac{1}{\tau_{r1}s} + \tau_{r2}s \right)$$

where $k_r = \frac{1}{a_1\tau_\mu k_C k_y k_o}$, $\tau_{r1} = \tau_{o1}$, $\tau_{r2} = \tau_{o2}$.

In Table 5.1 the common recommendations regarding the sequential correction are collected.

Object model	Time constants	Setting	Regulator	Regulator parameters
$\frac{k_o}{\tau_o s + 1}$	—	—	PI	$k_r = \frac{\tau_o}{\tau_\mu k_o}, \tau_r = \tau_i$
$\frac{k_o}{\tau_o s (\tau_\mu s + 1)}$	$\tau_o > 4\tau_\mu$	MO	P	$k_r = \frac{\tau_o}{2\tau_\mu k_o}$
		SO	PI	$k_r = \frac{\tau_o}{2\tau_\mu k_o}, \tau_r = 4\tau_\mu$
$\frac{k_o}{(\tau_\mu s + 1)(\tau_o s + 1)}$	$\tau_o > 4\tau_\mu$	MO	PI	$k_r = \frac{\tau_o}{2\tau_\mu k_o}, \tau_r = \tau_o$
		SO	PI	$k_r = \frac{\tau_o}{2\tau_\mu k_o}, \tau_{pe} = 4\tau_\mu$
$\frac{k_o}{(\tau_\mu s + 1)}$	—	MO	I	$k_\tau = \frac{1}{2\tau_\mu k_o}$
		SO	I	$k_r = \frac{4}{\tau_\mu k_o}$
$\frac{k_o}{(\tau_\mu s + 1)(\tau_{o1}\tau_{o2}s^2 + \tau_{o1}s + 1)}$	$\tau_{o1} > 16\tau_\mu$ $\tau_{o1} \leq 4\tau_{o2}$	MO	PID	$k_r = \frac{\tau_{o1}}{2\tau_\mu k_o}, \tau_{r1} = \tau_{o1}, \tau_{r2} = \tau_{o2}$
		SO	Compensatory	$k_r = \frac{\tau_{o1}}{2\tau_\mu k_o}, \tau_{r1} = \tau_{o1}, \tau_{r2} = \tau_{o2}, \tau_{r3} = 4\tau_\mu$
$\frac{k_o}{(\tau_\mu s + 1)(\tau'_{o1}s + 1)(\tau'_{o2}s + 1)}$	$4\tau_\mu > \tau'_{o2}$ $4\tau_\mu \leq \tau'_{o1}$	MO	PID	$k_r = \frac{\tau'_{o1}}{2\tau_\mu k_o}, \tau_{r1} = \tau'_{o1}, \tau_{r2} = \tau'_{o2}$
		SO	PID	$k_r = \frac{\tau'_{o1}}{2T_\mu k_o}, T_{r1} = 4\tau_\mu, \tau_{r2} = \tau'_{o2}$
	$\tau'_{o2} \geq 4\tau_\mu$ $\tau_{o2} < \tau'_{o1}$	MO	PID	$k_r = \frac{\tau'_{o1}}{2\tau_\mu k_o}, \tau_{r1} = \tau'_{o2}, \tau_{r2} = \tau'_{o2}$
		SO	PID	$k_r = \frac{\tau'_{o1}\tau'_{o2}}{8\tau_\mu^2 k_o}, \tau_{r1} = \tau'_{o2}, \tau_{r2} = 4\tau_\mu$
$\frac{k_o}{s(\tau_\mu s + 1)(\tau_{o1}\tau_{o2}s^2 + \tau_{o1}s + 1)}$	$\tau_{o1} > 16\tau_\mu$ $\tau_{o1} \leq 4\tau_{o2}$	MO	PID	$k_r = \frac{1}{2\tau_\mu k_o}, \tau_{r1} = \tau_{o1}, \tau_{r2} = \tau_{o2}$

Table 5.1 Regulators for sequential correction

5.4 Cascading

The principle of *cascading* proposes dividing the complex object into the maximum possible easily controlled sub-objects to arrange a multi-loop system. The number of loops is equal to the number of the sub-objects. Each loop includes the controller linked in such a way that the output of the previous controller specifies the behavior of the next one. Respective block-diagram of the looping cascade is presented in Fig. 5.4. The object of each outer controller includes both the appropriate sub-object and the inner loop keeping its own controller. Two signals are compared at the input of each controller, the loop set-point signal and the loop actual signal measured by the loop sensor.

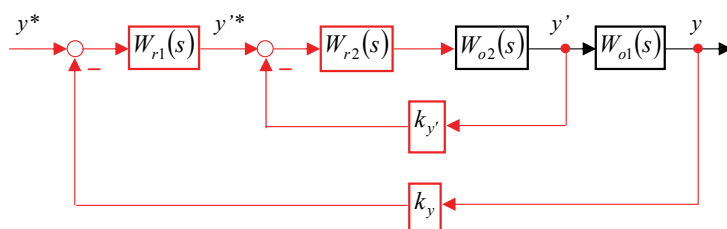


Fig. 5.4 Cascading

Clearly, cascading is used together with the principle of sequential correction. The large time constants of the loops are balanced by the corresponding controllers to decrease the loop inertia. Corrected loops have merely the small time constants and are described by the low-order transfer functions supported by the standard settings.

To tune the outer loop, the MO-tuned inner loop is approximated by the first-order unit which time constant equals to the doubled small time constant of the inner loop, that is

$$W_i(s) = \frac{k}{k_y} \cdot \frac{1}{2\tau_\mu^2 s^2 + 2\tau_\mu s + 1} \approx \frac{k}{k_y} \cdot \frac{1}{2\tau_\mu s + 1},$$

where k is a scale factor which reflects all the regulator gains to the single regulator input. For the programming controllers, k is defined by the signal scales. When the controllers are built on the op amps with the feedback resistance R_2 and the reference input resistance R_1 , $k = \frac{R_2}{R_1}$.

In the MO-tuned multi-loop system, each i -th loop has the transfer function

$$W_i(s) = \frac{k}{k_y} \cdot \frac{1}{2^i \tau_\mu s (2^{i-1} \tau_\mu s (2^{i-2} \tau_\mu s \dots (2^{i-i} \tau_\mu s + 1) \dots + 1) + 1) + 1}$$

If an inner loop is of SO-tuned, the following filter is to be inserted ahead the inner loop to tune the outer loop:

$$W_f(s) = \frac{1}{4\tau_\mu s + 1}$$

As a result, the inner loop transfer function will be as follows:

$$W_i(s) = \frac{k}{k_y} \cdot \frac{1}{8\tau_\mu^3 s^3 + 8\tau_\mu^2 s^2 + 4\tau_\mu s + 1} \approx \frac{k}{k_y} \cdot \frac{1}{4\tau_\mu s + 1}$$

In the SO-tuned multi-loop system, each i -th loop has the transfer function

$$W_i(s) = \frac{k}{k_y} \cdot \frac{1}{8(2^{i-1} \tau_\mu)^3 s^3 + 8(2^{i-1} \tau_\mu)^2 s^2 + 4(2^{i-1} \tau_\mu)^2 s + 1}$$

Thus, since the number of loops grows, the controller and the outer loop time constants grow, being doubled in each new loop. In other words, every loop steps down twice the system speed response and the drive precision.

A *jog* of the cascading systems is executed sequentially for each close loop starting, possibly, from the inner loop. If the inner loop has the *factory setting* (for instance, the current loop), the jog will begin with the next loop (for example, the speed loop).

Initially the P-controller is included into the loop. By the gradually increasing of its gain, the response of the moving system is examined upon the small step input signals thus preventing the saturation. As the close loop gain grows, the loop transient time is reduced along with its overshoot magnification. As the process obtains the oscillating feature, the gain stops to increase and even slightly decreases. If this way does not provide the demanded frequency band, the system must be tested for resonance and non-linearity, which restrict the bandwidth.

After that, the highest possible integral component is included into the controller. By gradual decreasing of its time constant, the step response of the moving non-saturated system is examined again. Along with the integral time constant lowering, the loop overshoot increases and, as its value overcomes the permissible level, the integral change is to be finished.

If the loop response remains insufficiently fast, the differential component can be included into the loop. By gradual increasing of its gain, the step response of the moving non-saturated system is examined once again. Along with the differential time constant growing, the loop overshoot increases and, as its value overcomes the permissible level, the tuning will be finished.

Thereupon, the regulator restriction components are switched on. Now, the input signals are to be increased to test the non-linear system response. This is the last step of the loop jog following which the jog of the next outer loop can start.

6 Tuning the Electric Drives

6.1 Speed control

The goal of the variable speed electric drives is to keep the prescribed motor speed stable and independent of the load and supply disturbances. To ensure the speed control has the required wide control range, as even the lowest speeds need to be detected accurately, a high-resolution tachometer and a processor with an extremely short sampling time are often required. This, in turn, demands a speed controller of high processing capacity and power.

To provide the speed sensing, the tachometer the signal of which is proportional to the speed is mounted directly on the motor shaft. The set-point value ω^* (desired speed) is continuously compared with the actual value ω in the control system. The speed difference determined in this way is used by the speed controller to regulate the power stage of the converter in such a manner that the motor reduces the controller difference. This represents a close loop speed regulating circuit.

In Fig. 6.1 (a) the block diagram of the converter-fed electric drive with the negative speed feedback is presented which satisfies to the above shown Fig. 4.4 (b). In this speed-stabilizing circuit the control object is described by the transfer functions of the power converter $W_C(s)$ and the motor $W_M(s)$, the feedback includes the speed sensor $W_\omega(s)$, whereas the speed regulator $W_{r\omega}(s)$ processes an error between the set-point ω^* and the actual speed signal.

I joined MITAS because
I wanted **real responsibility**



Month 16
I was a construction supervisor in the North Sea advising and helping foremen solve problems

Real work
International opportunities
Three work placements



The Graduate Programme
for Engineers and Geoscientists
www.discovermitas.com



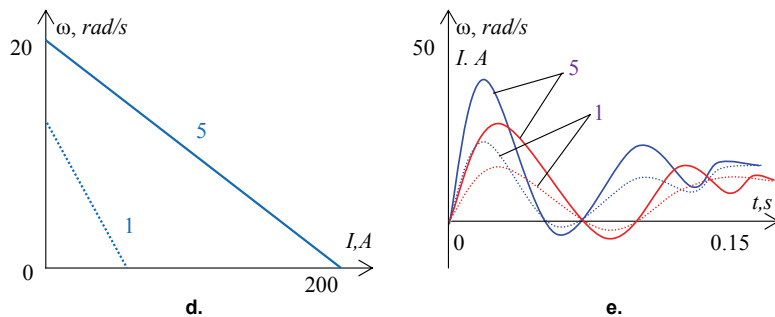
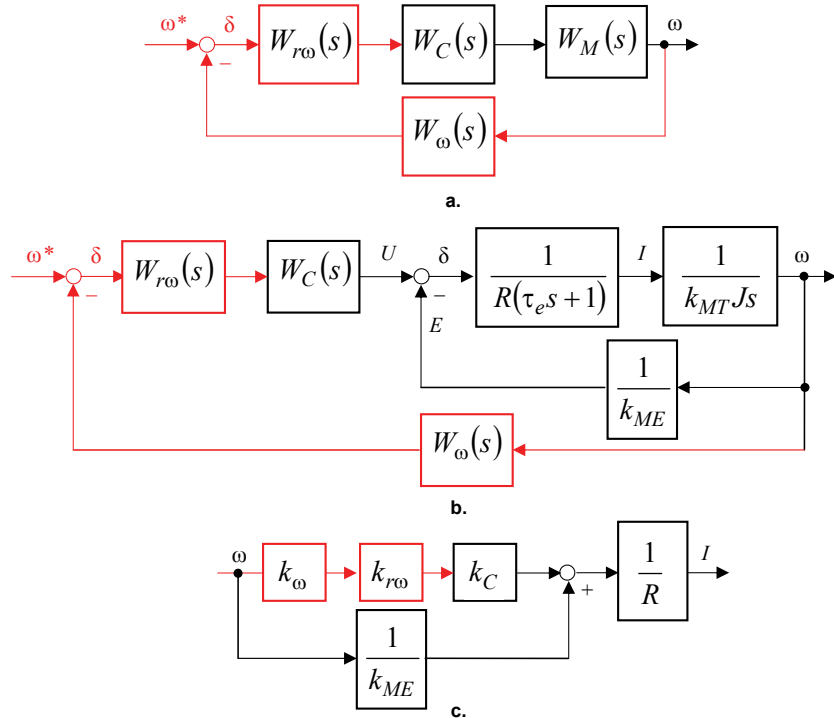


Fig. 6.1 Block diagrams and characteristics of electric drive with negative speed feedback

The detailed block diagram of the same electric drive is shown in Fig. 6.1 (b). Unlike the previous diagram, the motor is presented here by the close loop of the three sections from above shown Fig. 4.1 (f). The diagram denotes the following values: $\tau_e = \frac{L}{R}$ – electromagnetic time constant, $R = R_M + R_C$ – resistance of the motor and converter common circuit, R_M – motor resistance, R_C – power converter resistance, $L = L_M + L_C$ – inductance of the motor and converter common circuit, L_M – motor inductance, L_C – power converter inductance, k_{MT}, k_{ME} – the motor torque and EMF gains from (4.3), $J = J_M + J_L$ – the moment of inertia of the electric drive, accounting the motor and the load reflected to the motor shaft.

In Fig. 6.1 (c) this diagram is reorganized for the steady state drive performance with the current as the output value. The static rigidity of the circuit is as follows:

$$\beta_I = \frac{dI}{d\omega} = \frac{1 + k_{ME}k_Ck_{r\omega}k_\omega}{k_{ME}R}.$$

Thus, the electric drive enveloped by the negative speed feedback has more rigid static characteristics as compared with the natural motor characteristic, $\beta_I = \frac{1}{k_{ME}R_M}$. Along with the growth of the regulator gain $k_{r\omega}$ the rigidity also raises, $\beta_I \rightarrow \infty$. The same concerns the torque rigidity which, assuming the equivalence $T = \frac{I}{k_{MT}}$, is described as follows:

$$\beta = \frac{dT}{d\omega} = \frac{1 + k_{ME}k_Ck_{r\omega}k_\omega}{k_{ME}k_{MT}R}.$$

In Fig. 6.1 (d, e) some examples are shown for the electric drive with the following data: $U_M = 220$ V, $I_M = 5.4$ A, $\omega_M = 105$ rad/s, $R_M = 0.68$ Ω, $L_M = 0.002$ H, $J_M = 0.09$ kgm², $J_L = 0.008$ kgm², $T_s = 1$ Nm, $k_\omega = 1$ rad/(Vs). The static and dynamic characteristics are built for two variants of the speed regulator gain, $k_{r\omega} = 1$ and $k_{r\omega} = 5$. As follows from the diagrams, an increase of the static rigidity is accompanied by the oscillation growth.

In Fig. 6.2 (a) another variant of the speed-stabilizing system is shown. Here, the positive current feedback is implemented using the current regulator $W_{rl}(s)$ and the current sensor $W_I(s)$ instead of the negative speed feedback. The structural reorganization resulted in the static rigidity found from Fig. 6.2 (b) as follows:

$$\beta_I = \frac{dI}{d\omega} = \frac{\frac{1}{k_{ME}}}{R - k_C k_{rl} k_I}.$$

Here, along with the growth of the current gain k_{rl} , the rigidity reaches infinity at $k_C k_{rl} k_I = R$ and even becomes negative at $k_C k_{rl} k_I > R$ in the unstable mode of operation.

In practice the *combined feedback* is used also known as the *EMF feedback* or the *IR-compensation*. In Fig. 6.2 (c), following the algebraic summing of the voltage sensor signal with the current sensor signal, the EMF output $E = U - IR$ is produced. The static rigidity of the system with the *EMF regulator* $W_{rE}(s)$ is as follows:

$$\beta_I = \frac{dI}{d\omega} = \frac{1 + k_C k_{rE} k_E}{k_{ME} R}$$

and tends to infinity along with the growth of the EMF gain k_{rE} . As k_{rE} is sufficiently small, such feedback has quite low efficiency.

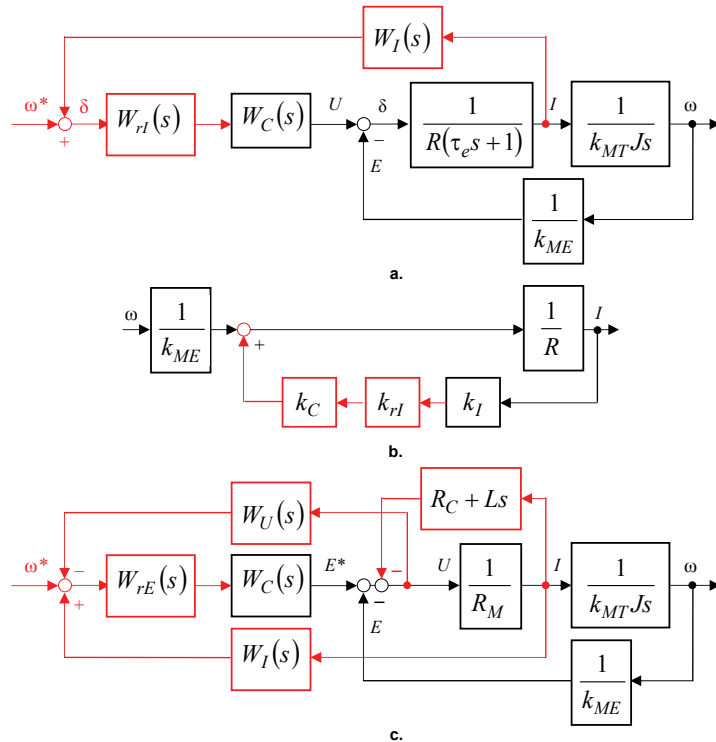


Fig. 6.2 Block diagrams of electric drive with current and combined feedbacks



In Fig. 6.3 (a) the block diagram of the close loop variable-speed electric drive is shown which conforms to Fig. 4.1 (b) and Fig. 6.1 (a).

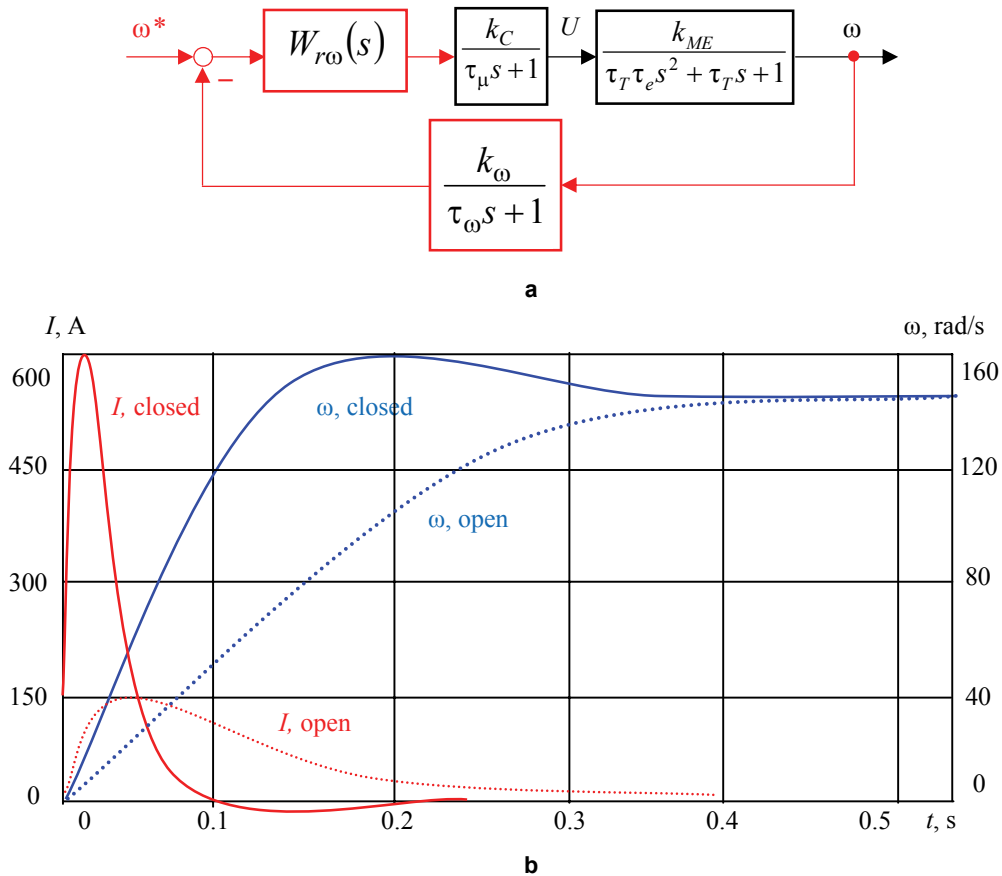


Fig. 6.3 Block diagram and transients of variable-speed electric drive

The control object has the transfer function

$$W_o(s) = \frac{k_o}{(\tau_{\mu} s + 1) \cdot (\tau_{o1} \tau_{o2} s^2 + \tau_{o1} s + 1)},$$

where $k_o = k_C k_{ME} k_\omega$, $\tau_\mu = \tau_C + \tau_\omega$, $\tau_{o1} = \tau_T$, $\tau_{o2} = \tau_e$. To obtain the optimum settings, the speed controller is to be designed as a PID-controller with the three components which can be separately tuned:

$$W_{r\omega}(s) = k_r \left(1 + \frac{1}{\tau_{r1} s} + \tau_{r2} s \right).$$

Instead, the compensatory regulator can also be applied,

$$W_{r\omega}(p) = k_r \left(1 + \frac{1}{\tau_{r1} s} + \tau_{r2} s \right) \left(1 + \frac{1}{\tau_{r3} s} \right).$$

Accordingly the sequential correction principle, multiple setting variants are possible here. The MO tuning ensures the *fast response* of the set-point ω^* processing with a small speed error δ_ω . At the same time, it provides the *slow response* of the disturbance T_L processing with the sizable overshoot but with no steady-state error δ_ω . Herewith the speed recovery time is proportional to the ratio of τ_o and τ_μ . The SO setting ensures the fast non-periodic processes with a small error of the disturbance processing. It has the slow response of the set-point processing with the sizable overshoot and without the steady-state error.

If $16\tau_\mu < \tau_{o1} \leq 4\tau_{o2}$, the MO setting will require the PID-controller with $k_r = \frac{\tau_{o1}}{2\tau_\mu k_o}$, $\tau_{r1} = \tau_{o1}$, $\tau_{r2} = \tau_{o2}$. The SO setting needs in the compensatory controller with $\tau_{r3} = 4\tau_\mu$.

In other cases the PID-controller is applied with $\tau'_{o1o2} = \frac{\tau_{o1}}{2} \pm \sqrt{\left(\frac{\tau_{o1}}{2}\right)^2 - \tau_{o1}\tau_{o2}}$ to reach the MO setting in which the parameters are to be as follows: $k_r = \frac{\tau'_{o1}}{2\tau_\mu k_o}$, $\tau_{r1} = \tau'_{o1}$, $\tau_{r2} = \tau'_{o2}$. Herewith, for $\tau_{o2} < 4\tau_\mu \leq \tau_{o1}$ the SO setting will be reached at $k_r = \frac{\tau'_{o1}}{2\tau_\mu k_o}$, $\tau_{r1} = 4\tau_\mu$, $\tau_{r2} = \tau'_{o2}$, whereas for $4\tau_\mu \leq \tau_{o2} < \tau_{o1}$ at $k_r = \frac{\tau'_{o1}\tau'_{o2}}{8\tau_\mu^2 k_o}$ the demanded time constants are $\tau_{r1} = \tau'_{o2}$ and $\tau_{r2} = 4\tau_\mu$.

For example, let the dc motor has the following rated data: $U_M = 110$ V, $I_M = 13$ A, $\omega_M = 157$ rad/s,

$R_M = 0.53$ Ω, $L_M = 0.005$ H, $J_M = 0.025$ kgm². The parameters of the thyristor rectifier are as

follows: $k_C = 11$, $R_C = 0.12$ Ω, $L_C = 0.016$ H, $T_C = 0.006$ s. The load data, reflected to the motor

shaft are as follows: $J_L = 0.055$ kgm², $T_s = 7$ Nm. The speed sensor parameters are as follows:

$k_\omega = 0.12$ rad/(Vs), $T_\omega = 0.0015$ s. The following parameters are to be calculated for the block

diagram: $k_{MT} = k_{ME} = \frac{\omega_M}{U_M - I_M R_M} = 1.54$ rad/(Vs), $R = R_M + R_C = 0.65$ Ω, $L = L_M + L_C = 0.02$ H,

$J = J_M + J_L = 0.08$ kgm², $\tau_T = JRk_{ME}k_{MT} = 0.125$ s, $T_e = \frac{L}{R} = 0.03$ s. Define the small time constant

as $\tau_\mu = \tau_C + \tau_\omega = 0.0075$ s. As $\tau_T > 4\tau_e$, the transfer function of the control object is converted as

$$W_o(s) = \frac{k_C k_{ME} k_\omega}{(\tau_\mu s + 1)(\tau_{o1}s + 1)(\tau_{o2}s + 1)},$$

where

$$\tau_{o1,o2} = \frac{\tau_T}{2} \pm \sqrt{\frac{\tau_T^2}{4} - \tau_T \tau_e} = 0.075 \text{ and } 0.05 \text{ s.}$$

The obtained loop has the parameter ratio of $4\tau_\mu < \tau_{o2} < \tau_{o1}$. The PID-controller provides here both the MO setting ($k_{r\omega} = \frac{\tau_{o1}}{2\tau_\mu\tau_C k_{ME} k_\omega} = 2.45$, $\tau_{r1} = \tau_{o1} = 0.075$ s, $\tau_{r2} = \tau_{o2} = 0.05$ s) and the SO setting ($k_{r\omega} = \frac{\tau_{o1}\tau_{o2}}{8\tau_\mu^2 k_C k_{ME} k_\omega} = 4.10$, $\tau_{r1} = \tau_{o2} = 0.05$ s, $\tau_{r2} = 4\tau_\mu = 0.03$ s). Figure 6.3 (b) displays two pairs of the transients, the first for the MO setting and the second for the open-ended system.

6.2 Combined speed-current control

As the single-loop variable-speed electric drives do not control the torque they can satisfactorily adjust the speed only at the constant load. To unstable loading the multi-loop systems suit better. The block diagram of the double-loop speed controlled motor drive is shown in Fig. 6.4. In this cascading system, the inner loop controls the current whereas the outer loop controls the motor angular frequency i.e. the system speed. The output signal from the speed controller serves as the set-point of the current loop. The current controller compares the set-point and the actual values and generates the control signals that are routed to the control stage of the power converter. The current loop is the innermost control loop of the system and must therefore respond very quickly, as this will determine the quick action of the higher-level speed controller.

In the past four years we have drilled
81,000 km
That's more than **twice** around the world.

Who are we?
We are the world's leading oilfield services company. Working globally—often in remote and challenging locations—we invent, design, engineer, manufacture, apply, and maintain technology to help customers find and produce oil and gas safely.

Who are we looking for?
We offer countless opportunities in the following domains:

- Engineering, Research, and Operations
- Geoscience and Petrotechnical
- Commercial and Business

If you are a self-motivated graduate looking for a dynamic career, apply to join our team.

What will you be?

Schlumberger

careers.slb.com



Click on the ad to read more

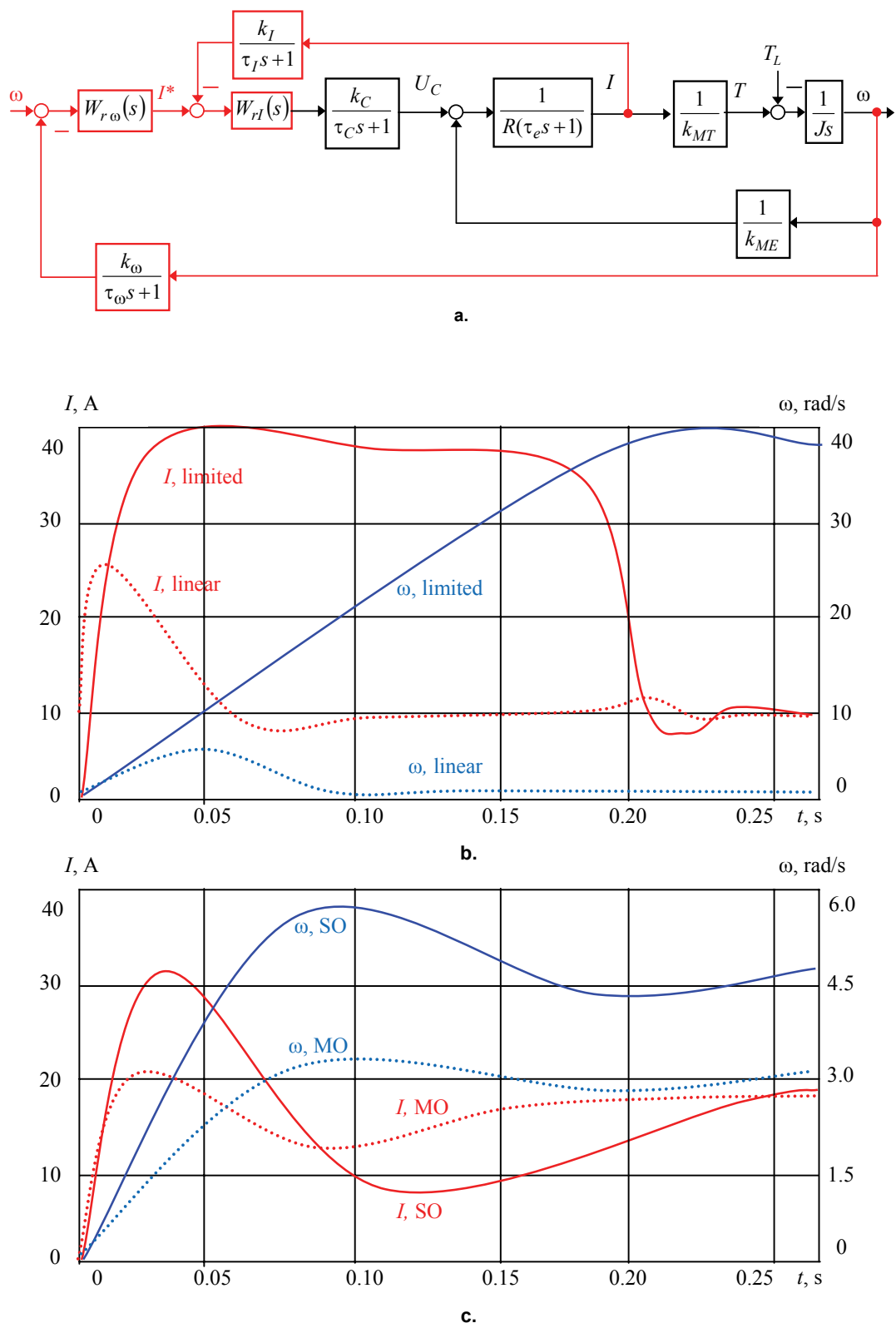


Fig. 6.4 Block diagram and transients of an electric drive with speed and torque control

The current loop has the following transfer function of the control object:

$$W_{oI}(s) = \frac{k_C k_I k_{MT} k_{ME} J_s}{(T_n p + 1)(R k_{MT} k_{ME} J_s (\tau_e s + 1) + 1)(\tau_I s + 1)} = \frac{\frac{1}{R} k_C k_I \tau_T s}{(\tau_{\mu I} s + 1)(\tau_T \tau_e s^2 + \tau_T s + 1)}$$

To compensate the large time constants τ_T, τ_e in accordance of the sequential correction principle, the compensatory controller is recommended,

$$W_{rl}(s) = \frac{k_{rl}}{s} \left(1 + \frac{1}{\tau_{r1} s} + \tau_{r2} s \right)$$

the following parameters of which provide the MO setting:

$$\tau_{\mu I} = \tau_C + \tau_I, \quad k_{rl} = \frac{R}{2\tau_{\mu I} k_C k_I}, \quad \tau_{r1} = \tau_T, \quad \tau_{r2} = \tau_e.$$

In the case of the transistor power converters, which operate at high switching frequencies of more than ten kilohertz, the converter inertia is ignored.

The current loop is usually calculated assuming the demanded current restriction at the fixed speed value, that is at $s\omega = 0$, ignoring the EMF feedback $\frac{1}{k_{ME}}$. Herewith the control object of the current loop is described by the following transfer function:

$$W_{oI}(s) \approx \frac{k_C k_I}{(\tau_{\mu I} s + 1) R (\tau_e s + 1)}$$

To control this object, the PI-controller is used which is tuned with the MO setting

$$k_{rl} = \frac{\tau_e R}{2\tau_{\mu I} k_C k_I}, \quad \tau_{rl} = \tau_e.$$

At this tuning, assuming $\tau_e \gg \tau_{\mu I}$, the loop should operate without the steady-state error therefore the system is expected to have the fast response on the supply perturbations.

Nevertheless, in the majority of cases the small steady-state error remains due to the EMF feedback. To reach the acceptable accuracy, the current regulator is to be jogged or the EMF influence must be compensated, for instance by the LPF or by the non-linear correction. In the former case the quick action drops whereas the circuit is complicated in the latter case.

In the servo drives the current loop is closed and tuned by the manufacturer. To increase the accuracy, this tuning can be self-corrected periodically. For this purpose, at the beginning of operation the motor is momentary wired to the testing dc source ($f_1 = 0$) to measure the actual stator resistance, $R_0 = \frac{U}{I}$. Then, in action, the parameters of the current regulator are constantly recalculated meaning the actual resistance drift which can be estimated using the thermo-sensor signals as follows:

$$R = R_0 \left(1 + \frac{\tau^\circ - \tau_0^\circ}{235 - \tau_0^\circ} \right)$$

where R_0, τ_0 are the resistance and the temperature of the cold motor.

Following the tuning, the current loop is considered as the part of the control object in relation to the outer speed loop.

In the transfer function of the control object of the speed loop, the optimized current loop, the compensated EMF feedback, and the scaled combined inputs are presented as follows:

$$W_o(s) = \frac{1}{2\tau_{\mu I} s + 1} \cdot \frac{1}{J_s} \cdot \frac{k_\omega}{\tau_\omega s + 1} = \frac{k_\omega}{J k_I k_{MT} s (\tau_{\mu\omega} s + 1)}$$

where $\tau_{\mu\omega} = 2\tau_{\mu I} + \tau_\omega$. To get the MO setting in the speed loop, the P-controller is preferable,

$$W_{r\omega}(s) = k_{r\omega} = \frac{J k_I k_{MT}}{2\tau_{\mu\omega} k_\omega}$$

Such approach is known as the single-integrated system design.

To provide the SO setting, the PI-controller with the same gain and the time constant $\tau_{r\omega} = 4\tau_{\mu\omega}$ is applied. This approach is known as the double-integrated system design. In distinct from the single-integrated system, it provides the slower set-point and supply disturbance responses but has no steady-state torque errors. Nevertheless, the dynamic speed sag at the load jump still remains.

As an example, the transients of the single-integrated system are presented in Fig. 6.4 (b). The system has the following parameters: $U_M = 110$ V, $I_M = 13$ A, $\omega_M = 157$ rad/s, $R_M = 0.53$ Ω, $L_M = 0.005$ H, $J_M = 0.025$ kgm², $k_C = 11$, $R_C = 0.12$ Ω, $L_C = 0.016$ H, $\tau_C = 0.006$ s, $J_L = 0.055$ kgm², $T_s = 7$ Nm, $k_\omega = 0.12$ rad/(Vs), $\tau_\omega = 0.0015$ s, $k_I = 0.092$ A/V, $\tau_I = 0.0015$ s, $k_{rI} = 1.3$, $T_{rI} = 0.03$ s, $k_{r\omega} = 2.86$, $I_{max} = 40$ A. The drive response on the speed set-point step of 5 rad/s is shown by the first couple of the curves. As the sizable current spikes are dangerous for the electric drive, the regulators are supplied by the input limiters. The dotted trace pair displays the drive performance in the linear regulator bond, whereas the solid couple shows the running up 40 rad/s at the current limiting.

Figure 5.2 (c) illustrates the response on the 5 rad/s step by both the single-integrated and the double-integrated systems of the same parameters and $\tau_{r\omega} = 0.066$ s.

6.3 Path control

The block diagram of the close loop electric drive with the path control is shown in Fig. 6.5 (a). The control object has the transfer function

$$W_o(s) = \frac{k_C k_{ME} k_\varphi}{s(\tau_{\mu\varphi}s + 1) \cdot (\tau_T \tau_e s^2 + \tau_T s + 1)}$$

where $\tau_{\mu\varphi} = \tau_C + \tau_\varphi$. As the sequential correction principle states, to countervail the object inertia, the regulator has to be described by the transfer function of the fourth order,

$$W_{r\varphi}(s) = k_{r\varphi} s \left(1 + \frac{1}{\tau_{r1}s} + \tau_{r2}s \right) \left(1 + \frac{1}{\tau_{r3}s} \right)$$

associated with the parameters:

$$k_{r\varphi} = \frac{\tau_T}{a_1 \tau_{\mu\varphi} k_C k_{ME} k_\varphi}, \quad \tau_{r1} = \tau_T, \quad \tau_{r2} = \tau_e, \quad \tau_{r3} = a_2 \tau_{\mu\varphi}.$$

**STUDY FOR YOUR MASTER'S DEGREE
IN THE CRADLE OF SWEDISH ENGINEERING**

Chalmers University of Technology conducts research and education in engineering and natural sciences, architecture, technology-related mathematical sciences and nautical sciences. Behind all that Chalmers accomplishes, the aim persists for contributing to a sustainable future – both nationally and globally.

Visit us on **Chalmers.se** or **Next Stop Chalmers** on facebook.

CHALMERS
UNIVERSITY OF TECHNOLOGY

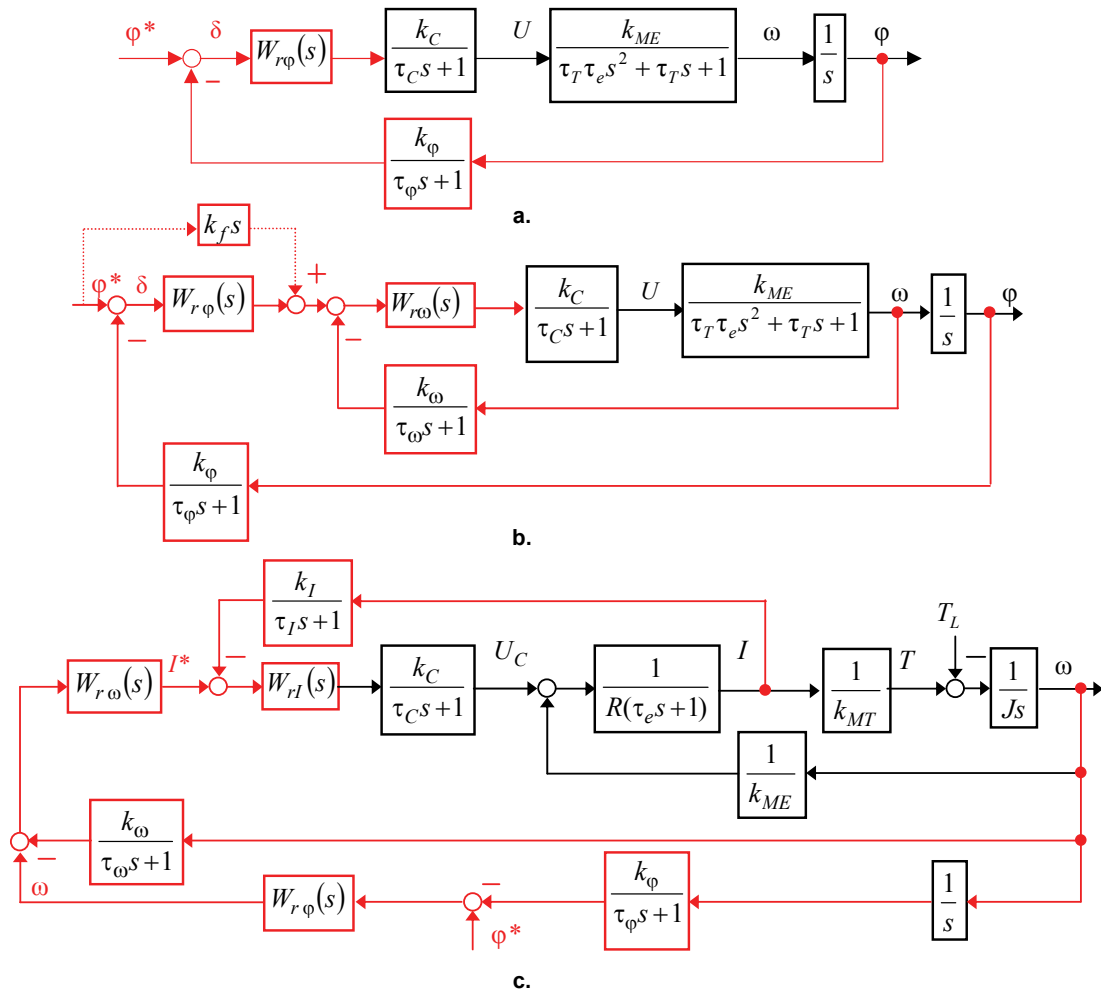


Fig. 6.5 Block diagrams of an electric drive with path control

According to Fig. 5.1, to provide the nearest to the EO setting, select $a_1 = 3$ and $a_2 = 9$. The tuning similar to the MO setting is obtained by selection $a_1 = 2.25$ and $a_2 = 6$. The SO setting is accessible at $a_1 = 2$ and $a_2 = 4$. Usually, the implementation and tuning of such a controller is sufficiently complex, thus the conventional approach assumes the system decomposition to some cascades, typically the path and the speed ones.

The block diagram of the double-loop path controlled electric drive with an inner speed loop is shown in Fig. 6.5 (b). In this cascading system, the inner loop controls the motor angular frequency whereas the outer loop controls the path that the load travels. The external position set-point φ^* is the reference variable used by the system. The error δ between the position set-point φ^* and position actual value serves as the input signal for the path regulator which produces the relevant set-point speed for the motor. The speed set-point and actual values are compared in the lower-level speed regulator. The output signal of the speed regulator is routed to the gate circuit which generates the control signals for the power converter control stages.

The block diagram of the triple-loop path controlled electric drive with the inner speed and current loops is shown in Fig. 6.5 (c).

Let the system has the MO-tuned speed loop

$$W(s) = \frac{1}{k_\omega(2\tau_{\mu\omega}s + 1)}$$

where $\tau_{\mu\omega} = \tau_C + \tau_\omega$ or $\tau_{\mu\omega} = 2\tau_{\mu I} + \tau_\omega$. The object of the path controller is described by the transfer function

$$W_o(s) = \frac{k_\phi}{k_\omega s(2\tau_{\mu\phi}s + 1)},$$

where $\tau_{\mu\phi} = 2\tau_{\mu\omega} + \tau_\phi$. To obtain the EO setting of the path loop, the P-controller is to be used with a gain

$$W_r(s) = k_r = \frac{k_\omega}{4\tau_{\mu\phi}k}$$

To obtain the MO setting of the path loop, the twofold gain is required,

$$W_{r\phi}(s) = k_{r\phi} = \frac{k_\omega}{2\tau_{\mu\phi}k_\phi}$$

**INDEPENDENT MINDED
LIKE YOU**

We believe in equality, sustainability and a modern approach to learning. How about you?
Apply for a Master's Programme in Gothenburg, Sweden.

PS. Scholarships available for Indian students!

www.gu.se/education

To obtain the SO setting of the path loop, the PI-controller is needed with the same gain and the time constant $\tau_{r\phi} = 4\tau_{\mu\phi}$. In this case, an LPF has to be placed between the path and speed controllers with a transfer function $W_f(s) = \frac{1}{4\tau_{\mu\omega}s + 1}$. As a result, the transfer function of the control object is reduced to the third-order model, which can be corrected by the above described regulators.

The choice of the path setting is defined by the drive dynamic and static requirements. In the steady state mode, the use of the SO-tuned PI-controller results in the following transfer function of the open loop path control system:

$$W_{open}(s) = \frac{4\tau_{\mu\omega}s + 1}{8\tau_{\mu\phi}^2 s^2 (\tau_{\mu\phi}s + 1)}$$

This setting provides the step response of high quality without the steady-state path error. At the same time, integration always deteriorates the drive dynamics due to the slowing of the motor starting and the raising of the drive overshoot.

As shown above in Fig. 2.5 (c), the predictive control which uses a feedforward signal is an effective method to drop the steady-state error without excessive dynamic errors. One possible way to introduce the feedforward loop is shown by the dotted lines in the path control block diagram of Fig. 6.5 (b). Here, the feedforward controller with the transfer function of the differentiator $k_f s$ is connected across the path P-controller. The transfer function of the path-controlled drive is as follows:

$$W(s) = \frac{\frac{k_f}{k_{r\phi}} s + 1}{k_\phi (2\tau_{\mu\phi}^2 s^2 + 2\tau_{\mu\phi}s + 1)}.$$

As this equation implies, the feedforward loop may act differently on the drive static and dynamic responses. To estimate it, examine the transfer function in respect to the path error:

$$W_\delta(s) = \frac{\delta}{\varphi^*} = \frac{1}{k_\phi} - W(s) = \frac{2\tau_{\mu\phi}^2 s^2 + 2\tau_{\mu\phi}s - \frac{k_f}{k_{r\phi}}}{k_\phi (2\tau_{\mu\phi}^2 s^2 + 2\tau_{\mu\phi}s + 1)}.$$

While the system operates at the constant speed ($s = 0$), the steady-state speed error is equal to

$$\delta_\omega = \frac{\omega}{k_\phi} \left(2\tau_{\mu\phi} - \frac{k_f}{k_{r\phi}} \right).$$

The system speed quality

$$\frac{\omega}{\delta_\omega} = \frac{k_\phi}{2\tau_{\mu\phi} - \frac{k_f}{k_{r\phi}}}$$

aspires to infinitive since

$$k_f = 2\tau_{\mu\phi} k_{r\phi} = \frac{k_\omega}{k_\phi}.$$

Other values of k_f result in the overbalancing or misbalancing. Since the feedforward is effective only within the certain range of input signals, this has neither to act on the system control response nor on its response to disturbances. Therefore, it is usually switched off from the control circuit during the starting and breaking operations.

6.4 Electric drives with elastic load

The behavior of the double mass elastic system shown in Fig. 6.6 (a) is described by the inertia ratio γ_J , the elastic torque T_β described by (3.3), the motor T_M and the load T_L torques, the referred solid factor c_β from (3.1), the inner friction factor β_L from (3.2), the period of the free oscillations τ_β given by (3.4), the mechanism free oscillation period at the immovable motor τ_c from (3.5), the period of the motor shaft oscillation at the immovable mechanism τ_M from (3.6), and the damping factors ξ_β and ξ_c of elastic oscillations defined by (3.7).



Linköping University –
innovative, highly ranked,
European

Interested in Engineering and its various branches? Kick-start your career with an English-taught master's degree.

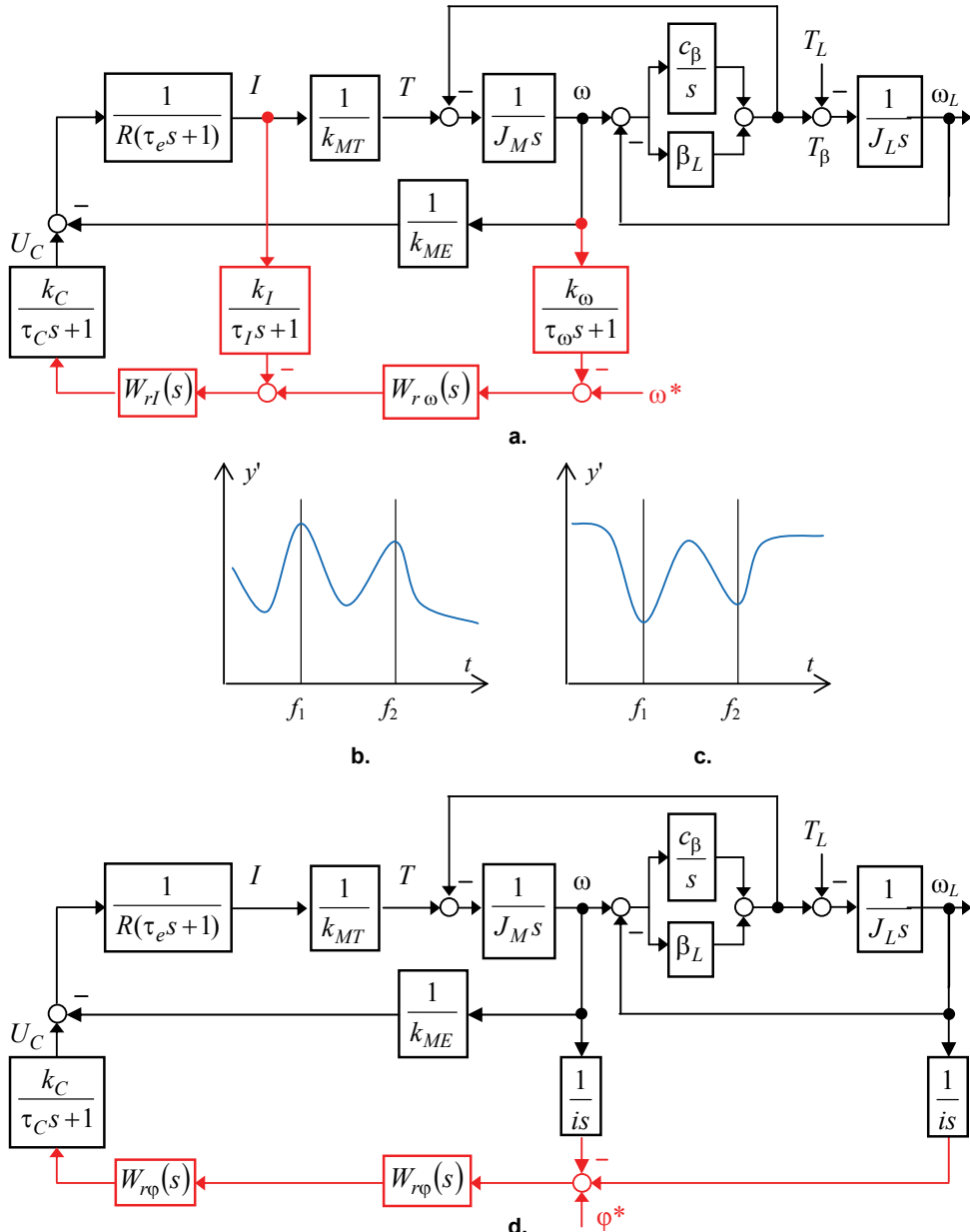
[→ Click here!](#)

ll.U LINKÖPING
UNIVERSITY





Click on the ad to read more

**Fig. 6.6** Block diagrams and frequency responses of an electric drive with elastic load

The transfer function of the open-ended elastic system in regard to the disturbance T_L without the motor reference is as follows:

$$W_{open}(s) = \frac{T_\beta}{T_L} = \frac{\frac{1}{\gamma_J}}{\frac{\tau_\beta^2 s^2 + 2\xi_\beta \tau_\beta s + 1}{\tau_\beta^2 s^2 + 2\xi_\beta \tau_\beta s + 1}}.$$

At weak damping ξ_β the open-ended elastic system is usually described as a conservative section (3.8) with the following transfer function:

$$W_{open}(s) = \frac{\frac{1}{\gamma_J}}{\frac{\tau_\beta^2 s^2 + 1}{\tau_\beta^2 s^2 + 1}}.$$

The transfer function in regard to the motor torque is as follows:

$$W_T(s) = \frac{T_\beta}{T} = \frac{\tau_\beta^2 c_\beta (2\xi_\beta \tau_\beta s + 1)}{\tau_\beta^2 s^2 + 2\xi_\beta \tau_\beta s + 1} \approx \frac{\frac{J_L}{\gamma_J}}{\tau_\beta^2 s^2 + 1}.$$

The elastic torque changes reciprocally upon the motor torque alternation. The equation of the second mass motion is as follows:

$$W_{T2}(s) = \frac{\omega_L}{T} = \frac{2\xi_\beta \tau_\beta s + 1}{(J_M + J_L)s(\tau_\beta^2 s^2 + 2\xi_\beta \tau_\beta s + 1)} \approx \frac{\frac{1}{J_L J_M \gamma_J}}{s(\tau_\beta^2 s^2 + 1)}.$$

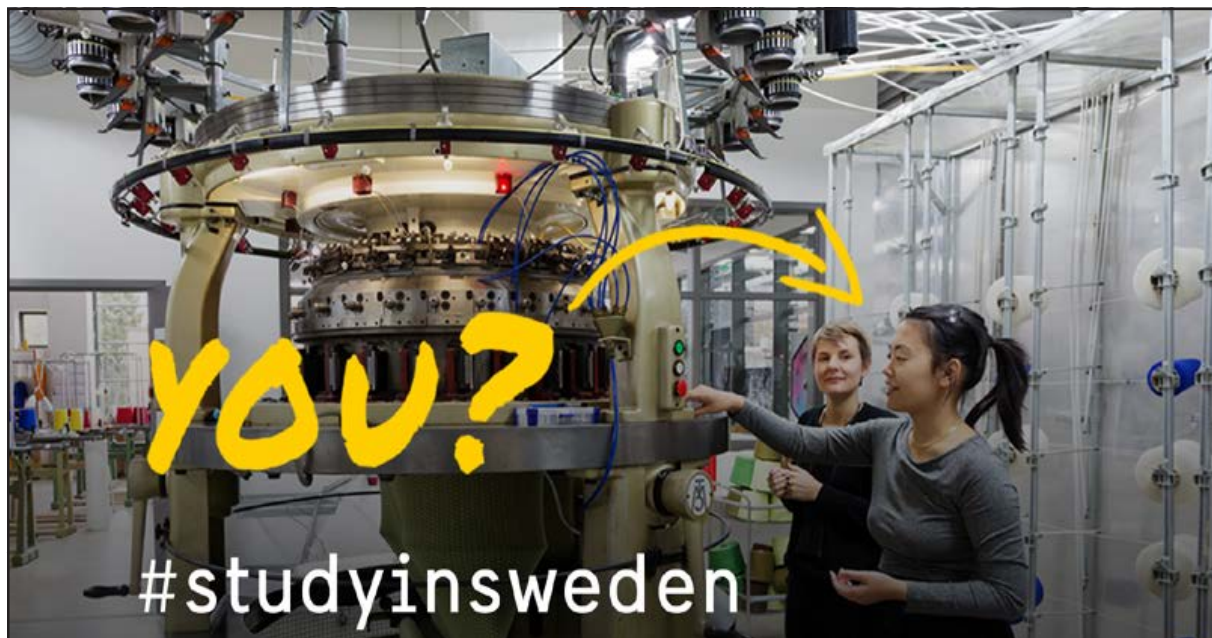
The transfer function in regard to the motor speed is as follows:

$$W_\omega(s) = \frac{\omega_L}{\omega} = \frac{2\xi_\beta \tau_\beta s + 1}{\gamma_J \tau_\beta^2 s^2 + 2\xi_\beta \tau_\beta s + 1} \approx \frac{1}{\gamma_J \tau_\beta^2 s^2 + 1}.$$

The transfer function of the speed loop object with the optimized current loop, the scaled inputs, and compensated counter-EMF can be presented as follows:

$$W_{o1}(s) = \frac{1}{2\tau_{\mu I}s + 1} \cdot \frac{1}{\gamma_J J_M s} \cdot \frac{k_\omega}{\tau_\omega s + 1} \cdot \frac{W_2(s)}{W_1(s)} = W_o(s) \cdot \frac{W_2(s)}{W_1(s)}$$

where



Striking a match, reconnecting with your family through Skype or over a phone network from Ericsson, refurbishing your apartment at IKEA or driving safely in your Volvo - none of this would be possible if not for Sweden. Swedish universities offer over 900 international master's programmes taught entirely in English.

Don't just pick a place - pick a future.
[>studyinsweden.se](http://studyinsweden.se)



Click on the ad to read more

The simple method to avoid an operation at the resonant frequencies relates to the generation of the especial set-point laws known as the *frequency window skip (jump frequency method)*. Unfortunately, this solution is unacceptable for the tracking and programmable systems which require the accurate processing of the broad set-point spectres.

Another approach is based on the inclusion of the correcting devices into the control system. For this purpose the electric drives are supplied by the filters, primarily the LPF, *resonance suppression filters*, and *adaptive vibration suppression controls*. Particularly, in the Mitsubishi servo drives such filters are allocated behind the speed regulator outputs.

Figure 6.6 (b) presents the frequency response of the elastic load with two resonant splashes at the frequencies f_1 and f_2 . To define these frequencies, the driven mechanism is subjected to the identification process by its swinging at small amplitudes using the built-in amplitude-frequency analysers. If the frequency response is unknown, the filters will be tuned directly on the object.

The LPF are tuned at the first resonance frequency, approximately $f_1 = \frac{k}{2\pi\gamma_J}$ where k is the open-ended system gain. Herewith, the transient character is preserved though the gain is γ_J times reduced as compared with the hard system.

More effective are the anti-resonant sections on the basis of the second-order BSF tuned for the particular resonant frequency bands. As the operation frequency catches these bands, the filters reduce the open-ended system gain. The *notch frequency* and the *gain decreasing depth* of the BSF are selected manually or with the help of the specific adaptation instruments. For this purpose, first, the low speed gain is assigned and the search of the BSF frequency starts aiming to suppress the resonant frequencies. The search starts from the high (1000 Hz) frequencies with the gradual their reducing (up to 100 Hz). Following the frequency finding, the regulator gain increases and the filter tuning repeats until the maximum bandwidth will be reached. Figure 6.6 (c) illustrates the tuning results of two BSF which have suppressed the resonant splashes of Fig. 6.6 (b).

The tracking and positioning electric drives with the elastic loads are locked either through the motor shaft or through the mechanism shaft, or they are supplied by the two position encoders as shown in Fig. 6.6 (d). The first variant meets the low tracking requirements, thus the system conditions are similar to those of the adjustable-speed drives. For the second and third variants, the dynamical object properties essentially depend on the joint machine-regulator parameters. Besides, the system quality is affected by the control loop backlashes and gaps which reduce the drive bandwidth resulting in the self-oscillations. The influence of these sources may be decreased by the elevation of the drive damping abilities.